博士論文

The fundamental studies for the exact excitation calculation; spin-orbit coupling in the all-electron mixed basis approach and normalization in quasiparticle theory by the Ward identity

（厳密な励起状態計算のための基礎研究；全電子混合基底法におけるスピン軌道相互作用と準粒子理論における Ward 恒等式による規格化）

横浜国立大学大学院

理工学府

Takeru Nakashima

（中嶋武）

学位授与　2022 年 3 月

YOKOHAMA NATIONAL UNIVERSITY

DOCTORAL THESIS

The fundamental studies for the exact excitation calculation; spin-orbit coupling in the all-electron mixed basis approach and normalization in quasiparticle theory by the Ward identity

Author:
Takeru NAKASHIMA

A thesis submitted in fulfillment of the requirements for the degree of Doctor of Science

in the

Graduate School of Engineering Science

March 18, 2022

“ふしぎだと思うこと、これが科学の芽です。よく観察してたしかめ、そして考えること、これが科学の茎です。そうして最後になぞがとける、これが科学の花です。”

朝永振一郎

Acknowledgements

I would like to express my deepest appreciation to Prof. Kaoru Ohno and Prof. Hannes Raebiger as supervisors. Advice given by them has been a great help in studying the topics involved in this doctoral thesis. Also, I am deeply grateful to my mother Kazuko for her help and support.

List of publications

This thesis consists of an overview of the following publications

1. Takeru Nakashima and Kaoru Ohno. "Spin-Orbit Coupling in All-electron Mixed Basis Approach". *Annalen der Physik*, 531 9: 1900060 (2019)[1];

   I carried out the theoretical work, proposed to the new calculation method for the spin-orbit coupling, wrote the code, ran the calculations, and wrote the paper.

2. Takeru Nakashima and Hannes Raebiger, and Kaoru Ohno. "Normalization of exact quasiparticle wave functions in the Green's function method guaranteed by the Ward identity". *Physical Review B* 104 20: L2011116 (2021)[2];

   I elucidated that the vertex correction plays a role of normalization factor of quasiparticle wave functions, their derivation for an inhomogeneous system, and that the Dyson equation can be hermitized under Baym-Kadanoff's conservation law, gave the interpretation of the extended Kohn-Sham equation, and wrote the paper.

Contents

List of Abbreviations

AEMB	**A**ll-Electron **M**ixed **B**asis
AO	**A**tomic **O**rbital
APW	**A**ugemented **P**lane **W**aves
BSE	**B**ethe-**S**alpeter **E**quation
BSSE	**B**asis **S**et **S**uperposition **E**rror
DFT	**D**ensity **F**unctional **T**heory
GGA	**G**eneralized **G**radient **A**pproximation
HF	**H**artree-**F**ock
HK	**H**ohenberg-**K**ohn
IPE	**I**nverse **P**hoto**E**mission
KS	**K**ohn-**S**ham
LCAO	**L**inear **C**ombination of **A**tomic **O**rbitals
LDA	**L**ocal **D**ensity **A**pproximation
LMTO	**L**inear **M**uffin-**T**in **O**rbitals
MBPT	**M**any-**B**ody **P**erturbation **T**heory
MO	**M**olecular **O**rbital
PAW	**P**rojector **A**ugmented **W**aves
PE	**P**hoto**E**mission
PW	**P**lane **W**ave
QP	**Q**uasi**P**article
QPWF	**Q**uasi**P**article **W**ave **F**unction
SOC	**S**pin-**O**rbit **C**oupling
SOS	**S**pin-**O**rbit **S**plitting
TOMBO	**TO**hoku **M**ixed **B**asis **O**rbital
XPS	**X**-ray **P**hotoelectron **S**pectroscopy

List of Symbols

a_0	Bohr radius
$\boldsymbol{r}$	Position vector
t	Time coordinate
i	Abbreviation for position and time coordinates; $(\boldsymbol{r}_i, t_i)$
$\boldsymbol{k}$	Wave number vector
$\boldsymbol{G}$	Reciprocal lattice vector
$\boldsymbol{p}$	Momentum vector
$\boldsymbol{L}$	Orbital angular momentum
$\boldsymbol{S}$	Spin operator
$\boldsymbol{E}$	Electric field vector
n	Principal quantum number
l	Angular momentum quantum number
m	Magnetic quantum number
σ	Pauli's spin matrix
H	Hamiltonian for many-particle system
$\psi(r)$	Electron annihilation Schrödinger operator
$\psi^\dagger(r)$	Electron creation Schrödinger operator
$\psi(i)$	Electron annihilation Heisenberg operator; $i = (\boldsymbol{r}_i, t_i)$
$\psi^\dagger(i)$	Electron creation Heisenberg operator; $i = (\boldsymbol{r}_i, t_i)$
∂_t	Partial differentiation with respect to time, $\partial/\partial t$
ω	Angular frequency
μ	Occupied levels or chemical potential
ν	Empty levels
λ	Both occupied and empty levels or arbitrary parameter
Σ	Self-energy
v^H	Hartree potential
M	Mass term; $M = \Sigma - v^H$
G_0	One-particle Green's function for non-interacting system
G_0^{-1}	Inverse one-particle Green's function for non-interacting system
G	One-particle Green's function
G^{-1}	Inverse one-particle Green's function
ϵ	Dielecteric function
ϵ^{-1}	Inverse dielecteric function
P	Polalization function
K	Two-particle Green's function
L	Two-particle correlation function
ρ	Electron density (matrix)
Ψ_0^N	Ground state for N-electron system
E_0^N	Ground energy for N-electron system
$E_\lambda^{N\pm1}$	λ-th excited energy for $(N \pm 1)$-electron system

Chapter 1

Introduction

At the beginning of the 20th century, quantum mechanics was established and it became possible to make theoretical predictions on various properties of materials. Many theoretical approaches have appeared in order to study physical phenomena. As one of them, the first-principles calculation is the great one which gives the good agreement with various experimental results. This method also has the great advantage that it is applicable to any target calculation compared with other approaches, because the least number of parameters are just needed in its calculation. It is, however, well known that first-principles calculation become more cumbersome with the size of target system. For this reason, it is long-standing subject in first-principles approach to introduce the approximations with reducing the computational cost and still preserving their physical features. This doctoral thesis includes the two studies based on the first-principles calculation, and I tried to introduce new calculation method and theory to solve the above problem in those studies.

Generally, the one-particle effective Schrödinger equation is taken as first-principles in quantum mechanics, and there are several calculation methods relying on the one-particle picture; especially, this doctoral thesis is based on density functional theory (DFT) and many-body Green's function which are famous theories[3–8]. DFT is developed by P. Hohenberg, W. Kohn, and L. J. Sham mainly, and their calculation results are widely applied for much more sophisticated calculations including the Green's function approach (W. Kohn was awarded Nobel Prize in Chemistry in 1998 for developing DFT). These theories have been applied to calculate several physical phenomena such as stable structures, excitation energies, transition matrices related to photo absorptions, direct and inverse photoemission, etc.

Photoemission, inverse photoemission, and photo absorption in optical experiments are useful to obtain information on electronic states of materials (see Fig. 1.1)[9]. In a direct photoemission experiment, the final state on the material has one hole which was originally occupied by a photoelectron. Since the energy and momentum conservation laws are satisfied in the direct photoemission process among the photoelectron, the photoelectron gives the excitation energy and the energy level information of occupied states. On the other hand, in a similar way, inverse photoemission gives the excitation energy and the energy level information of unoccupied (which is called empty) states. (Notice that photoabsorption is a little different from direct and inverse photoemission, and a more complicated process appears because the excited electrons stay in the material interacting with the holes created in that process.) A hole state created in direct photoemission process is affected by surrounding electrons, so its behavior is different from a bare hole. Therefore, the hole affected by other electrons around the hole is called quasi-hole (see Fig. 1.2). For similar reason, an electron created in inverse photoemission process does not exist as a bare electron in the material, but is affected by surrounding electrons. This electron affected by the surrounding electrons is called quasi-electron (see Fig. 1.2). In this

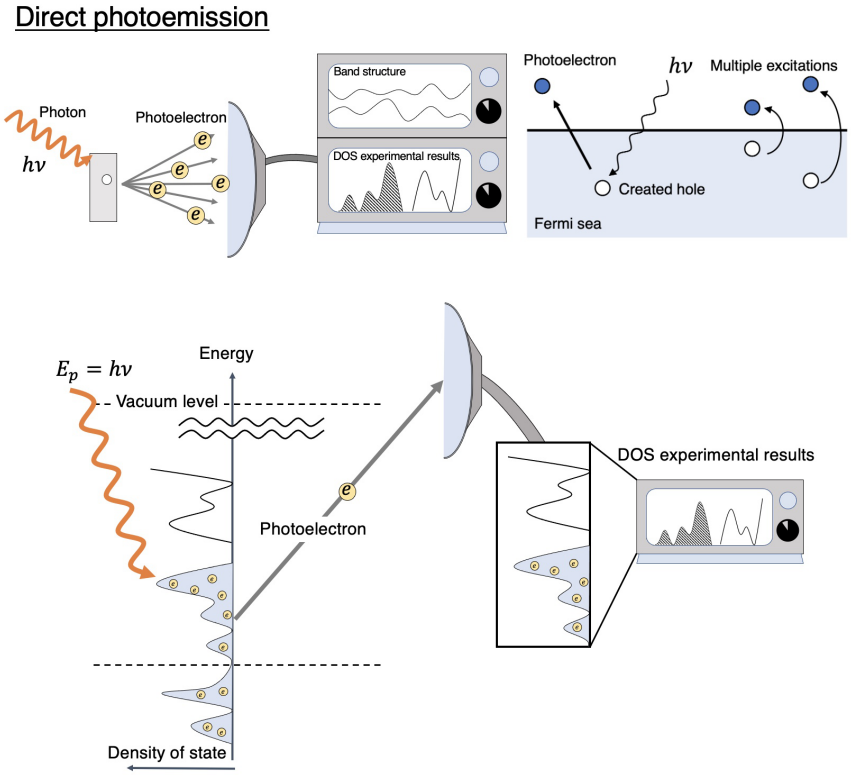

FIGURE 1.1: Schematic figure of direct photoemission. A photon injected into the system gives energy to an electron, which is excited and leaves the system as a photoelectron. The observation of the photoelectron gives information of density of state, energy levels, and so on.

doctoral thesis, I call both quasi-hole and quasi-electron as quasiparticle (QP) for simplicity[10–12]. This QP obeys the one-particle effective Schrödinger equation, which is called the Dyson equation for QP or the QP equation. The QP equation is cumbersome and is difficult to solve without approximations, which means this method needs expensive computational cost in the original procedure. So, the development of good approximations and methods is important to improve discrepancies with experimental spectra and calculated ones. In my first study, I developed a new precise method to calculate the spin-orbit coupling with Kohn-Sham (KS) DFT framework, as published in *Annalen der Physik*, 531. 9 (2019): 1900060. [1] (see section 1.1 and details are given in chapter 3), and in the second one, I elucidated the validity to normalize quasiparticle wave functions (QPWFs) in QP theory, showed that the Dyson equation can be hermitized under Baym-Kadanoff's conservation law, and gave the interpretation of the extended KS equation, as published in *Physical Review B*. 104. 20 (2021): L201116. [2] (see section 1.2 and details are given in chapter 4).

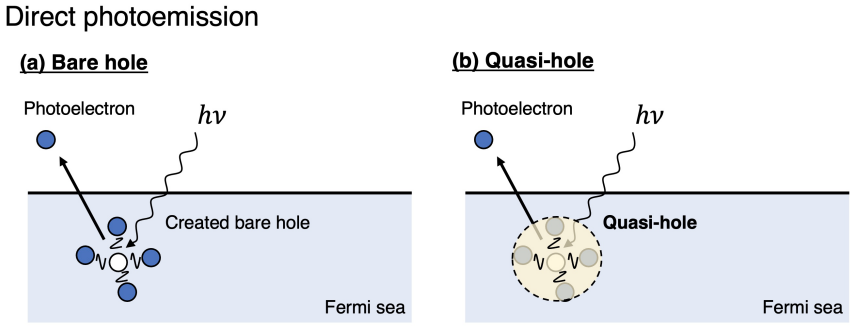

FIGURE 1.2: In a material, a bare particle can not be observed, and one particle picture have to be applied to the collective electron taking other electrons. Therefore, in QP theory, quasi-hole in direct photoemission and quasi-electron in the inverse photoemission have to be treated. (a) denotes the original bare hole schematic picture, but this picture can not be observed by actual experiments, *i.e.*, direct photoemission. (b) denotes the quasi-hole schematic picture, which can be applied to the actual electron picture.

1.1 Spin-orbit coupling in QP theory

For accuracy of calculation which reproduces optical experiments, spin dependent effects are also important. One of physical phenomena related to them is the spin-orbit coupling (SOC), which is derived from the Dirac equation in the classical limit[13]. Specifically, for the Hamiltonian including the SOC, angular momentum and spin are not good quantum numbers, and the SOC induces band spin splitting which may produce spin currents in spintronics devices. Therefore, it is important to develop quasiparticle (QP) theory including the SOC effects in order to promote active studies on spintronics and new phenomena related to spin properties.

In QP theory, SOC calculation is cumbersome because even non-spin dependent QP equation requires expensive computational cost. As a solution to the cumbersome problem, generally Kohn-Sham (KS) density functional theory (DFT) orbitals are used to calculate the SOC splitting because the quasiparticle wave functions (QPWFs) are thought to be very similar to the KS orbitals. This approximation are based on the assumption that the screening effects from the core electrons for the SOC are considered relatively small[14, 15], and this approach is the main methods used widely.

In previous papers[15, 16], the SOC has been calculated by using both the pseudo potential and all-electron methods. In those calculations, the SOC has two different forms, *i.e.*, the $\boldsymbol{S} \cdot \boldsymbol{L}$ form under the spherical symmetry of the Coulomb potential, $V(\boldsymbol{r}) \simeq V(|\boldsymbol{r}|)$, and the exact original form derived from the Dirac equation[13]. we have to treat the exact form in order to precisely treat valence electrons existing in the intermediate space of nuclei. The reason is that generally the Coulomb potential does not satisfy spherical symmetry $V(\boldsymbol{r} - \boldsymbol{R}_n) \neq V(|\boldsymbol{r} - \boldsymbol{R}_n|)$ in the interatomic region, where $\boldsymbol{r}$ and $\boldsymbol{R}_n$ denote the electron and nucleus position coordinates, respectively. As a solution for this difficulty, I propose to apply the $\boldsymbol{S} \cdot \boldsymbol{L}$ form near the nuclei and the exact form in the intermediate space among nuclei with all-electron mixed basis (AEMB) approach[17]. AEMB expands one-particle wave function as both local basis (numerical atomic orbitals) and non-local basis (plane waves). This study was reported in Takeru Nakashima and Kaoru Ohno. "Spin-Orbit Coupling

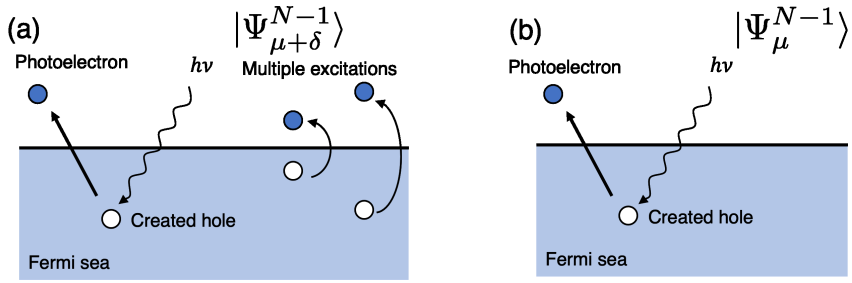

FIGURE 1.3: Many excited states in the photoemission: (a) Illustration of an excited state including some hole states, (b) Illustration of an excited state including only one hole state, which is the main final state observed in the photoemission.

in All-Electron Mixed Basis Approach". *Annalen der Physik*, 531 9: 1900060 (2019).[1]. Details are discussed in chapter 3. The purpose of chapter 3 is to develop a method to calculate SOC with AEMB, which takes into account both the contribution from valence electrons in the intermediate space between nuclei, where spherical symmetry is broken, and the contribution from inner orbitals. This method can be applied to combine the SOC and QP theory in perturbation theory.

1.2 The finite number problem in QP theory

Generally, Kohn-Sham (KS) orbitals are taken as initial values for quasiparticle (QP) calculation[9, 14, 18–21]. But, it is empirically known that in the actual calculation, the number of the quasiparticle wave functions (QPWFs) for occupied levels is finite and the same number equal to the number of electrons in the system, *i.e.* the number of KS orbitals. This is inconsistent with theoretical requirements, that the number of the QPWFs is infinite. In recent QP calculations, these QPWFs obtained in actual calculation are normalized in order to conserve the electron number, albeit there is no clear justification for such normalization. I try to elucidate the justification of this treatment focusing on the Ward identity and explain the relationship between the normalization and the Ward identity by physical intuition. Additionally, I elucidate that the QP equation can be divided into two equations, which have the real part of the QP energy and the imaginary part of the QP energy as eigenvalues, respectively. The equation having the real part of the QP energy as eigenvalue can be regarded as the extended KS equation, whose eigenstates are non-orthogonal mutually.

There are a lot of excitations in many-body excited states $|\Psi^{N-1}_{\mu}\rangle$ in photoemission process. We can classify these states into the state, including multi hole and Auger like process, (see Fig. 1.3 (a)) and the state, including only one hole state (see Fig. 1.3 (b)). I consider that the state, including one hole only, is the main state observed in photoemission. This physical intuition can be related to the limited vertex function and the Ward identity[22, 23]. The Ward identity is derived from the vertex function when taking the limit of energy and momentum transfers between three points of the vertex function, that is, the situation of the Ward identity means that the energy and momentum transfer in terms of the Coulomb interaction does not appear. Then, the Ward identity corresponds to the multiple excitations not related to the main QP state, which means that the Ward identity can be treated as renormalized factor for QP state (see Fig. 4.1 and details in chapter 4). I consider that the Ward identity leads to the state including one quasi-hole picture. So, the Ward

identity guarantees that the electron number is conserved and makes the QPWFs normalized. (This interpretation is justified from the fact that the Ward identity is proved by the continuity equation for the electron number[7, 24].) This study was reported in Takeru Nakashima, Hannes Raebiger, and Kaoru Ohno. "Normalization of exact quasiparticle wave functions in the Green's function method guaranteed by the Ward identity". *Physical Review B*, 104 20: L201116 (2021).[2]. Details are discussed in chapter 4. The purpose of chapter 4 is to elucidate the relationship between the normalization of the QPWFs and the vertex correction in QP theory, and introduce the extended KS equation under Baym-Kadanoff's conservation law. In other words, this study gives the justification of the normalized QPWFs and the physical intuition of the Ward identity.

1.3 The organization of doctoral thesis

In chapter 2, I explain the theory basis for my main studies; specifically, density functional theory (DFT), spin-orbit coupling (SOC) and their forms, all-electron mixed basis (AEMB), and Green's function theory. This doctoral thesis contains two main studies, *i.e.*, (i) the development of the calculation of SOC in the AEMB in chapter 3 and (ii) the elucidation for the relation between the vertex correction and the normalization of the quasiparticle wave function (QPWFs) in chapter 4. In chapter 5, summary is given.

Chapter 2

Theoretical framework

In this chapter, I explain some previous key theories and studies of relevant topics. Section 2.1 is devoted to the explanation of density functional theory (DFT) because the spin-orbit coupling (SOC) is calculated within Kohn-Sham (KS) DFT in the first study; *Annalen der Physik*, 531:1900060 (2019)[1]. Section 2.2 is devoted to the SOC, which is an important relativistic correction derived from the Dirac equation. Section 2.3 is devoted to the explanation of the all-electron mixed basis (AEMB). This method is applied to calculate the SOC effects contributed from both core and valence electrons efficiently. Section 2.4 is devoted to the brief explanation of the Green's function method, QP theory, and some theories related to the second study; *Physical Review B* 104: L2011116 (2021)[2].

2.1 Density functional theory

Density functional theory (DFT) is one of the most powerful tools to study material properties and has been widely used in various fields[3, 4, 25]. DFT is composed of two theories, *i.e.*, Hohenberg-Kohn (HK) theorem and Kohn-Sham (KS) theory[3, 4]. According to HK theorem, physical quantities in the ground state can be expressed as a functional of the electron density. HK theorem gave the basis to calculate physical properties depending on only the electron density. This great success led to KS theory, which allows us to use a set of non-interacting one-particle effective Schrödinger equations (called KS equations) instead of true many-body Schrödinger equation. In the following, let me introduce these theories.

2.1.1 Hohenberg-Kohn theorem

Suppose that a general Hamiltonian H is

$$H = \int d\boldsymbol{r}\psi^\dagger(\boldsymbol{r})\left(T(\boldsymbol{r}) + U_{\text{ext}}(\boldsymbol{r})\right)\psi(\boldsymbol{r}) + \frac{1}{2}\int d\boldsymbol{r}_1 d\boldsymbol{r}_2 v(\boldsymbol{r}_1 - \boldsymbol{r}_2)\psi^\dagger(\boldsymbol{r}_1)\psi^\dagger(\boldsymbol{r}_2)\psi(\boldsymbol{r}_2)\psi(\boldsymbol{r}_1), \quad (2.1)$$

where ψ and $\psi^\dagger$ are, respectively, electron's annihilation and creation field operators, the first term is the one-particle operator including a kinetic term T and a local external potential term U_{ext}, and the second term represents an electron-electron Coulomb interaction. (Please notice that we use the Hartree atomic unit $m = e = \hbar = 1$ for simplicity.) Symbolically each term in Eq. (2.1) is represented by $H = T + U_{\text{ext}} + V$; T, U_{ext}, and V denote, respectively, the kinetic energy, the local external potential, and the electron-electron Coulomb interaction. The electron density $n(r)$, which is key physical quantity in DFT, is defined by

$$n(\boldsymbol{r}) = \langle\, \Psi_0^N \,|\, \psi^\dagger(\boldsymbol{r})\psi(\boldsymbol{r}) \,|\, \Psi_0^N \,\rangle, \quad (2.2)$$

where Ψ_0^N denotes a ground state for a system composed of N electrons, satisfying the true Schrödinger equation

$$H \,|\, \Psi_0 \,\rangle = E_0^N \,|\, \Psi_0^N \,\rangle.$$

We can consider that the electron density is determined by the external potential uniquely, which is trivial, but on the other hand it is not clear that the external potential U_{ext} is determined by the eletron density $n(\boldsymbol{r})$ uniquely. This unique property is shown by *reductio ad absurdum*.

Firstly, consider the following two eigenvalue problems

$$H \,|\, \Psi \,\rangle = E \,|\, \Psi \,\rangle \quad (2.3a)$$
$$H' \,|\, \Psi' \,\rangle = E' \,|\, \Psi' \,\rangle, \quad (2.3b)$$

where Ψ, Ψ' are the ground states respectively, and H' is H with U_{ext} replaced by the different external potential U'_{ext}. We assume that these ground states Ψ and Ψ' give the same electron density $n(\boldsymbol{r})$. The minimal property of the ground state shows that

$$E' = \langle\, \Psi' \,|\, H' \,|\, \Psi' \,\rangle < \langle\, \Psi \,|\, H' \,|\, \Psi \,\rangle = \langle\, \Psi \,|\, H + U'_{\text{ext}} - U_{\text{ext}} \,|\, \Psi \,\rangle, \quad (2.4)$$

so that

$$E' < E + \int d\boldsymbol{r} \left[U'_{\text{ext}}(\boldsymbol{r}) - U_{\text{ext}}(\boldsymbol{r}) \right] n(\boldsymbol{r}). \tag{2.5a}$$

In the same way, we get

$$E < E' + \int d\boldsymbol{r} \left[U_{\text{ext}}(\boldsymbol{r}) - U'_{\text{ext}}(\boldsymbol{r}) \right] n(\boldsymbol{r}). \tag{2.5b}$$

Equations (2.5) show the contradiction,

$$E + E' < E + E'. \tag{2.6}$$

Therefore, from *reductio ad absurdum*, the electron density $n(\boldsymbol{r})$ is a unique functional of the external potential U_{ext}, *i.e.*, $n[U_{\text{ext}}]$, which is called the first HK theorem.

Secondly, the each term (kinetic and interaction terms) is also the functional of the electron density since the ground state Ψ is the functional of the electron density. We therefore define

$$F[n] = \langle \Psi \mid (T + V) \mid \Psi \rangle, \tag{2.7}$$

where $F[n]$ is generally called universal function, valid for any number of particles and any external potential. Using $F[n]$, the total energy for the ground states is

$$E_{U_{\text{ext}}} = \int d\boldsymbol{r} U_{\text{ext}}(\boldsymbol{r}) n(\boldsymbol{r}) + F[n], \tag{2.8}$$

which equals the ground state energy for the correct $n(\boldsymbol{r})$. As an additional condition, $n(\boldsymbol{r})$ should satisfy the following equation

$$N[n] = \int d\boldsymbol{r} n(\boldsymbol{r}) = N. \tag{2.9}$$

The energy functional

$$\mathcal{E}_{U_{\text{ext}}}[\Psi'] = \langle \Psi' \mid U_{\text{ext}} \mid \Psi' \rangle + \langle \Psi' \mid (T + V) \mid \Psi' \rangle, \tag{2.10}$$

has the minimum value for the correct ground state Ψ and suppose that Ψ' corresponds to the ground state for the different external potential U'_{ext}. From Eq. (2.10), the following inequality is satisfied

$$\mathcal{E}_{U_{\text{ext}}}[\Psi'] = \int U_{\text{ext}}(\boldsymbol{r}) n'(\boldsymbol{r}) d\boldsymbol{r} + F[n'] > \mathcal{E}_{U_{\text{ext}}}[\Psi] = \int U_{\text{ext}}(\boldsymbol{r}) n(\boldsymbol{r}) d\boldsymbol{r} + F[n], \tag{2.11}$$

which shows that the the correct density among all electron densities corresponding to any external potential U_{ext} makes the total energy functional $\mathcal{E}_{U_{\text{ext}}}$ get minimal. This is called second HK theorem. This HK theorem makes the electron density the basic variable for the recent studies. In next section, we derive the KS theory from HK theorem.

2.1.2 Kohn-Sham theory

By using HK theorem, we can transform a many-body problem into a virtual single-particle problem, *i.e.*, one-particle effective Schrödinger equation which is called KS equation. From HK theorem, total energy for any system is determined by electron density $n(\boldsymbol{r})$. The classical Coulomb interaction (which is the Hartree term) is separated from the universal function $F[n]$ for convenience

$$F[n] = \frac{1}{2}\int d\boldsymbol{r}_1 d\boldsymbol{r}_2 v(\boldsymbol{r}_1 - \boldsymbol{r}_2) n(\boldsymbol{r}_1) n(\boldsymbol{r}_2) + G[n], \tag{2.12}$$

where $G[n]$ is a universal function like $F[n]$. Equation (2.8) becomes

$$E = \int U_{\text{ext}}(\boldsymbol{r}) n(\boldsymbol{r}) d\boldsymbol{r} + \frac{1}{2}\int d\boldsymbol{r}_1 d\boldsymbol{r}_2 v(\boldsymbol{r}_1 - \boldsymbol{r}_2) n(\boldsymbol{r}_1) n(\boldsymbol{r}_2) + G[n]. \tag{2.13}$$

It is very difficult to find the explicit form of $G[n]$, so we introduce a non-interacting kinetic energy $T_s[n]$ with density $n(\boldsymbol{r})$

$$G[n] = T_s[n] + E_{xc}[n], \tag{2.14}$$

where $E_{xc}[n]$ is called exchange-correlation term. Restriction conditions, Eq. (2.9), gives

$$\delta N = \int \delta n(\boldsymbol{r}) d\boldsymbol{r} = 0. \tag{2.15}$$

The method of Lagrange multiplier with Eqs. (2.8), (2.12), and (2.15), shows

$$\delta\left(E[n] - \alpha N\right) = \int d\boldsymbol{r}\left[U_{\text{ext}}(\boldsymbol{r}) + \int d\boldsymbol{r}' v(\boldsymbol{r} - \boldsymbol{r}') n(\boldsymbol{r}') + \frac{\delta T_s[n]}{\delta n(\boldsymbol{r})} + \frac{\delta E_{xc}[n]}{\delta n(\boldsymbol{r})} - \alpha\right]\delta n(\boldsymbol{r}). \tag{2.16}$$

Assume that the electron density for the non-interacting system is represented by

$$n(\boldsymbol{r}) = \sum_{i=1}^{N} |\phi_i(\boldsymbol{r})|^2, \tag{2.17}$$

and that the kinetic energy for the non-interacting system is

$$T_s[n] = -\frac{1}{2}\sum_{i=1}^{N}\int d\boldsymbol{r}\phi_i^*(\boldsymbol{r})\nabla^2\phi_i(\boldsymbol{r}). \tag{2.18}$$

Combining Eqs. (2.16), (2.17), and (2.18) gives a one-particle effective Schrödinger equation giving the same electron density with the true many-particle system interacting each other

$$\left(-\frac{1}{2}\nabla^2 + U_{\text{ext}}(\boldsymbol{r}) + \int d\boldsymbol{r}' v(\boldsymbol{r} - \boldsymbol{r}') n(\boldsymbol{r}') + \frac{\delta E_{xc}[n]}{\delta n(\boldsymbol{r})}\right)\phi_i(\boldsymbol{r}) = \varepsilon_i\phi_i(\boldsymbol{r}), \tag{2.19}$$

which is called the KS equation, their eigenvalues are called KS eigenvalues or KS energies, and eigenstates are called KS eigenstates or KS orbitals. This theory is called KS theory[4].

KS theory is applied to predict the band structures observed by the photoemission and inverse photoemission, and photo absorption experiments with no justification. The KS eigenvalues and eigenstates are treated as each electron's energy and orbital in the material, but it is well known that those treatment is incorrect and the

energy gap is underestimated by KS theory due to the discontinuity in the correlation functional with electron density[14, 18, 19, 26–29] (of course, it is already shown in the previous studies that the identification of KS orbitals and quasiparticle wave functions (QPWFs) only near the Fermi level is good approximation[14, 26, 30, 31]). The Kohn and Sham(1965)'s original paper[4] proposed the simple approximation as

$$E_{\mathrm{xc}}[n] = \int n(\boldsymbol{r})\varepsilon_{\mathrm{xc}}(n(\boldsymbol{r}))d\boldsymbol{r}, \tag{2.20}$$

where $\varepsilon_{\mathrm{xc}}(n(\boldsymbol{r}))$ is calculated from a homogeneous system with electron density $n(\boldsymbol{r})$. This approximation is called local density approximation (LDA) and has been used widely[25] (spin dependent LDA was also introduced[5]). Also other famous approximations are introduced to improve the LDA results. As one of them, generalized gradient approximation (GGA) takes into account the correction for the gradient of the local density $\nabla n(\boldsymbol{r})$.[25, 32–35]. These approximation forms lead to removal of the ambiguity in the effective potential $\delta E_{\mathrm{xc}}/\delta n$ from the exchange-correlation function E_{xc}.

LDA and GGA have the advantage of being simple in form due to their locality. It is well known that the LDA and GGA are appropriate for calculations of clusters including s- and p-orbitals; but on the other hand not appropriate for some system including d-orbitals. In order to get the precise calculation for complex systems, we have to consider the non-local term[35, 36] or have to take into account orbital dependent correction like Hubbard $+U$ approach. The justification of this non-locality is already proven by A. Seidl, A. Görling, P. Vogl, J. A. Mahewski, and M. Levy(1996), whose method is famous as generalized KS equation[37]. In this aspect of the non-locality importance, the self-energy correction in QP theory is very essential too, and it is big problem to clarify the relation between QP theory and KS theory (the second study[2] gives one solution for this problem).

2.2 Spin-orbit coupling

The spin-orbit coupling (SOC) is one of the relativistic effects derived from the Dirac equation[13, 38]. The SOC is responsible for energy level splitting and fine structure, playing the important role for spintronics devices because the SOC reduces band gaps and gives band structures as the sources inducing spin currents. For this reason, developing a new method for the SOC calculation is noticeable to activate these fields.

2.2.1 Spin-orbit coupling around nuclei

The exact SOC is defined by[13, 38]

$$H_{\mathrm{SOC}} = -\frac{1}{4c^2}\sigma \cdot (\boldsymbol{E} \times \boldsymbol{p}) = \frac{1}{2c^2}\boldsymbol{S} \cdot (\nabla V \times \boldsymbol{p}), \tag{2.21}$$

where σ is the Pauli's spin matrix, $\boldsymbol{S} = \sigma/2$ is the spin operator, $\boldsymbol{E} = -\nabla V$ is the electric field, $\boldsymbol{p} = -i\nabla$ is the momentum operator, and $c = 137.036$ is the light velocity in Hartree atomic unit ($m = e = \hbar = 1$). Generally, Eq. (2.21) is used for plane wave basis calculation in homogeneous electron systems. Here, we can introduce a symmetry approximation

$$V(\boldsymbol{r} - \boldsymbol{R}_n) \simeq V(|\boldsymbol{r} - \boldsymbol{R}_n|), \tag{2.22}$$

for the potential in the neighborhood around each nucleus because the Coulombic potential is mainly contributed from the nearest nucleus, in neighborhood around each nucleus. For brevity, take the coordinate of nucleus as the origin and $\nabla V \times \boldsymbol{p}$ becomes

$$\nabla V \times \boldsymbol{p} \simeq \frac{1}{r}\frac{\partial V(r)}{\partial r}\boldsymbol{L}, \tag{2.23}$$

where $\boldsymbol{L} = \boldsymbol{r} \times \boldsymbol{p}$ denotes orbital angular momentum operator. Using Eqs. (2.22) and (2.23), Eq. (2.21) becomes

$$H_{\mathrm{SOC}} = \frac{1}{2c^2}\frac{1}{r}\frac{\partial V(r)}{\partial r}\boldsymbol{S} \cdot \boldsymbol{L}. \tag{2.24a}$$

This equation is rewritten as

$$H_{\mathrm{SOC}} = \frac{1}{2c^2}\frac{1}{r}\frac{\partial V(r)}{\partial r}\frac{1}{2}\left(S_+L_- + S_-L_+\right) + S_zL_z, \tag{2.24b}$$

where $\boldsymbol{S} = \left(S_x, S_y, S_z\right)$ and $S_\pm = S_x \pm iS_y$ operating on spin state, called the spin ladder operator, satisfy following equations

$$S_+ \left| s_z = +\frac{1}{2} \right\rangle = 0, \tag{2.25a}$$

$$S_+ \left| s_z = -\frac{1}{2} \right\rangle = \left| s_z = +\frac{1}{2} \right\rangle, \tag{2.25b}$$

$$S_- \left| s_z = +\frac{1}{2} \right\rangle = \left| s_z = -\frac{1}{2} \right\rangle, \tag{2.25c}$$

$$S_- \left| s_z = +\frac{1}{2} \right\rangle = 0. \tag{2.25d}$$

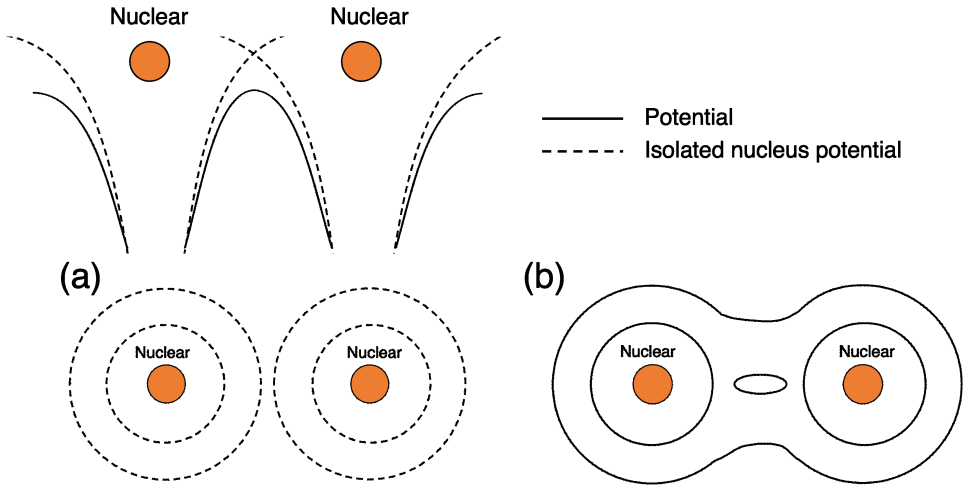

FIGURE 2.1: Structure and contour lines of potentials; dotted lines denote the isolated atomic potential contour lines and solid lines denote the total Coulomb potential contour lines; (a) illustration for isolated contours, (b) illustration for total contours.

Also $L_\pm = L_x \pm iL_y$, operating on orbital momentum state like $S_\pm$, satisfy following equations

$$L_\pm \,|\, l, m \,\rangle = \sqrt{l(l+1) - m(m \pm 1)} \,|\, l, m \pm 1 \,\rangle. \tag{2.26}$$

Especially, $L_\pm \,|\, l, m \,\rangle = 0$ in the case $l < |m \pm 1|$. From these relations, Eqs. (2.24) under Eq. (2.22) is valid near the nucleus; on the other hand this approximation is not valid in interatomic regions, where the potential has a non-symmetric form (see Fig. 2.1). The matrices of Eq. (2.24) are easily calculated by the orthogonality of atomic orbitals $|\, n, l, m, s_z \,\rangle = |\, n, l, m \,\rangle \,|\, s_z \,\rangle$; $\langle\, n', l', m' \,|\, n, l, m \,\rangle = \delta_{n',n}\delta_{l',l}\delta_{m',m}$

$$\langle\, n', l', m' \,|\, L_\pm \,|\, n, l, m \,\rangle = \sqrt{l(l+1) - m(m \pm 1)} \langle\, n', l', m' \,|\, n, l, m \pm 1 \,\rangle. \tag{2.27}$$

Therefore, Eqs. (2.24) are suitable for *ab initio* calculations with local atomic basis. On the other hand, the SOC contributed from valence electrons, including d- and f-orbitals, have to be calculated by the exact SOC form equation (2.21). That is because d- and f-orbitals are expanded broadly in the interatomic regions (see Fig. 2.2). In my thesis, Takeru Nakashima and Kaoru Ohno. "Spin-Orbit Coupling in All-Electron Mixed Basis Approach". *Annalen der Physik*, 531 9: 1900060 (2019).[1], I propose a new calculation method taking into account the full SOC effects contributed from the core and valence electrons using the both SOC forms, Eqs. (2.21) and (2.24)

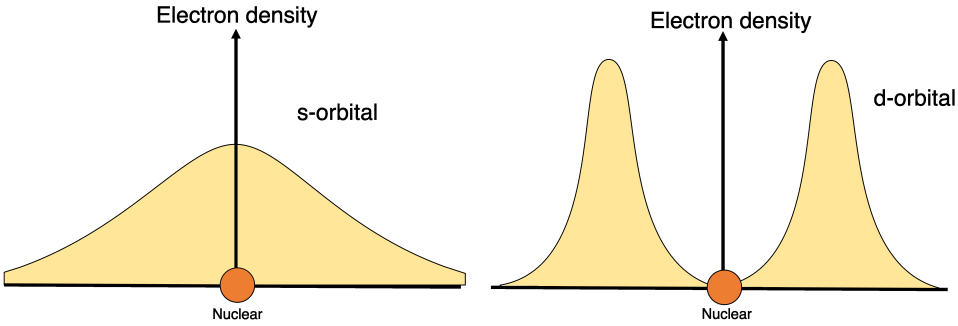

FIGURE 2.2: Each electron density for s- and d-orbital around nucleus is represented schematically. This sketches show that d-orbitals are expanded and may deform the potential in the intermediate space between nuclei

2.3 All-electron mixed basis approach

First-principles calculation is highly dependent on the capability of computer, and their computational cost is dependent on various methods for first-principles calculations. One of the issues related to the computational cost is choice of basis functions. This means that the computational cost is lower when the wave function is well represented by a small set of basis functions. There are several basis approaches developed in order to perform the precise calculation efficiently.

Linear combination of atomic orbitals (LCAO) can enable us to treat the localized wave functions like inner orbitals efficiently. But, LCAO has the intrinsic problem of incomplete basis set, which has difficulty in perturbation theory or spectral expansion. LCAO approach such as Gaussian basis approach has the basis set superposition error (BSSE) too.

In order to remove these problems, it is very important to develop a new method which combines the PW expansion technique with the LCAO technique to remove pseudopotentials in the PW expansion methods and to make the basis set complete in the LCAO methods. This is the main idea to introduce the all-electron mixed basis (AEMB) approach[17].

AEMB expands one-particle wave functions as both local basis and non-local basis[17, 39],

$$|\,\phi\,\rangle = \sum_i |\,\phi_i^{\mathrm{L}}\,\rangle C_i^{\mathrm{L}} + \sum_j |\,\phi_j^{\mathrm{NL}}\,\rangle C_j^{\mathrm{NL}}, \tag{2.28}$$

where ϕ_i^{L} and ϕ_j^{NL} denote local and non-local basis, respectively, and if those basis show orthogonality each other, their coefficients are $C_i^{\alpha} = \langle\,\phi_i^{\alpha}\,|\,\phi\,\rangle$. Our method takes local basis as numerical isolated atomic orbitals (AOs) and non-local basis as plane waves (PWs). For example, the Kohn-Sham (KS) wave function is expanded as

$$\phi_\lambda(\boldsymbol{r}) = \sum_{jnlm} c^{\mathrm{AO}}_{\lambda,jnlm}\phi^{\mathrm{AO}}_{jnlm}(\boldsymbol{r}-\boldsymbol{R}_j) + \frac{1}{\sqrt{\Omega}}\sum_{\boldsymbol{G}} c^{\mathrm{PW}}_{\lambda,\boldsymbol{G}} e^{i\boldsymbol{G}\cdot\boldsymbol{r}} \tag{2.29a}$$

$$= \sum_{jnlm} c^{\mathrm{AO}}_{\lambda,jnlm} R_{nl}(r_j) Y_{lm}(\hat{\boldsymbol{r}}_j) + \frac{1}{\sqrt{\Omega}}\sum_{\boldsymbol{G}} c^{\mathrm{PW}}_{\lambda,\boldsymbol{G}} e^{i\boldsymbol{G}\cdot\boldsymbol{r}}, \tag{2.29b}$$

where $R_{nl}(\boldsymbol{r}_j)$ and $Y_{lm}(\hat{\boldsymbol{r}}_j)$ are the radial function and the spherical harmonics of

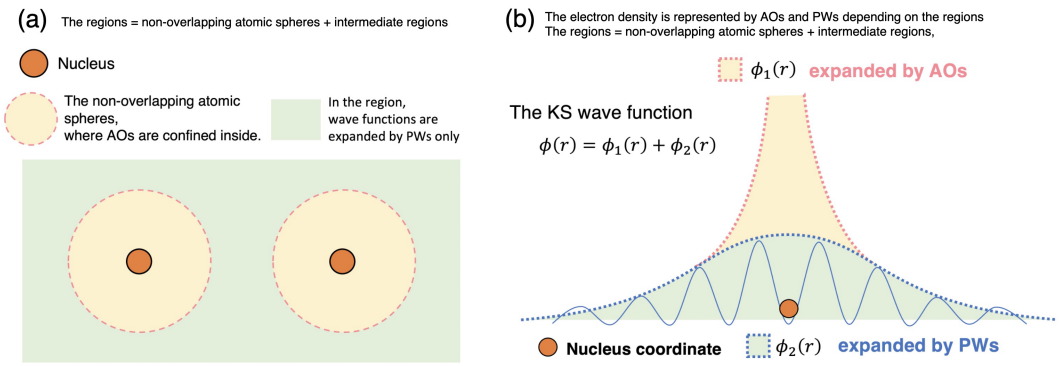

FIGURE 2.3: (a) The schematic two regions, composed of the non-overlapping atomic spheres and the interatomic regions. In the non-overlapping atomic sphere, the wave function is represented by the linear combination of AOs and PWs. On the other hand, in the interatomic region, the wave function is expanded by PWs only. (b) The true wave function is represented by both yellow region and green region. In yellow region, the wave function is represented by AOs and in green region, the wave function is represented by PWs. Therefore, this separation treatment says that the wave function is represented by AOs and PWs in the non-overlapping atomic spehere and the wave function in the regions except non-overlapping atomic sphere is represented by PWs only.

each atom, $\boldsymbol{r}_j = \boldsymbol{r} - \boldsymbol{R}_j$, $\hat{\boldsymbol{r}}_j = \boldsymbol{r}_j / r_j$, $\boldsymbol{R}_j$ denotes nucleus coordinate, Ω is the volume of the unit cell, $\boldsymbol{G}$ is reciprocal lattice vector. Here j, n, l, and m are atomic species, principal quantum number, angular momentum quantum number, and magnetic quantum number, respectively. In our code, TOMBO[1, 17, 40–45], the atomic wave function is composed of cubic harmonics instead of spherical harmonics and the matrix calculation is performed analytically. AOs describe the cusp-like behavior in the wave function near the nuclei. All AOs are confined inside the non-overlapping atomic spheres, which remove the computation of complicated overlap integrals between AOs centered at adjacent atoms (see Fig. 2.3)[17]. In our code, TOMBO, the numerical atomic orbital is obtained from the Herman-Skillman code. The Herman-Skillman code gives numerical atomic orbitals solving the Hartree-Fock equation self-consistently. Therefore, those numerical atomic orbitals include the screening effect partially, which means that the orbitals tend to be broader than the hydrogen-like orbitals.

2.4 Green's function theory

The first application of the Green's function technique in physics is introduced into quantum field theory[46, 47] and their applications are well known already[8, 48–53]. Recently, a method has been applied to condensed matter physics, *i.e.* strong correlation theory and first-principles calculation, mainly based on Hedin's method[6–8, 54]. The Green's function gives various information, excitation energies in many-body systems, ionization energy, transition density matrix, and polarizability and so on, without knowing the explicit wave function[7, 53–55]. Additionally, the Green's function approach is very convenient to give the one-particle picture in perturbation theory. In this chapter, I put brief explanations about the basic knowledge and general applications of the Green's function method and the Hedin's approach.

2.4.1 One- or two-particle Green's function

Originally, the Green's function is the concept appearing in mathematics (details in appendix A). Here, we focus on the Green's function appearing as a propagator in quantum field theory and condensed matter physics. There are a lot of great texts, reviews, and papers[7–9, 48, 50–55].

The one-particle Green's function for electron field (zero temperature) is defined by

$$G(1,2) = -i\langle\, \Psi_0^N \,|\, T\left[\psi(1)\psi^\dagger(2)\right] \,|\, \Psi_0^N \,\rangle \;;\; \langle\, \Psi_0^N \,|\, \Psi_0^N \,\rangle = 1, \tag{2.30}$$

where numbers are abbreviations for position and time coordinates, *i.e.* $i = (\boldsymbol{r}_i, t_i)$, $\psi(i)$ and $\psi^\dagger(i)$ denote electron annihilation and creation field Heisenberg operator, respectively,

$$\psi(i) = e^{+iHt_i}\psi(\boldsymbol{r}_i)e^{-iHt_i}, \tag{2.31a}$$
$$\psi^\dagger(i) = e^{+iHt_i}\psi^\dagger(\boldsymbol{r}_i)e^{-iHt_i}, \tag{2.31b}$$

in the Heisenberg representation, while $\psi(\boldsymbol{r}_i)$ and $\psi^\dagger(\boldsymbol{r}_i)$ electron annihilation and creation operator in the Schrödinger representation (notice that Eqs. (2.31) are no longer valid if $\partial H/\partial t \neq 0$). $T[\cdots]$ is Wick's time ordered product[56], and Ψ_0^N is the N-particle ground state as $H\,|\,\Psi_0^N\,\rangle = E_0^N\,|\,\Psi_0^N\,\rangle$, defined by Eq. (2.1). Wick's time ordered product is defined by

$$T\left[A_1(t_1)A_2(t_2)\right] = A_1(t_1)A_2(t_2)\Theta(t_1 - t_2) - A_2(t_2)A_1(t_1)\Theta(t_2 - t_1), \tag{2.32}$$

where A_i corresponds to an electron field operator, *i.e.* fermion operator, and Θ is the Heaviside's step function

$$\Theta(t_1 - t_2) = \begin{cases} 1 \;;\; t_1 - t_2 > 0 \\ 0 \;;\; t_1 - t_2 < 0 \end{cases}. \tag{2.33}$$

In the general Green's function method in classical quantum mechanics, it is helpful to suppose the time translational symmetry, *i.e.* G(1,2) depends only on the difference $t_1 - t_2$, for convenience

$$G(1,2) = G(\boldsymbol{r}_1, \boldsymbol{r}_2 | t_1 - t_2). \tag{2.34a}$$

Upon taking the time Fourier transformation, Eq. (2.34a) becomes

$$G(\boldsymbol{r}_1, \boldsymbol{r}_2|\omega) = \int d\tau\, G(\boldsymbol{r}_1, \boldsymbol{r}_2|\tau) e^{+i\omega\tau}. \tag{2.34b}$$

Equations (2.34) make any one-particle physical value $\langle A \rangle$ computable. Suppose that any one-particle physical operator like kinetic operator

$$A = \int d\boldsymbol{r}\, \psi^\dagger(\boldsymbol{r}) A(\boldsymbol{r}) \psi(\boldsymbol{r}), \tag{2.35}$$

which leads to

$$\begin{aligned}
\langle A \rangle &= \int d\boldsymbol{r} \langle\, \Psi_0^N \,|\, \psi^\dagger(\boldsymbol{r}) A(\boldsymbol{r}) \psi(\boldsymbol{r}) \,|\, \Psi_0^N \,\rangle \\
&= \int d\boldsymbol{r}_1 d\boldsymbol{r}_2 \delta(\boldsymbol{r}_1 - \boldsymbol{r}_2) \langle\, \Psi_0^N \,|\, \psi^\dagger(\boldsymbol{r}_2) A(\boldsymbol{r}_1) \psi(\boldsymbol{r}_1) \,|\, \Psi_0^N \,\rangle \\
&= -\int d\boldsymbol{r}_1 d\boldsymbol{r}_2\, \delta(\boldsymbol{r}_1 - \boldsymbol{r}_2) A(\boldsymbol{r}_1) \langle\, \Psi_0^N \,|\, T\left[\psi(\boldsymbol{r}_1 0) \psi^\dagger(\boldsymbol{r}_2 0^+)\right] \,|\, \Psi_0^N \,\rangle.
\end{aligned}$$

Using Eq. (2.30), $\langle A \rangle$ can be represented by the one-particle Green's function $G(\boldsymbol{r}_1, \boldsymbol{r}_2|0^-)$ in time space, where 0^- denotes a negative infinitesimal number,

$$\langle A \rangle = -i \int d\boldsymbol{r}_1 \boldsymbol{r}_2\, \delta(\boldsymbol{r}_1 - \boldsymbol{r}_2) A(\boldsymbol{r}_1) G(\boldsymbol{r}_1, \boldsymbol{r}_2|0^-). \tag{2.36a}$$

Here, please notice that $G(\boldsymbol{r}_1, \boldsymbol{r}_2|0^-) = G(\boldsymbol{r}_1 t, \boldsymbol{r}_2 t^+)$ because we suppose the time translational invariance. Owing to Eqs. (2.34), $\langle A \rangle$ can be represented also by $G(\boldsymbol{r}_1, \boldsymbol{r}_2|\omega)$ in ω space

$$\langle A \rangle = -i \int d\boldsymbol{r}_1 d\boldsymbol{r}_2 \int \frac{d\omega}{2\pi} \delta(\boldsymbol{r}_1 - \boldsymbol{r}_2) A(\boldsymbol{r}_1) G(\boldsymbol{r}_1, \boldsymbol{r}_2|\omega) e^{-i\omega 0^-}. \tag{2.36b}$$

From Eqs. (2.36), specifically electron density $n(r) = \psi^\dagger(r)\psi(r)$ becomes

$$\langle n(\boldsymbol{r}) \rangle = -iG(\boldsymbol{r}, \boldsymbol{r}|0^-) = \int \frac{d\omega}{2\pi} G(\boldsymbol{r}, \boldsymbol{r}|\omega) e^{-i\omega 0^-}. \tag{2.37}$$

Above discussion shows that if the one-particle Green's function is known, easily one-particle physical value is calculated. (Please notice that we do not explain the Green's function $G(k|\cdots)$ for wave number space because we do not focus on a homogeneous electron system, where G(1,2) depends on the difference $\boldsymbol{r}_1 - \boldsymbol{r}_2$, in this doctoral thesis.)

The two-particle Green's function[47] is defined, like the one-particle Green's function G Eq. (2.30), by

$$K(1,2;3,4) = -\langle\, \Psi_0^N \,|\, T\left[\psi(1)\psi(2)\psi^\dagger(4)\psi^\dagger(3)\right] \,|\, \Psi_0^N \,\rangle \;;\; \langle\, \Psi_0^N | \Psi_0^N \,| = \rangle 1. \tag{2.38}$$

Equation (2.38) can be applied to two-particle physical value in similar way of the one-particle Green's function, like Eqs. (2.36). Specifically, the electron-electron Coulomb interaction $E_{\text{int}} = \langle V \rangle$ can be calculated by the two-particle Green's function

$$E_{\text{int}} = \frac{1}{2} \int d\boldsymbol{r}_1 d\boldsymbol{r}_1 v(\boldsymbol{r}_1 - \boldsymbol{r}_2) K(\boldsymbol{r}_1 0, \boldsymbol{r}_2 0; \boldsymbol{r}_1 0^+, \boldsymbol{r}_2 0^+), \tag{2.39}$$

where also please notice that $K(\boldsymbol{r}_1 0, \boldsymbol{r}_2 0; \boldsymbol{r}_1 0^+, \boldsymbol{r}_2 0^+) = K(\boldsymbol{r}_1 t, \boldsymbol{r}_2 t; \boldsymbol{r}_1 t^+, \boldsymbol{r}_2 t^+)\ \forall t$, under time translational invariance. Equations (2.1), (2.36), and (2.39) show that total energy $E_{\text{total}} = \langle T \rangle + \langle U \rangle + \langle V \rangle$ is

$$\begin{aligned} E_{\text{total}} = -i \int d\boldsymbol{r}_1 d\boldsymbol{r}_2 \delta(\boldsymbol{r}_1 - \boldsymbol{r}_2) \left(T(\boldsymbol{r}_1) + U_{\text{ext}}(\boldsymbol{r}_1) \right) G(\boldsymbol{r}_1, \boldsymbol{r}_2 | 0^-) \\ + \frac{1}{2} \int d\boldsymbol{r}_1 d\boldsymbol{r}_1 v(\boldsymbol{r}_1 - \boldsymbol{r}_2) K(\boldsymbol{r}_1 0, \boldsymbol{r}_2 0; \boldsymbol{r}_1 0^+, \boldsymbol{r}_2 0^+). \end{aligned} \tag{2.40}$$

Above discussion implies that the Green's function has a lot of information related to one- and two-particle behaviors. Therefore, if the Green's function is known, we can know various physical properties. As one of the famous examples, the spectral function (which is observed in photoemission and inverse photoemission) is calculated by the Green's function. In order to explain the spectral function, we need to explain quasiparticle wave functions (QPWFs) and quasiparticle (QP) energies, and I put the details in latter section. Spectral function $A(r_1, r_2|\omega)$ in frequency space is related with the one-particle Green's function $G(r_1, r_2|\omega)$ as follows

$$\text{Re}\left(G(\boldsymbol{r}_1, \boldsymbol{r}_2|\omega)\right) = P \int d\omega' \frac{A(\boldsymbol{r}_1, \boldsymbol{r}_2|\omega')}{\omega' - \omega}, \tag{2.41a}$$

$$\text{Im}\left(A(\boldsymbol{r}_1, \boldsymbol{r}_2|\omega)\right) = -\frac{1}{\pi} \text{Im}\left(G(\boldsymbol{r}_1, \boldsymbol{r}_2|\omega)\right) \text{sgn}(\omega - \mu), \tag{2.41b}$$

where $\text{P} \int \cdots$ denotes Cauchy principal value, μ is a chemical potential, and sgn is the sign function defined by

$$\text{sgn}(x) = \Theta(x) - \Theta(-x). \tag{2.42}$$

Spectral function is represented by QPWFs and plays an important role for Lehmann representation, which is used in self-consistent GW approach[57, 58].

2.4.2 Dyson equation

Section 2.4.1 explains that the Green's function gives one- or two-particle information and leads to easy calculations of various physical values. Here, we have to consider a method to obtain the Green's function in actual calculations.

Consider the Heisenberg equation of motion for electron annihilation operator

$$\begin{aligned} i\frac{\partial}{\partial t_1}\psi(1) &= [\psi(1), H] \\ &= h(1)\psi(1) + \int d3v(1,3)\psi^\dagger(3)\psi(3)\psi(1), \end{aligned} \tag{2.43}$$

where H is represented by

$$H = \int d\boldsymbol{r}\psi^\dagger(\boldsymbol{r})h(\boldsymbol{r})\psi(\boldsymbol{r}) + \frac{1}{2}\int d\boldsymbol{r}_1 d\boldsymbol{r}_2 v(\boldsymbol{r}_1 - \boldsymbol{r}_2)\psi^\dagger(\boldsymbol{r}_1)\psi^\dagger(\boldsymbol{r}_2)\psi(\boldsymbol{r}_2)\psi(\boldsymbol{r}_1), \tag{2.44}$$

where $h(\boldsymbol{r}) = T(\boldsymbol{r}) + U_{\text{ext}}(\boldsymbol{r})$ is one-electron operator; $T(\boldsymbol{r}) = -\nabla^2/2$ is kinetic energy and $U_{\text{ext}}(\boldsymbol{r})$ is external potential, and anti-commutation of electron field operators are used

$$\left[\psi(\boldsymbol{r}_1), \psi^\dagger(\boldsymbol{r}_2)\right]_+ = \delta(\boldsymbol{r}_1 - \boldsymbol{r}_2), \tag{2.45a}$$

$$\left[\psi(\boldsymbol{r}_1), \psi(\boldsymbol{r}_2)\right]_+ = 0, \tag{2.45b}$$

$$\left[\psi(\boldsymbol{r}_1)^\dagger, \psi^\dagger(\boldsymbol{r}_2)\right]_+ = 0, \tag{2.45c}$$

and $v(1,3) = v(\boldsymbol{r}_1 - \boldsymbol{r}_3)\delta(t_1 - t_3)$ is introduced. Multiplying $\psi^\dagger(2)$ by both sides of Eq. (2.43) and taking Wick's time ordered and inner product with ground state Ψ_0^N for Eq. (2.44), we obtain a governing equation composed of the one-particle Green's function G and the two-particle Green's function K

$$i\frac{\partial}{\partial t_1}G(1,2) - h(\boldsymbol{r})G(1,2) + i\int d3v(1,3)K(1,3^-;2,3^+) = \delta(1,2), \tag{2.46}$$

where $\delta(1,2) = \delta(\boldsymbol{r}_1 - \boldsymbol{r}_2)\delta(t_1 - t_2)$ and the following relation is used[48],

$$T\left[\frac{\partial}{\partial t_1}\psi(1)\psi^\dagger(2)\right] = \frac{\partial}{\partial t_1}T\left[\psi(1)\psi^\dagger(2)\right] - \delta(1,2).$$

Here, we have to notice that there are several time orders for the two-particle Green's function as follows

$$\int d3\; v(1,3)T\left[\psi^\dagger(3^+)\psi(3^-)\psi(1)\psi^\dagger(2)\right] \tag{2.47a}$$

$$= \int d3\; v(1,3)T\left[\psi^\dagger(3^+)\psi(3)\psi(1^-)\psi^\dagger(2)\right] \tag{2.47b}$$

$$= \int d3\; v(1,3)T\left[\psi^\dagger(3^{++})\psi(3^+)\psi(1)\psi^\dagger(2)\right] \tag{2.47c}$$

$$= \int d3\; v(1,3)T\left[\psi^\dagger(3^+)\psi(3)\psi(1^+)\psi^\dagger(2)\right] \tag{2.47d}$$

$$= \int d3\; v(1^+,3)T\left[\psi^\dagger(3^+)\psi(3)\psi(1)\psi^\dagger(2)\right] \tag{2.47e}$$

$$= \int d3\; v(1,3^-)T\left[\psi^\dagger(3^+)\psi(3)\psi(1)\psi^\dagger(2)\right]. \tag{2.47f}$$

The expression used for discussion depends on papers, and there are still other representations. In order to make Eq. (2.46) solvable self-consistently, introduction of the following integral transformation is important

$$\int d3\Sigma(1,3)G(3,2) = -i\int d3v(1,3)K(1,3^-;2,3^+). \tag{2.48}$$

This integral kernel Σ is called self-energy, and the main difficulty in the Green's function approach is how to obtain the practical form of this kernel. Substitute Eq. (2.48) into Eq. (2.46), we obtain

$$i\frac{\partial}{\partial t_1}G(1,2) - h(\boldsymbol{r}_1)G(1,2) - \int d3\Sigma(1,3)G(3,2) = \delta(1,2), \tag{2.49a}$$

which is called Dyson equation in differential form in time space. Also, taking time Fourier transformation to Eq. (2.49a) gives

$$\omega G(\boldsymbol{r}_1,\boldsymbol{r}_2|\omega) - h(\boldsymbol{r}_1)G(\boldsymbol{r}_1,\boldsymbol{r}_2|\omega) - \int d\boldsymbol{r}_3\Sigma(\boldsymbol{r}_1,\boldsymbol{r}_3|\omega)G(\boldsymbol{r}_3,\boldsymbol{r}_2|\omega) = \delta(\boldsymbol{r}_1-\boldsymbol{r}_2), \tag{2.49b}$$

which is called Dyson equation in the frequency space, and the time Fourier transformation for the self-energy is introduced like the one-particle Green's function

$$\Sigma(\boldsymbol{r}_1,\boldsymbol{r}_2|t_1-t_2) = \int \frac{d\omega}{2\pi}\Sigma(\boldsymbol{r}_1,\boldsymbol{r}_2|\omega)e^{-i\omega(t_1-t_2)}. \tag{2.50}$$

Using Eqs. (2.40) and (2.48), electron-electron Coulomb interaction E_{int} is

$$E_{\text{int}} = +\frac{i}{2}\int d(12)\Sigma(1,2)G(2,1^+), \tag{2.51a}$$

which is also represented by

$$E_{\text{int}} = +\frac{i}{2}\int d\boldsymbol{r}_1 d\boldsymbol{r}_2\frac{d\omega}{2\pi}\Sigma(\boldsymbol{r}_1,\boldsymbol{r}_2|\omega)G(\boldsymbol{r}_2,\boldsymbol{r}_1|\omega)e^{+i\omega 0^+}. \tag{2.51b}$$

These E_{int} representations with self-energy are called Galitskii-Migdal formula[48]. Then, we can easily calculate the total energy with the one-particle Green's function[48]

$$E_{\text{total}} = -i\int d(12)\left[\delta(1,2)h(1) - \frac{1}{2}\Sigma(2,1)\right]G(1,2^+). \tag{2.52}$$

Classically, there are two trends in the Green's function approach studies[53]; one is based on the Heisenberg equation of motion and another is many-body perturbation theory (MBPT) relying on Gell-Mann& Low's adiabatic theorem and Wick's theorem for zero temperature (Bloch-Dominics theorem for finite temperature)[56, 59–61]. MBPT is currently the dominant approach because it is very difficult to obtain the self-energy based on the Heisenberg equation of motion[6, 52, 62, 63]. In MBPT, self-energy $\Sigma(1,2)$ is divided into Hartree term $v_H(1)\delta(1,2)$ and mass term $M(1,2)$ for convenience

$$M(1,2) = +i\int d(34)G(1,3)W(1^+,4)\widetilde{\Gamma}(3,2;4). \tag{2.53}$$

In this doctoral thesis, in order to distinguish between self-energy and self-energy except the Hartree term, Σ is called the self-energy and M is treated as the self-energy except the Hartree term, which is called mass term to avoid confusion. W denotes

dynamically screened Coulomb interaction defined by

$$W(1,2) = \int d3\, \epsilon^{-1}(1,3)v(3,2), \tag{2.54}$$

where ϵ^{-1} denotes the inverse (longitudinal) dielectric matrix. The inverse dielectric matrix is calculated by

$$\epsilon^{-1}(1,2) = \delta(1,2) + \int d(34)v(1,3)\widetilde{\chi}(3,2), \tag{2.55}$$

where $\widetilde{\chi}$ denotes the (irreducible) polarizability. In actual calculation, ϵ^{-1} is obtained by Adler-Wiser's pertubative random-phase approximation[64, 65] or using the following relation, $\epsilon(k)^{-1} = \epsilon^{-1}(k)$ for homogeneous system. Also, substituting Eq. (2.55) into Eq. (2.54), we understand that the dynamically screened Coulomb interaction satisfies the following integral equation

$$W(1,2) = v(1,2) + \int d(34)W(1,3)\widetilde{\chi}(3,4)v(4,2), \tag{2.56}$$

and (irreducible) polarizability is defined by

$$\widetilde{\chi}(1,2) = -iG(1,3)G(4,1^+)\widetilde{\Gamma}(3,4;2). \tag{2.57}$$

$\widetilde{\Gamma}$ denotes scalar (irreducible) vertex function defined by the following integral equation

$$\widetilde{\Gamma}(1,2;3) = \delta(1,2)\delta(2,3) + \int d(4567)\, \frac{\delta M(1,2)}{\delta G(4,5)} G(4,6)G(7,5)\widetilde{\Gamma}(6,7;3). \tag{2.58}$$

From Eqs. (2.49), we obtain the inverse Green's function $G^{-1}(1,3)$, satisfying

$$\int d3 G^{-1}(1,3)G(3,2) = \delta(1,2), \tag{2.59}$$

and analytically defined by

$$G^{-1}(1,3) = \left(i\frac{\partial}{\partial t_1} - h(1)\right)\delta(1,3) - \Sigma(1,3), \tag{2.60}$$

Suppose the non-interacting Green's function G_0^{-1} satisfying

$$\int d3\, G_0^{-1}(1,3)G_0(3,2) = \left(i\frac{\partial}{\partial t_1} - h(1)\right) G_0(1,2) = \delta(1,2). \tag{2.61}$$

Combining Eqs. (2.60) and (2.61) shows that the Dyson equation (2.49a) is

$$\int d3 \left(G_0^{-1}(1,3) - \Sigma(1,3)\right) G(3,2) = \delta(1,2), \tag{2.62}$$

which gives that

$$G(1,2) = G_0(1,2) + \int d(34)G_0(1,3)\Sigma(3,4)G(4,2). \tag{2.63}$$

This is also the Dyson equation. These Eqs. (2.53), (2.56), (2.57), (2.58), and (2.63) are represented by Fig. 2.4 (a), (b), (c), (d), and (e), respectively. These 5 coupled equa-

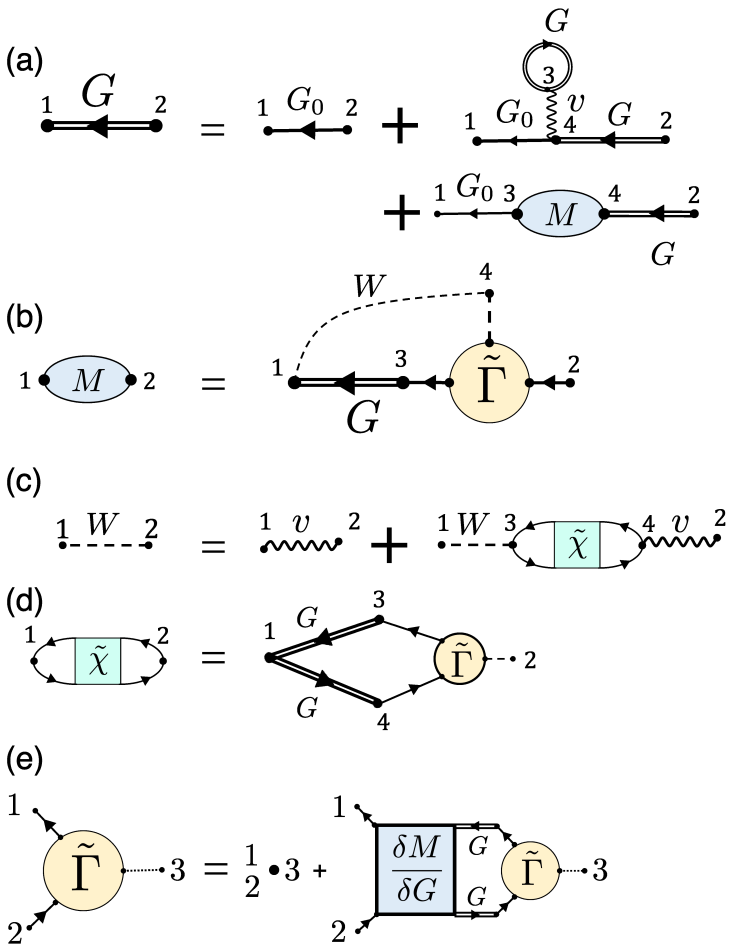

FIGURE 2.4: Hedin's coupling 5 equations represented by Feynman diagram[7].

tions are introduced by Hedin (1965)[6] and solved self-consistently like Fig. 2.5. We have to notice that it is very difficult to solve the 5 coupled equations self-consistently. so the GW approximation has great meaning in this Hedin's calculation, and that brief explanation for GW approximation is put in the next subsection[6–9, 54, 58, 66].

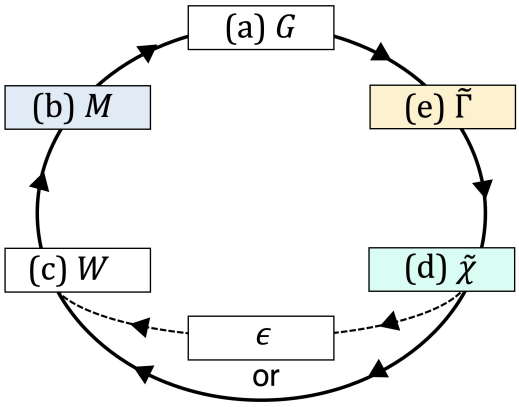

FIGURE 2.5: Flow chart to solve the Hedin's 5 coupled equations self-consistenly

2.4.3 GW approximation

GW approximation makes the Hedin's coupled equations solvable, and actually gives good agreement with experimental results[6–9, 14, 18–21, 54, 58, 66]. The difficulty to solve Hedin's 5 coupled equations self-consistently is accompanied in the vertex function $\widetilde{\Gamma}$. Hedin introduced the approximation for $\widetilde{\Gamma}$ as[6, 54]

$$\widetilde{\Gamma}(1,2;3) \simeq \delta(1,2)\delta(2,3), \tag{2.64}$$

which corresponds to neglect the second term in Eq. (2.58) and reduces the Hedin's 5 coupled equations into 4 coupled simple equations

$$G(1,2) = G_0(1,2) + \int d(34) G_0(1,3)\Sigma(3,4)G(4,2), \tag{2.65a}$$

$$M(1,2) = +iG(1,2)W(1^+,2), \tag{2.65b}$$

$$W(1,2) = v(1,2) + \int d(34) W(1,3)\widetilde{\chi}(3,4)v(4,2), \tag{2.65c}$$

$$\widetilde{\chi}(1,2) = -iG(1,2)G(2,1^+). \tag{2.65d}$$

Here please notice that $\Sigma(1,2) = \delta(1,2)v_H(1) + M(1,2)$. The form of Eq. (2.65b) is symbolically GW, that is why this approximation is called GW approximation. GW approximation neglects the calculation step for $\widetilde{\Gamma}$ part (e) in Fig. 2.5. This simple approximation leads to more reasonable calculations compared with the full Hedin's 5 coupled equations approach. In terms of computational cost, the GW approaches are preferred in a lot of previous papers and shows the great successes.

2.4.4 Baym-Kadanoff's conservation law

As another approach to obtain a self-energy form in MBPT, Baym-Kadanoff's conservation law is very famous method to give a good approximation form of the two-particle Green's function K[7, 67, 68]. In Baym and Kadanoff's original paper (1961)[67], there are three conditions in order to conserve macroscopic physical values; as examples, number, momentum, total angular momentum, and energy, and so on. Specifically, Baym and Kadanoff's three conditions are as follows

A. For a given approximate two-particle Green's function K, the approximate G satisfies both left- and right-eigenvalue equations, described later such as Eqs. (2.69).

B. The two-particle Green's function K satisfies the following symmetry

$$K(1,3;1^+,3^+) = K(3,1;3^+,1^+).$$

C. The two-particle effective interaction $\Xi = \delta M/\delta G$ satisfies the following symmetry

$$\Xi(1,2;3,4) = \Xi(2,1;4,3). \tag{2.66}$$

It is very important that mainly, if conditions (A) and (B) are satisfied, the one-particle Green's function G obtained from the Dyson equation satisfies all the conservation laws[67]. These three conditions proposed by Baym and Kadanoff (1961)[67] are equal to be one condition proposed by Baym (1962)[68]. Briefly, the equal condition proposed by Baym (1962) [68] is as follows

D. the self-energy has the $\langle \Phi-\text{derivable} \rangle$ representation

$$\Sigma(1,2) = \frac{\delta\Phi}{\delta G(2,1)}, \tag{2.67}$$

analogous to the Luttinger-Ward functional Φ[49, 69, 70] such as Fig. 2.6.

In MBPT, taking together from these diagram derived from Φ leads to the conservations of macroscopic physical values. In other respect, Eq. (2.67) guarantees that the left-Dyson equation

$$-i\frac{\partial}{\partial t_2}G(1,2) - h(2)G(1,2) - \int d3G(1,3)\bar{\Sigma}(3,2) = \delta(1,2), \tag{2.68}$$

and right-Dyson equation (2.49a) have the same self-energy kernel, $\Sigma = \bar{\Sigma}$[7]. For simplicity, it is useful to introduce the following abstract form in frequency space

$$(\omega - h - \Sigma(\omega))\, G(\omega) = 1, \tag{2.69a}$$
$$G(\omega)\, (\omega - h - \Sigma(\omega)) = 1, \tag{2.69b}$$

where $G(\boldsymbol{r}_1,\boldsymbol{r}_2|\omega) = \langle \boldsymbol{r}_1 \,|\, G(\omega) \,|\, \boldsymbol{r}_2 \rangle$[71]. These are the left- and right-eigenvalue problems in frequency space similar to conventional ones[26]. Equations (2.69) play important roles in my study[2] for the normalization of QPWFs, which leads to the extended Kohn-Sham equation.

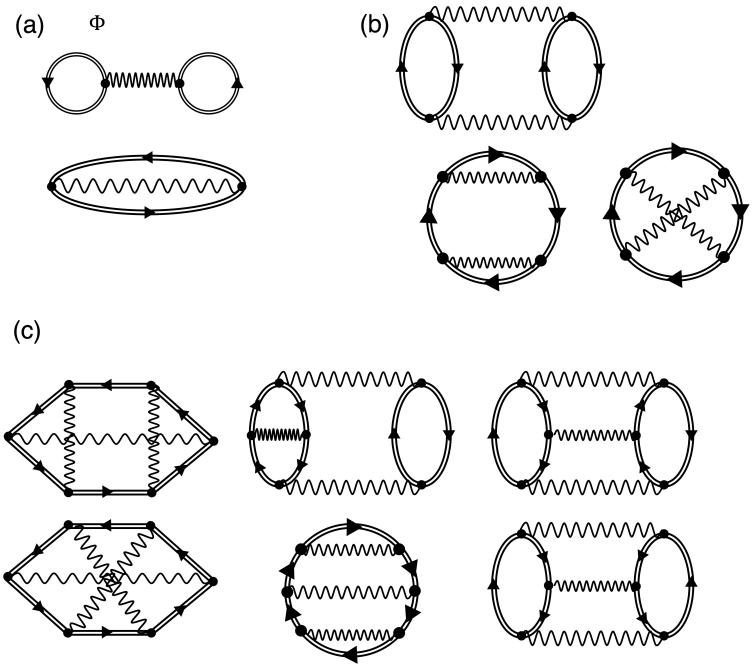

FIGURE 2.6: The functional Φ for Baym-Kadanoff's conservation law; (a), (b), and (c) is first, second, and third order terms on potential, respectively, example Φ diagram. Especially, (a) gives the Hartree-Fock diagrams.

2.4.5 Quasiparticle wave function

One of the advantages in the Green's function approach is that it can be used to calculate arbitrary physical quantities without explicit wave functions. But, of course, one can also introduce virtual single-particle wave functions, which is called QPWFs. QPWFs have two forms in the zero temperature Green's function approach.

$$\phi_\mu(1) = \langle\, \Psi_\mu^{N-1} \,|\, \psi(1) \,|\, \Psi_0^N \,\rangle, \tag{2.70a}$$
$$\phi_\nu(1) = \langle\, \Psi_0^N \,|\, \psi(1) \,|\, \Psi_\nu^{N+1} \,\rangle, \tag{2.70b}$$

where $\Psi_\lambda^{N\pm1}$ are eigenstates for $(N \pm 1)$-particle system, satisfying $H \,|\, \Psi_\mu^{N-1} \,\rangle = E_\mu^{N-1} \,|\, \Psi_\nu^{N-1} \,\rangle$ and $H \,|\, \Psi_\nu^{N+1} \,\rangle = E_\nu^{N+1} \,|\, \Psi_\nu^{N+1} \,\rangle$, and they denote occupied (occ) and emptied (emp) states, respectively (also, Eqs. (2.70b) and (2.70b) are called quasi-hole and quasi-electron, respectively). Because $\psi(1)$ is Heisenberg representation, Eqs. (2.70) become

$$\phi_\lambda(1) = \phi_\lambda(\boldsymbol{r}_1) e^{-i\varepsilon_\lambda t_1}, \tag{2.71}$$

where ϵ_λ denotes

$$\varepsilon_\mu = E_0^N - E_\mu^{N-1}, \tag{2.72a}$$
$$\varepsilon_\nu = E_\nu^{N+1} - E_0^N, \tag{2.72b}$$

together, and the suffix μ and ν denote occ and emp states respectively. QPWFs in position component are defined by

$$\phi_\mu(\boldsymbol{r}_1) = \langle\, \Psi_\mu^{N-1} \,|\, \psi(\boldsymbol{r}_1) \,|\, \Psi_0^N \,\rangle, \tag{2.73a}$$

$$\phi_\nu(\boldsymbol{r}_1) = \langle\, \Psi_0^N \,|\, \psi(\boldsymbol{r}_1) \,|\, \Psi_\nu^{N-1} \,\rangle. \tag{2.73b}$$

Using the commutation relation of electron creation and annihilation operators Eq. (2.45a), we can obtain the completeness represented by QPWFs[44],

$$\begin{aligned}
\delta(\boldsymbol{r}_1 - \boldsymbol{r}_2) &= \langle\, \Psi_0^N \,|\, [\psi(\boldsymbol{r}_1)\psi^\dagger(\boldsymbol{r}_2) + \psi^\dagger(\boldsymbol{r}_2)\psi(\boldsymbol{r}_1)] \,|\, \Psi_0^N \,\rangle \\
&= \sum_{\nu\in\text{emp}} \langle\, \Psi_0^N \,|\, \psi(\boldsymbol{r}_1) \,|\, \Psi_\nu^{N+1} \,\rangle \langle\, \Psi_\nu^{N+1} \,|\, \psi^\dagger(\boldsymbol{r}_2) \,|\, \Psi_0^N \,\rangle \\
&\qquad + \sum_{\mu\in\text{occ}} \langle\, \Psi_0^N \,|\, \psi^\dagger(\boldsymbol{r}_2) \,|\, \Psi_\mu^{N-1} \,\rangle \langle\, \Psi_\mu^{N-1} \,|\, \psi(\boldsymbol{r}_1) \,|\, \Psi_0^N \,\rangle \\
&= \sum_{\lambda\in\text{all}} \phi_\lambda(\boldsymbol{r}_1)\phi_\lambda^*(\boldsymbol{r}_2) \\
&= \sum_{\mu\in\text{occ}} \phi_\mu(\boldsymbol{r}_1)\phi_\mu^*(\boldsymbol{r}_2) + \sum_{\nu\in\text{emp}} \phi_\nu(\boldsymbol{r}_1)\phi_\nu^*(\boldsymbol{r}_2).
\end{aligned} \tag{2.74}$$

This equation is derived from the completeness condition in Fock space

$$1 + \sum_{N=1} \frac{1}{N!} \sum_i |\, \Psi_i^N \,\rangle\langle\, \Psi_i^N \,| \;= I_{\text{Fock}}\,;\; \langle\, \Psi_i^N \,|\, \Psi_{i'}^{N'} \,\rangle = \delta_{N,N'}\delta_{i,i'}, \tag{2.75}$$

where I_{Fock} denotes the identity operator for the Fock space. Equation (2.74) means that any state $|\, f \,\rangle$ in one-particle space is expanded by QPWFs, $|\, f \,\rangle = \sum_\lambda |\, \phi_\lambda \,\rangle\langle\, \phi_\lambda \,|\, f \,\rangle$, which are defined as $f(x) = \langle\, x \,|\, f \,\rangle$ and $\phi_\lambda(x) = \langle\, x \,|\, \phi_\lambda \,\rangle$. This interesting point is that $\{\phi_\lambda\}$ is not orthogonal each other due to the self-energy's dependent on QP energy, $\Sigma(\varepsilon_\lambda)$. Especially, the electron density matrix $\rho(1,2) = \langle\, \Psi_0^N \,|\, \psi^\dagger(2)\psi(1) \,|\, \Psi_0^N \,\rangle$ is represented by

$$\begin{aligned}
\rho(1,2) &= \langle\, \Psi_0^N \,|\, \psi^\dagger(2)\psi(1) \,|\, \Psi_0^N \,\rangle = \sum_{\mu\in\text{occ}} \langle\, \Psi_0^N \,|\, \psi^\dagger(2) \,|\, \Psi_\mu^{N-1} \,\rangle \langle\, \Psi_\mu^{N-1} \,|\, \psi(1) \,|\, \Psi_0^N \,\rangle \\
&= \sum_{\mu\in\text{occ}} \phi_\mu^*(2)\phi_\mu(1) = \sum_{\mu\in\text{occ}} \phi_\mu^*(\boldsymbol{r}_2)\phi_\mu(\boldsymbol{r}_1) e^{-i\varepsilon_\mu(t_1-t_2)},
\end{aligned} \tag{2.76}$$

which means that the electron density is represented by infinite number of occ QPWFs. (This requirement that the representation for the electron density needs the infinite number of occ QPWFs makes the QP calculation very difficult.)

The one-particle Green's function, Eq. (2.30), is represented by QPWFs

$$G(1,2) = -i\phi_\mu(\boldsymbol{r}_1)\phi_\mu(\boldsymbol{r}_2)e^{-i\varepsilon_\mu(t_1-t_2)}\Theta(t_1-t_2) + i\phi_\nu(\boldsymbol{r}_1)\phi_\nu(\boldsymbol{r}_2)e^{-i\varepsilon_\nu(t_1-t_2)}\Theta(t_2-t_1), \tag{2.77a}$$

and Eq. (2.34b) becomes

$$G(\boldsymbol{r}_1,\boldsymbol{r}_2|\omega) = \sum_\mu \frac{\phi_\mu(\boldsymbol{r}_1)\phi_\mu^*(\boldsymbol{r}_2)}{\omega - \epsilon_\mu - i0^+} + \sum_\nu \frac{\phi_\nu(\boldsymbol{r}_1)\phi_\nu^*(\boldsymbol{r}_2)}{\omega - \epsilon_\nu + i0^+}, \tag{2.77b}$$

where 0^+ is infinitesimal number. Using Eqs. (2.49b) and (2.77b), the residue around each QP energy like Fig. 2.7 gives the Dyson equation for each QPWF

$$h(\boldsymbol{r}_1)\phi_\lambda(\boldsymbol{r}_1) + \int d\boldsymbol{r}_3 \Sigma(\boldsymbol{r}_1,\boldsymbol{r}_2|\epsilon_\lambda)\phi_\lambda(\boldsymbol{r}_2) = \epsilon_\lambda\phi_\lambda(\boldsymbol{r}_1), \tag{2.78a}$$

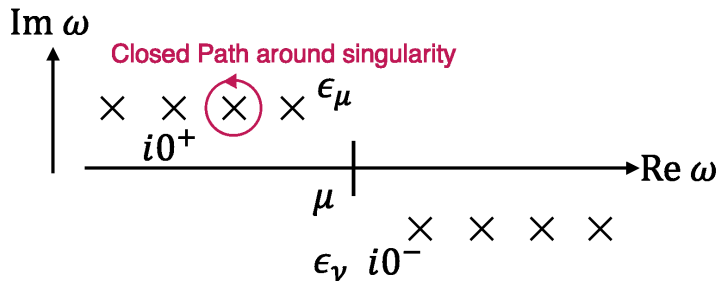

FIGURE 2.7: The residue around each QP energy in frequency space.

which is also called the QP equation. The KS wave functions and QPWFs are considered to be very similar, and generally the KS states are treated as initial states in actual QP calculations like Fig. 2.8[9, 14, 19, 20, 28]. The number of occ QPWFs obtained in such calculation is finite (which is equal to the electron number). This is in contradiction with the requirement that original QP theory has infinite number of occupied states (mathematically which is shown in Eq. (2.76) and the norms of the QPWFs are less than one $\langle \phi_\lambda \,|\, \phi_\lambda \rangle \leq 1$). The explanation for the norm of QPWFs is put in subsection 4.2.2.

As remarkable feature, the present study[2] proved that QPWFs also obey the left- and right-eigenvalue problems similar to conventional ones[26]. This requirement is very surprising and interesting. From Eq. (2.69b) in the same way, we obtain the left-eigenvalue problem

$$h(\boldsymbol{r}_2)\phi^*_\lambda(\boldsymbol{r}_2) + \int d\boldsymbol{r}_3 \phi^*_\lambda(\boldsymbol{r}_3)\Sigma(\boldsymbol{r}_3,\boldsymbol{r}_2|\varepsilon_\lambda) = \phi^*_\lambda(\boldsymbol{r}_2)\varepsilon_\lambda. \tag{2.78b}$$

Equations (2.78a) and (2.78b) look complicated, then it is helpful to introduce the abstract forms like Eq. (2.69) for simplicity

$$(h + \Sigma(\epsilon_\lambda)) \,|\, \phi_\lambda \rangle = \epsilon_\lambda \,|\, \phi_\lambda \rangle, \tag{2.79a}$$
$$\langle \phi_\lambda \,|\, (h + \Sigma(\epsilon_\lambda)) = \langle \phi_\lambda \,|\, \epsilon_\lambda. \tag{2.79b}$$

These left- and right-eigenvalue equations are very useful relation in various discussions and play important roles to derive the extended KS equation in my thesis; Takeru Nakashima, Hannes Raebiger, and Kaoru Ohno. "Normalization of exact quasiparticle wave functions in the Green's function method guaranteed by the Ward identity". *Physical Review B*, 104 20: L201116 (2021).[2]. The details for the extended KS equation are explained in chapter 4.

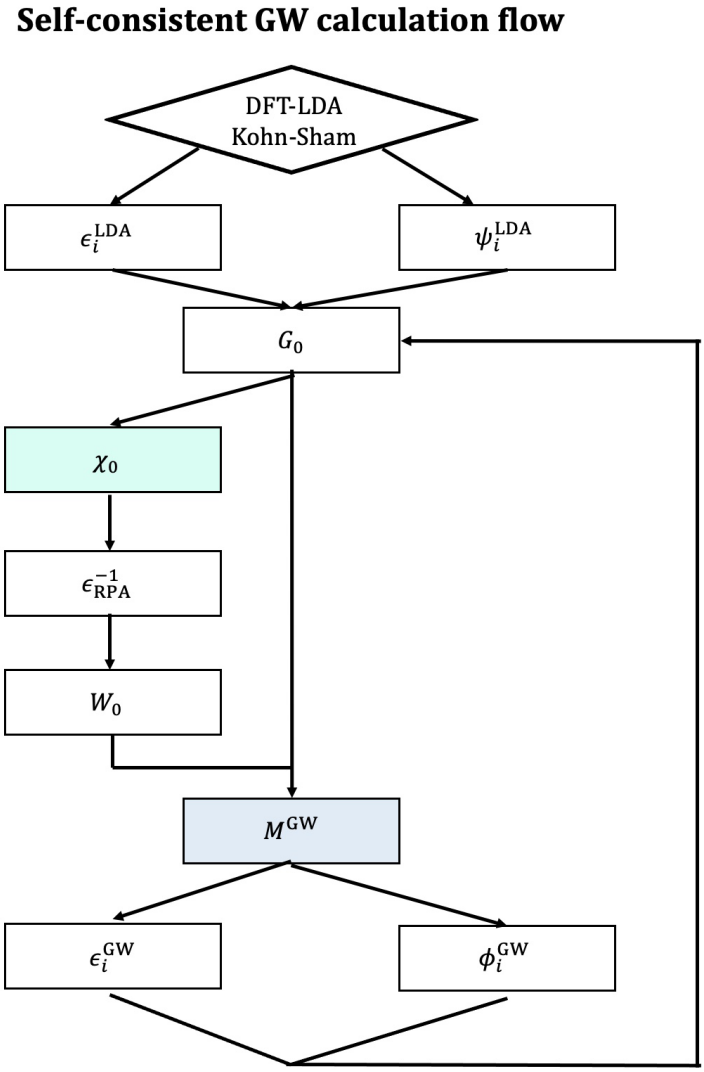

FIGURE 2.8: The example flow chart for the self-consistent GW calculation

Chapter 3

New method to calculate the SOC with AEMB

This chapter shows a new method to calculate the spin-orbit coupling (SOC) (see chapter 2.2) with all-electron mixed basis (AEMB) approach (see chapter 2.3), and this study is reported in the following paper; Takeru Nakashima and Kaoru Ohno. "Spin-Orbit Coupling in All-electron Mixed Basis Approach". *Annalen der Physik*, 531 9: 1900060 (2019).[1]. The SOC is the one of the relativistic effects derived from the Dirac equation, as explained in chapter 2[13]. The SOC splits band structures, which play important roles in spintronics devices[72, 73]. I tried to develop a new calculation method to improve difficulties of combining the quasiparticle (QP) theory and the SOC calculation, and hope that the present study will be useful for the active study in spintronics fields.

It is very difficult to include the SOC directly in the QP equation because even only the QP equation requires much more computational cost to solve. In order to avoid this computational difficulty, the present method makes use of the similarity between the quasiparticle wave functions (QPWFs) and Kohn-Sham (KS) orbitals[14, 15], that is, the SOC splitting is taken as perturbation and calculated by using KS orbitals. Their results are combined with results from QP theory.

In the framework of KS theory to calculate the SOC, there is the SOC form problems (which is already discussed in subsection 2.2). The exact Hamiltonian for the SOC is represented by Eq. (2.21)

$$H_{\mathrm{SOC}} = -\frac{1}{4c^2}\sigma\cdot(\boldsymbol{E}\times\boldsymbol{p}) = \frac{1}{2c^2}\boldsymbol{S}\cdot(\nabla V\times\boldsymbol{p}),$$

and under spherical symmetric approximation for the effective potential $V(\boldsymbol{r}-\boldsymbol{R}_n)\simeq V(|\boldsymbol{r}-\boldsymbol{R}_n|)$ in KS theory, H_{SOC} becomes

$$H_{\mathrm{SOC}} = \frac{1}{2c^2}\frac{1}{r}\frac{\partial V(r)}{\partial r}\boldsymbol{S}\cdot\boldsymbol{L}.$$

This equation is also represented by

$$H_{\mathrm{SOC}} = \frac{1}{2c^2}\frac{1}{r}\frac{\partial V(r)}{\partial r}\frac{1}{2}\left(S_+L_- + S_-L_+\right) + S_zL_z,$$

using the ladder operators defined in subsection 2.2. It is clear that Eqs. (2.24) are not valid in the intermediate space between nucleus (see Fig. 2.1).

In actual first-principles calculations, the choice of basis is very important problem, *i.e.*, atomic-like basis, free electron-like basis, or mixed basis. It is well known that atomic-like basis set is suitable for calculations of the target wave functions localizing around nucleus. Because of this property, the atomic-like basis set tends to

be applied to the isolated system. On the other hand, the free electron-like basis set is suitable for the target wave functions expanding in space, specifically like valence electrons related to bonds. Therefore, the free electron-like basis set tends to be applied to the crystal systems using pseudo-potentials. There are various basis choice problems, but I omit the details here because that is not main problem for the present study (the basis problem is explained briefly in subsection 2.3).

In my study, I try to take into account the SOC correction from both the core electrons around the nuclei and the valence electrons in the intermediate space among nuclei, using the AEMB. In the AEMB method, a spherical domain is set around each nucleus, and where the wave function is expressed in terms of both numerical atomic orbital and plane wave basis (see Eqs. (2.29) and section 2.3)

$$\phi_\lambda(\boldsymbol{r}) = \sum_{jnlm} c^{\mathrm{AO}}_{\lambda,jnlm}\phi^{\mathrm{AO}}_{jnlm}(\boldsymbol{r}-\boldsymbol{R}_j) + \frac{1}{\sqrt{\Omega}}\sum_{\boldsymbol{G}} c^{\mathrm{PW}}_{\lambda,\boldsymbol{G}} e^{i\boldsymbol{G}\cdot\boldsymbol{r}}, \tag{3.1a}$$

$$= \sum_{jnlm} c^{\mathrm{AO}}_{\lambda,jnlm} R_{nl}(r_j) Y_{lm}(\hat{\boldsymbol{r}}_j) + \frac{1}{\sqrt{\Omega}}\sum_{\boldsymbol{G}} c^{\mathrm{PW}}_{\lambda,\boldsymbol{G}} e^{i\boldsymbol{G}\cdot\boldsymbol{r}}, \tag{3.1b}$$

where $R_{nl}(\boldsymbol{r}_j)$ and $Y_{lm}(\hat{\boldsymbol{r}}_j)$ are the radial function and the spherical harmonics of each atom, $\boldsymbol{r}_j = \boldsymbol{r} - \boldsymbol{R}_j$, $\hat{\boldsymbol{r}}_j = \boldsymbol{r}_j/r_j$, $\boldsymbol{R}_j$ denotes nucleus coordinate, Ω is the volume of the unit cell, $\boldsymbol{G}$ is reciprocal lattice vector. Here j, n, l, and m are atomic species, principal quantum number, angular momentum quantum number, and magnetic quantum number, respectively. Outside the spherical domain, the wave function is represented in the plane wave basis only

$$\phi_\lambda(\boldsymbol{r}) = \frac{1}{\sqrt{\Omega}}\sum_{\boldsymbol{G}} c^{\mathrm{PW}}_{\lambda,\boldsymbol{G}} e^{i\boldsymbol{G}\cdot\boldsymbol{r}}. \tag{3.2}$$

This method is very suitable for the calculation of the SOC, which incorporates the asymmetry of the nuclear potential (see Figs. 2.1-2.3). For the atomic orbital basis in the spherical domain around each nucleus, the SOC representation matrix is calculated from Eq. (2.24), and the SOC representation for plane wave basis is calculated from Eq. (2.21). In the following, I explain the formulation to calculate these SOC matrices, how to get the final results, and the agreement of the calculation results with the experimental results.

3.1 Spin-orbit coupling in Kohn-Sham theory

The original spin-orbit coupling (SOC) in the one-electron Hamiltonian is expressed by Eq. (2.21). In the all-electron mixed basis (AEMB) approach, atomic orbitals (AOs) are well localized inside the non-overlapping atomic sphere, where the potential around the j-th atom can be regarded as spherically symmetric, $V_j(r_j)$, to a very good approximation (see Figs. 2.1-2.3). Then, the electric field can be expressed as

$$\boldsymbol{E} = -\nabla V_j = -\frac{\boldsymbol{r}_j}{r_j}\frac{dV_j}{dr_j},$$

where $\boldsymbol{r}_j = \boldsymbol{r} - \boldsymbol{R}_j$ denotes the electron coordinate around the nuclear position $\boldsymbol{R}_j$. Therefore, using the angular momentum $\boldsymbol{L} = \boldsymbol{r}_j \times \boldsymbol{p}$, we can rewrite Eq. (2.21) as

$$H_{\mathrm{SOC}} = \frac{1}{2c^2}\frac{1}{r_j}\frac{dV_j}{dr_j}\boldsymbol{S}\cdot\boldsymbol{L}. \tag{3.3}$$

In the AEMB approach, the Kohn-Sham (KS) wave function of the λ-th level is expressed as

$$\varphi_\lambda(\boldsymbol{r}) = \frac{1}{\sqrt{\Omega}}\sum_{\boldsymbol{G}} c_{\boldsymbol{G}}^{\lambda} e^{i\boldsymbol{G}\cdot\boldsymbol{r}} + \sum_{jnlm} c_{jnlm}^{\lambda}\sum_{nlm} R_{nl}(r_j)K_{lm}(\hat{\boldsymbol{r}}_j) \tag{3.4a}$$

$$= \sum_{\boldsymbol{G}} c_{\boldsymbol{G}}\langle\, \boldsymbol{r} \,|\, \boldsymbol{G}\,\rangle + \sum_{jnlm} c_{jnlm}\langle\, \boldsymbol{r} \,|\, jnlm\,\rangle, \tag{3.4b}$$

where Ω is the volume of the unit cell, $c_{\boldsymbol{G}}^{\lambda}$ and c_{jnlm}^{λ} are the expansion coefficients, $\boldsymbol{G}$ is the reciprocal lattice vector, and $R_{nl}(r_j)$ and $K_{lm}(\hat{\boldsymbol{r}}_j)$ represent, respectively, the numerical radial function in logarithmic mesh and the (angular part) cubic harmonics constituting the AO.

In my study, for simplicity, the local density approximation (LDA) is applied to Eq. (2.20), which leads to

$$\frac{\delta E_{xc}[n]}{\delta n(\boldsymbol{r})} = \epsilon_{xc}(n(\boldsymbol{r})) + \frac{\partial \epsilon_{xc}(n(\boldsymbol{r}))}{\partial n(r)} n(\boldsymbol{r}), \tag{3.5}$$

in Eq. (2.19). The effective KS potential V is defined by

$$V(\boldsymbol{r}) = \int d\boldsymbol{r}' v(\boldsymbol{r}-\boldsymbol{r}')n(\boldsymbol{r}') + U_{\mathrm{ext}}(\boldsymbol{r}) + \epsilon_{xc}(n(\boldsymbol{r})) + \frac{\partial \epsilon_{xc}(n(\boldsymbol{r}))}{\partial n(r)} n(\boldsymbol{r}), \tag{3.6}$$

and the KS equation is represented by a simple form

$$\left(-\frac{1}{2}\nabla^2 + V(\boldsymbol{r})\right)\phi_i(\boldsymbol{r}) = \varepsilon_i\phi_i(\boldsymbol{r}). \tag{3.7}$$

Additionally, actual calculations in the present study are performed by using the following Hamiltonian

$$H_{\mathrm{KS}} = H_0 + H_{\mathrm{SOC}}, \tag{3.8a}$$

$$H_0 = -\frac{1}{2}\nabla^2 + V(\boldsymbol{r}) - \frac{\boldsymbol{p}^4}{8c^2} + \frac{1}{8c^2}\Delta V(\boldsymbol{r}). \tag{3.8b}$$

The present calculation takes the SOC Hamiltonian as perturbation.

3.1.1 SOC matrix calculated from spin states

In KS theory, for spin polarized system, KS effective potential V is dependent on spin states[5]. In order to calculate the SOC by this spin dependent potential, we calculate the SOC matrix defined by spin states as follows

$$\begin{aligned} H_{\mathrm{SOC}} &= \frac{1}{4c^2}\boldsymbol{S}\cdot\Big\{\nabla(V_\uparrow+V_\downarrow)\times\boldsymbol{p}\Big\}+\frac{1}{8c^2}\Big(\sigma_z\boldsymbol{S}+\boldsymbol{S}\sigma_z\Big)\cdot\Big\{\nabla(V_\uparrow-V_\downarrow)\times\boldsymbol{p}\Big\} \\ &= \frac{1}{4c^2}\boldsymbol{S}\cdot\Big\{\nabla(V_\uparrow+V_\downarrow)\times\boldsymbol{p}\Big\} \\ &+\frac{1}{8c^2}\Big(\,|\uparrow\rangle\langle\uparrow|\boldsymbol{S}-|\downarrow\rangle\langle\downarrow|\boldsymbol{S}+\boldsymbol{S}|\uparrow\rangle\langle\uparrow|-\boldsymbol{S}|\downarrow\rangle\langle\downarrow|\,\Big)\cdot\Big\{\nabla(V_\uparrow-V_\downarrow)\times\boldsymbol{p}\Big\}. \end{aligned} \tag{3.9}$$

Thus we have

$$\langle\uparrow|H_{\mathrm{SOC}}|\uparrow\rangle=\frac{1}{2c^2}\langle\uparrow|\boldsymbol{S}|\uparrow\rangle\cdot\Big\{\nabla V_\uparrow\times\boldsymbol{p}\Big\}, \tag{3.10a}$$

$$\langle\uparrow|H_{\mathrm{SOC}}|\downarrow\rangle=\frac{1}{4c^2}\langle\uparrow|\boldsymbol{S}|\downarrow\rangle\cdot\Big\{\nabla(V_\uparrow+V_\downarrow)\times\boldsymbol{p}\Big\}, \tag{3.10b}$$

$$\langle\downarrow|H_{\mathrm{SOC}}|\uparrow\rangle=\frac{1}{4c^2}\langle\downarrow|\boldsymbol{S}|\uparrow\rangle\cdot\Big\{\nabla(V_\uparrow+V_\downarrow)\times\boldsymbol{p}\Big\}, \tag{3.10c}$$

$$\langle\downarrow|H_{\mathrm{SOC}}|\downarrow\rangle=\frac{1}{2c^2}\langle\downarrow|\boldsymbol{S}|\downarrow\rangle\cdot\Big\{\nabla V_\downarrow\times\boldsymbol{p}\Big\}. \tag{3.10d}$$

For spherical potential for AOs defined inside the non-overlapping sphere, $\nabla V_\sigma\times\boldsymbol{p}$ can be replaced by $(1/r)(dV_\sigma/dr)\boldsymbol{L}$, and Eqs. (3.10a)-(3.10d) become

$$\langle\uparrow|H_{\mathrm{SOC}}|\uparrow\rangle=\frac{1}{2c^2}\langle\uparrow|\boldsymbol{S}|\uparrow\rangle\cdot\boldsymbol{L}\,\frac{1}{r}\frac{dV_\uparrow}{dr}, \tag{3.11a}$$

$$\langle\uparrow|H_{\mathrm{SOC}}|\downarrow\rangle=\frac{1}{4c^2}\langle\uparrow|\boldsymbol{S}|\downarrow\rangle\cdot\boldsymbol{L}\,\frac{1}{r}\frac{d}{dr}(V_\uparrow+V_\downarrow), \tag{3.11b}$$

$$\langle\downarrow|H_{\mathrm{SOC}}|\uparrow\rangle=\frac{1}{4c^2}\langle\downarrow|\boldsymbol{S}|\uparrow\rangle\cdot\boldsymbol{L}\,\frac{1}{r}\frac{d}{dr}(V_\uparrow+V_\downarrow), \tag{3.11c}$$

$$\langle\downarrow|H_{\mathrm{SOC}}|\downarrow\rangle=\frac{1}{2c^2}\langle\downarrow|\boldsymbol{S}|\downarrow\rangle\cdot\boldsymbol{L}\,\frac{1}{r}\frac{dV_\downarrow}{dr}. \tag{3.11d}$$

This treatment corresponds to the use of an averaged potential $(V_\uparrow+V_\downarrow)/2$ for the calculation of the off-diagonal terms in terms of spin states. There are three kinds of matrix elements for the SOC hamiltonian, PW-PW, PW-AO and AO-AO, to be calculated. Each calculation method for these kinds of matrix is explained next three subsections.

3.1.2 SOC matrix calculated from basis; PW-PW

The PW-PW matrix is calculated as follows

$$\begin{aligned}\langle \mathbf{G}, s_z \,|\, H_{SOC} \,|\, \mathbf{G}', s_z' \rangle &= \langle \boldsymbol{G}, s_z \,|\, \frac{1}{2c^2} \boldsymbol{S} \cdot (\nabla V \times \boldsymbol{p}) \,|\, \boldsymbol{G}', s_z' \rangle \\ &= \frac{1}{2c^2} \langle \boldsymbol{G}, s_z \,|\, \boldsymbol{S} \cdot (\nabla V \times \boldsymbol{p}) \,|\, \boldsymbol{G}', s_z' \rangle \\ &= \frac{1}{2c^2} \langle \boldsymbol{G} \,|\, (\nabla V \times \boldsymbol{p}) \,|\, \boldsymbol{G}' \rangle \cdot \langle s_z' \,|\, \boldsymbol{S} \,|\, s_z' \rangle, \end{aligned} \tag{3.12}$$

where $|\, \boldsymbol{G}, s_z \,\rangle$ denotes the direct product of the PW $|\, \boldsymbol{G} \,\rangle$ and the spin function $|\, s_z \,\rangle$ with the spin eigenvalue $s_z = \frac{1}{2}$ or $-\frac{1}{2}$. Since the potential is expanded in Fourier space as

$$V(\boldsymbol{r}) = \sum_{G''} \widetilde{V}_{G''} e^{iG'' \cdot \boldsymbol{r}}, \tag{3.13}$$

the PW-PW matrix elements can be identified to be

$$\langle \boldsymbol{G}, s_z \,|\, H_{\mathrm{SOC}} \,|\, \boldsymbol{G}', s_z' \rangle = \frac{i}{2c^2} \widetilde{V}_{\boldsymbol{G}-\boldsymbol{G}'} \langle s_z \,|\, \boldsymbol{S} \,|\, s_z' \rangle \cdot \left[\boldsymbol{G} \times \boldsymbol{G}' \right]. \tag{3.14}$$

Specifically, the PW-PW matrix depending on the spin eigenvalues is implemented into the code (TOMBO) as follows

(1) $s_z = s_z' = +\frac{1}{2}$

$$\langle \boldsymbol{G}, +\frac{1}{2} \,|\, H_{SOC} \,|\, \boldsymbol{G}', +\frac{1}{2} \rangle = i \frac{\widetilde{V}_{\boldsymbol{G}-\boldsymbol{G}'}}{4c^2} [\boldsymbol{G} \times \boldsymbol{G}']_z, \tag{3.15a}$$

(2) $s_z = s_z' = -\frac{1}{2}$

$$\langle \boldsymbol{G}, -\frac{1}{2} \,|\, H_{SOC} \,|\, \boldsymbol{G}', -\frac{1}{2} \rangle = -i \frac{\widetilde{V}_{\boldsymbol{G}-\boldsymbol{G}'}}{4c^2} [\boldsymbol{G} \times \boldsymbol{G}']_z, \tag{3.15b}$$

(3) $s_z = +\frac{1}{2}$, $s_z' = -\frac{1}{2}$

$$\langle \boldsymbol{G}, +\frac{1}{2} \,|\, H_{SOC} \,|\, \boldsymbol{G}', -\frac{1}{2} \rangle = i \frac{\widetilde{V}_{\boldsymbol{G}-\boldsymbol{G}'}}{4c^2} \left([\boldsymbol{G} \times \boldsymbol{G}']_x + \frac{1}{i} [\boldsymbol{G} \times \boldsymbol{G}']_y \right), \tag{3.15c}$$

(4) $s_z = -\frac{1}{2}$, $s_z' = +\frac{1}{2}$

$$\langle \boldsymbol{G}, +\frac{1}{2} \,|\, H_{SOC} \,|\, \boldsymbol{G}', -\frac{1}{2} \rangle = i \frac{\widetilde{V}_{\boldsymbol{G}-\boldsymbol{G}'}}{4c^2} \left([\boldsymbol{G} \times \boldsymbol{G}']_x - \frac{1}{i} [\boldsymbol{G} \times \boldsymbol{G}']_y \right), \tag{3.15d}$$

where the indices (x, y, z) represent the individual components. (Here, I assumed the spin unpolarized systems but the generalization to spin polarized systems is straightforward.)

3.1.3 SOC matrix calculated from basis; AO-AO

The SOC matrices (AO-AO, AO-PW) related to AOs are calculated by Eq. (3.3) and using the identity

$$\boldsymbol{S}\cdot\boldsymbol{L}=\frac{1}{2}(S_+L_-+S_-L_+)+S_zL_z, \tag{3.16}$$

which can be used for the spherical harmonics because AOs are well confined in the non-overlapping atomic sphere (this is explained in section 2.3). Here, $S_\pm = S_x \pm iS_y$ and $L_\pm = L_x \pm iL_y$ are ladder operators. From this expression Eq. (3.16), it is obvious that different l, l' pairs do not contribute,

$$\int Y^*_{lm}(\hat{\boldsymbol{r}}_j)\,(\boldsymbol{S}\cdot\boldsymbol{L})\,Y_{l'm'}(\hat{\boldsymbol{r}}_j)d\hat{\boldsymbol{r}}_j=\langle\, jlm\,|\,\boldsymbol{S}\cdot\boldsymbol{L}\,|\,jlm\,\rangle=0\;;\;l\neq l', \tag{3.17}$$

and it is only necessary to consider the matrix elements sandwiched with the same angular momentum quantum number l. The cubic harmonics K are defined as (here and hereafter we omit the suffix j)

$$K_{0,1}=Y_{0,0},\quad K_{11}=\frac{1}{\sqrt{2}}(Y_{1,1}-Y_{1,-1}),\quad K_{12}=\frac{i}{\sqrt{2}}(Y_{1,1}+Y_{1,-1}),\quad K_{13}=Y_{1,0}, \tag{3.18a}$$

$$K_{2,1}=\frac{1}{\sqrt{2}i}(Y_{2,2}-Y_{2,-2}),\quad K_{2,2}=\frac{1}{\sqrt{2}i}(Y_{2,1}-Y_{2,-1}),\quad K_{2,3}=\frac{1}{\sqrt{2}}(Y_{2,1}+Y_{2,-1}),$$
$$K_{2,4}=Y_{2,0},\quad K_{2,5}=\frac{1}{\sqrt{2}}(Y_{2,2}+Y_{2,-2}), \tag{3.18b}$$

$$K_{3,1}=\frac{1}{\sqrt{2}}(-Y_{3,2}+Y_{3,-2}),\quad K_{3,2}=\frac{1}{4}(-\sqrt{5}Y_{3,3}+\sqrt{3}Y_{1,1}-\sqrt{3}Y_{3,-1}+\sqrt{5}Y_{3,-3}),$$
$$K_{3,3}=-\frac{i}{4}(-\sqrt{5}Y_{3,3}+\sqrt{3}Y_{1,1}+\sqrt{3}Y_{3,-1}+\sqrt{5}Y_{3,-3}),$$
$$K_{3,4}=Y_{3,0},\quad K_{3,5}=\frac{1}{4}(-\sqrt{3}Y_{3,3}+\sqrt{5}Y_{1,1}-\sqrt{5}Y_{3,-1}-\sqrt{3}Y_{3,-3}),$$
$$K_{3,6}=-\frac{i}{4}(-\sqrt{3}Y_{3,3}-\sqrt{5}Y_{1,1}-\sqrt{5}Y_{3,-1}+\sqrt{3}Y_{3,-3}),\quad K_{3,7}=\frac{1}{\sqrt{2}}(Y_{3,2}+Y_{3,-2}), \tag{3.18c}$$

apart from the prefactor $\sqrt{(2l+1)!!}/\sqrt{4\pi}r^l$. In the TOMBO code [17], in the numerical part the cubic harmonics functions are used, therefore we have to consider the matrix element derived from the cubic harmonics K instead of spherical harmonics Y. This makes the analytical calculation of $\boldsymbol{S}\cdot\boldsymbol{L}$ matrix difficult because the ladder operating on cubic harmonics is cumbersome.

There is a orthonormalization relation between two cubic harmonics,

$$\int K_{l,m}(\hat{\boldsymbol{r}})K_{l',m'}(\hat{\boldsymbol{r}})d\hat{\boldsymbol{r}}=\delta_{ll'}\delta_{mm'}, \tag{3.19}$$

where $\hat{\boldsymbol{r}}$ denotes $\hat{\boldsymbol{r}}=\boldsymbol{r}/|\boldsymbol{r}|$. For the AO-AO matrix elements, we have

$$\langle\, jnlms_z\,|\,H_{\mathrm{SOC}}\,|\,jnlm's'_z\,\rangle=-\frac{1}{2c^2}\langle\, lms_z\,|\,\boldsymbol{S}\cdot\boldsymbol{L}\,|\,lm's'_z\,\rangle\int_0^\infty R^2_{nl}(r)\frac{dV_j(r)}{dr}rdr, \tag{3.20}$$

where $|\,lms_z\,\rangle$ denotes the direct product of the cubic harmonics $K_{l,m}$ and the spin function $|\,s_z\,\rangle$ with the spin eigenvalue $s_z=\frac{1}{2}$ or $-\frac{1}{2}$. For the s orbitals ($l=0$),

obviously

$$\langle\, 00s_z \,|\, \boldsymbol{S}\cdot\boldsymbol{L} \,|\, 00s'_z \,\rangle = 0, \tag{3.21}$$

where $s, s'_z = \frac{1}{2}, -\frac{1}{2}$. For the p orbitals ($l = 1$), we have

$$\langle\, 1ms_z \,|\, \boldsymbol{S}\cdot\boldsymbol{L} \,|\, 1m's'_z \,\rangle = \begin{pmatrix} 0 & \frac{i}{2} & 0 & 0 & 0 & \frac{1}{2} \\ -\frac{i}{2} & 0 & 0 & 0 & 0 & \frac{i}{2} \\ 0 & 0 & 0 & -\frac{1}{2} & -\frac{i}{2} & 0 \\ 0 & 0 & -\frac{1}{2} & 0 & -\frac{i}{2} & 0 \\ 0 & 0 & \frac{i}{2} & \frac{i}{2} & 0 & 0 \\ \frac{1}{2} & -\frac{i}{2} & 0 & 0 & 0 & 0 \end{pmatrix}, \tag{3.22a}$$

where the order of the element ms_z is $1\uparrow, 2\uparrow, 3\uparrow, 1\downarrow, 2\downarrow$, and $3\downarrow$. For the d orbitals ($l = 2$), we have

$$\langle\, 2ms_z \,|\, \boldsymbol{S}\cdot\boldsymbol{L} \,|\, 2m's'_z \,\rangle = \begin{pmatrix} 0 & 0 & 0 & 0 & -i & 0 & \frac{1}{2} & \frac{i}{2} & 0 & 0 \\ 0 & 0 & -\frac{i}{2} & 0 & 0 & -\frac{1}{2} & 0 & 0 & \frac{\sqrt{3}i}{2} & \frac{i}{2} \\ 0 & \frac{i}{2} & 0 & 0 & 0 & -\frac{i}{2} & 0 & 0 & \frac{\sqrt{3}}{2} & -\frac{1}{2} \\ i & 0 & 0 & 0 & 0 & 0 & -\frac{\sqrt{3}i}{2} & -\frac{\sqrt{3}}{2} & 0 & 0 \\ 0 & 0 & 0 & 0 & 0 & 0 & -\frac{i}{2} & \frac{1}{2} & 0 & 0 \\ 0 & -\frac{1}{2} & \frac{i}{2} & 0 & 0 & 0 & 0 & 0 & 0 & i \\ \frac{1}{2} & 0 & 0 & \frac{\sqrt{3}i}{2} & \frac{i}{2} & 0 & 0 & \frac{i}{2} & 0 & 0 \\ -\frac{i}{2} & 0 & 0 & -\frac{\sqrt{3}}{2} & \frac{1}{2} & 0 & -\frac{i}{2} & 0 & 0 & 0 \\ 0 & -\frac{\sqrt{3}i}{2} & \frac{\sqrt{3}}{2} & 0 & 0 & 0 & 0 & 0 & 0 & 0 \\ 0 & -\frac{i}{2} & -\frac{1}{2} & 0 & 0 & -i & 0 & 0 & 0 & 0 \end{pmatrix}, \tag{3.22b}$$

where the order of the element ms_z is $1\uparrow, 2\uparrow, 3\uparrow, 4\uparrow, 5\uparrow, 1\downarrow, 2\downarrow, 3\downarrow, 4\downarrow$, and $5\downarrow$. For the f orbitals ($l = 3$), we have

$$\langle\, 3ms_z \,|\, \boldsymbol{S}\cdot\boldsymbol{L} \,|\, 3m's'_z \,\rangle$$

$$= \begin{pmatrix} 0 & -\frac{3i}{4} & 0 & 0 & -\frac{\sqrt{15}i}{4} & 0 & 0 & 0 & 0 & -\frac{3}{4} & 0 & 0 & \frac{\sqrt{15}}{4} & 0 \\ \frac{3i}{4} & 0 & 0 & -\frac{\sqrt{15}i}{4} & 0 & 0 & 0 & 0 & 0 & -\frac{3i}{4} & 0 & 0 & -\frac{\sqrt{15}i}{4} & 0 \\ 0 & 0 & 0 & 0 & 0 & 0 & 0 & \frac{3}{4} & \frac{3i}{4} & 0 & \frac{\sqrt{15}}{4} & -\frac{\sqrt{15}i}{4} & 0 & 0 \\ 0 & \frac{\sqrt{15}i}{4} & 0 & 0 & \frac{i}{4} & 0 & 0 & 0 & 0 & -\frac{\sqrt{15}}{4} & 0 & 0 & \frac{1}{4} & i \\ \frac{\sqrt{15}i}{4} & 0 & 0 & -\frac{i}{4} & 0 & 0 & 0 & 0 & 0 & \frac{\sqrt{15}i}{4} & 0 & 0 & \frac{i}{4} & -1 \\ 0 & 0 & 0 & 0 & 0 & 0 & i & -\frac{\sqrt{15}}{4} & \frac{\sqrt{15}i}{4} & 0 & -\frac{1}{4} & -\frac{i}{4} & 0 & 0 \\ 0 & 0 & 0 & 0 & 0 & -i & 0 & 0 & 0 & 0 & -i & 1 & 0 & 0 \\ 0 & 0 & \frac{3}{4} & 0 & 0 & -\frac{\sqrt{15}}{4} & 0 & 0 & \frac{\sqrt{3}i}{4} & 0 & 0 & \frac{\sqrt{15}i}{4} & 0 & 0 \\ 0 & 0 & -\frac{3i}{4} & 0 & 0 & -\frac{\sqrt{15}i}{4} & 0 & -\frac{\sqrt{3}i}{4} & 0 & 0 & \frac{\sqrt{15}i}{4} & 0 & 0 & 0 \\ -\frac{3}{4} & \frac{3i}{4} & 0 & -\frac{\sqrt{15}}{4} & -\frac{\sqrt{15}i}{4} & 0 & 0 & 0 & 0 & 0 & 0 & 0 & 0 & 0 \\ 0 & 0 & \frac{\sqrt{15}}{4} & 0 & 0 & -\frac{1}{4} & i & 0 & -\frac{\sqrt{15}i}{4} & 0 & 0 & -\frac{i}{4} & 0 & 0 \\ 0 & 0 & \frac{\sqrt{15}i}{4} & 0 & 0 & \frac{i}{4} & 1 & -\frac{\sqrt{15}i}{4} & 0 & 0 & \frac{i}{4} & 0 & 0 & 0 \\ \frac{\sqrt{15}}{4} & \frac{\sqrt{15}i}{4} & 0 & \frac{1}{4} & -\frac{i}{4} & 0 & 0 & 0 & 0 & 0 & 0 & 0 & 0 & -i \\ 0 & 0 & 0 & -i & -1 & 0 & 0 & 0 & 0 & 0 & 0 & 0 & i & 0 \end{pmatrix}, \tag{3.22c}$$

where the order of the element ms_z is $1\uparrow, 2\uparrow, 3\uparrow, 4\uparrow, 5\uparrow, 6\uparrow, 7\uparrow, 1\downarrow, 2\downarrow, 3\downarrow, 4\downarrow, 5\downarrow, 6\downarrow$, and $7\downarrow$. All these matrices have zero diagonal elements only, because the cubic harmonics is expressed in either symmetric or antisymmetric combination of spherical harmonics with respect to the L_z eigenvalue, *i.e.*, the magnetic quantum number m, the expectation value of L_z sandwiched with the same cubic harmonics is always zero. (Note that the second index of the spherical harmonics is the magnetic quantum number m but the second index of the cubic harmonics is not the magnetic

quantum number.) The third factor in Eq. (3.20),

$$\frac{1}{2c^2}\int_0^\infty R_{nl}^2(r)\frac{dV_j(r)}{dr}rdr,$$

is calculated numerically in the code. (Radial function is defined numerically by modified Hermann-Skillman code, which takes into account a screened effect approximately.)

3.1.4 SOC matrix calculated from basis; PW-AO

For the PW-AO matrix elements $\langle\, \boldsymbol{G}s_z \,|\, H_{\mathrm{SOC}} \,|\, jnlm's'_z \,\rangle$, PWs are first expanded in terms of the cubic harmonics as

$$e^{i\boldsymbol{G}\cdot\boldsymbol{r}} = e^{i\boldsymbol{G}\cdot\boldsymbol{R}_j}\left[4\pi\sum_l i^l j_l(Gr_j)\sum_{m=1}^{2l+1} K_{lm}(\hat{\boldsymbol{G}})K_{lm}(\hat{\boldsymbol{r}}_j)\right], \tag{3.23}$$

where $j_l(x)$ is the spherical Bessel function, $\hat{\boldsymbol{G}} = \boldsymbol{G}/|\boldsymbol{G}|$, $\hat{\boldsymbol{r}}_j = \boldsymbol{r}_j/|\boldsymbol{r}_j|$. Therefore, the PW-AO matrix elements are obtained as

$$\begin{aligned}\langle\, \boldsymbol{G}s_z \,|\, H_{\mathrm{SOC}} \,|\, jnlm's'_z \,\rangle = \frac{(-i)^l}{2c^2}e^{-i\boldsymbol{G}\cdot\boldsymbol{R}_j}\sum_{m=1}^{2l+1}\langle\, lms_z \,|\, \boldsymbol{S}\cdot\boldsymbol{L} \,|\, lm's'_z \,\rangle K_{lm}(\hat{\boldsymbol{G}}) \\ \times\int_0^\infty j_l(Gr)\frac{dV_j}{dr}R_{nl}(r)rdr.\end{aligned} \tag{3.24}$$

The factor $\langle\, lms_z \,|\, \boldsymbol{S}\cdot\boldsymbol{L} \,|\, lm's'_z \,\rangle$ in Eq. (3.24) is calculated by using Eqs. (3.22). The final factor related to the radial functions in Eq. (3.24),

$$\int_0^\infty j_l(Gr)\frac{dV_j}{dr}R_{nl}(r)rdr,$$

is calculated numerically in the program code (TOMBO).

3.1.5 Diagonalization

There are two approaches to treat the SOC. One is to use perturbation theory and the other is to diagonalize the full Hamiltonian. In the former approach, I construct the matrix elements sandwiched by the eigenfunctions $\{\,|\,\lambda, s_z\,\rangle\}$ of the unperturbed Hamiltonian H_0 as Eq. (3.8)

$$H_0\,|\,\lambda, s_z\,\rangle = \varepsilon_\lambda\,|\,\lambda, s_z\,\rangle,$$

and then the SOC hamiltonian $H_{\rm SOC}$ matrices become

$$\begin{aligned}\langle\,\lambda s_z\,|\,H_{\rm SOC}\,|\,\lambda' s'_z\,\rangle &= \sum_{\boldsymbol{G}} c^{\lambda *}_{\boldsymbol{G}} \sum_{\boldsymbol{G}'} c^{\lambda'}_{\boldsymbol{G}'} \langle\,\boldsymbol{G} s_z\,|\,H_{\rm SOC}\,|\,\boldsymbol{G}' s'_z\,\rangle \\ &+ \left(\sum_{\boldsymbol{G}} c^{\lambda *}_{\boldsymbol{G}} \sum_{jnlm} c^{\lambda}_{jnlm} \langle\,\boldsymbol{G} s_z\,|\,H_{\rm SOC}\,|\,jnlm s'_z\,\rangle + c.c. \right) \\ &+ \sum_{jnlm} c^{\lambda *}_{jnlm} \sum_{m'} c^{\lambda}_{jnlm'} \langle\,jnlm s_z\,|\,H_{\rm SOC}\,|\,jnlm' s'_z\,\rangle, \end{aligned} \tag{3.25}$$

where c.c. means the complex conjugate. As an approximation, one may solve the secular equation

$$\begin{vmatrix} \langle\,\lambda\,\frac{1}{2}\,|\,H_{\rm SOC}\,|\,\lambda'\,\frac{1}{2}\,\rangle + (\varepsilon_\lambda - \varepsilon)\,\delta_{\lambda\lambda'} & \langle\,\lambda\,\frac{1}{2}\,|\,H_{\rm SOC}\,|\,\lambda'\,-\frac{1}{2}\,\rangle \\ \langle\,\lambda\,-\frac{1}{2}\,|\,H_{\rm SOC}\,|\,\lambda'\,\frac{1}{2}\,\rangle & \langle\,\lambda\,-\frac{1}{2}\,|\,H_{\rm SOC}\,|\,\lambda'\,-\frac{1}{2}\,\rangle + (\varepsilon_\lambda - \varepsilon)\,\delta_{\lambda\lambda'} \end{vmatrix} = 0, \tag{3.26}$$

in the degenerate complex of the states, $|\,\lambda s_z\,\rangle$ and $|\,\lambda' s'_z\,\rangle$, where the KS energies ε_λ and $\varepsilon_{\lambda'}$ are all the same. One can apply such an approach, for example, to the atomic spectra or to the calculation of the core electron binding energy (CEBE) of molecules or defects/surfaces/interfaces in X-ray photoelectron spectroscopy (XPS). A more accurate treatment is to solve Eq. (3.26) beyond the degenerate complex of the states, $|\,\lambda s_z\,\rangle$ and $|\,\lambda' s'_z\,\rangle$, where ε_λ and $\varepsilon_{\lambda'}$ can be different. This becomes equivalent to perform the full matrix diagonalization of $H + H_{\rm SOC}$.

3.2 Results and Discussion

For an isolated hydrogen-like atom, we can see the eigenvalues defined by resultant orbital angular momentum quantum number $j = l + s_z$ are split as

$$|\epsilon_{nlj=l+1/2} - \epsilon^0_{nl}| : |\epsilon_{nlj=l-1/2} - \epsilon^0_{nl}| = l : l+1, \tag{3.27}$$

so this result is used in checking the result of isolated atoms having a closed shell.

Table 3.1 shows the results calculated for the levels at the $^1S_0$ ground state of isolated rare gas atoms, Ne, Ar, and Kr. $E^{\rm calc}_{\rm SOC}$ and $E^{\rm calc}_{\rm SOC}(+{\rm SR})$ are the first-principles results obtained by diagonalizing the full $H + H_{\rm SOC}$ without and with the scalar relativistic correction (SR), respectively. The last column lists available experimental data [74–79] for comparison. The resulting spin-orbit splitting (SOS) $E^{\rm calc}_{\rm SOC}(+{\rm SR})$ for Ne, Ar, and Kr shows excellent agreement with the experimental data. These SOS values are observed in XPS experiments. It is known that the XPS results for one particular material could be diverse between different research and measurements; so if there are differences, those values are written on the lower right. From these results, we can see that our program works quite well. Figures 3.1 (a)-(e) show the energy

TABLE 3.1: SOS in units of eV calculated for rare gas atoms by using the full eigenvalue problem $\Delta E^{\rm calc}_{\rm SOC}$ and $\Delta E^{\rm calc}_{\rm SOC}(+{\rm SR})$, where (+SR) means the scalar relativistic correction. The available experimental values are also listed in the last column for comparison. (Tables from the publication[1])

Atom		Level	$\Delta E^{\rm calc}_{\rm SOC}$	$\Delta E^{\rm calc}_{\rm SOC}(+{\rm SR})$	Experiment
^{10}Ne	$^1S_0$	$2p$	0.103	0.103	0.097[a]
^{18}Ar	$^1S_0$	$2p$	2.209	2.211	$2.68^{\rm b}_{\pm 0.95}$
		$3p$	0.176	0.177	0.177[c]
^{36}Kr	$^1S_0$	$2p$	51.677	51.853	
		$3p$	7.482	7.387	
		$3d$	1.306	1.304	
		$4p$	0.615	0.597	0.666[d]
^{54}Xe	$^1S_0$	$3d$	12.91	12.92	12.6[e]
		$4p$	10.38	9.82	
		$4d$	2.59	2.58	
		$5p$	0.76	0.77	

[a] Ref.[74].
[b] Ref.[75].[76].
[c] Ref.[77].
[d] Ref.[78].
[e] Ref.[79].

diagram of the Kohn-Sham (KS) energy eigenvalues for some levels of the rare gas atoms. The fully diagonalized absolute energy levels (right side of each figure) are also quite reasonable. In fact, the p orbitals for $l = 1$ are split into two states, $j = \frac{3}{2}$ and $j = \frac{1}{2}$, and the energy shifts from ϵ^0_{nl} without complex calculations are analytically evaluated as $\frac{1}{2}\zeta_{n1}$ $(j = \frac{3}{2})$ and ζ_{n1} $(j = \frac{1}{2})$, *i.e.*, $\Delta\epsilon_{np_{\frac{3}{2}}-np} : \Delta\epsilon_{np_{\frac{1}{2}}-np} = 1 : 2$. Similarly for the d orbitals corresponding to $l = 2$, the energy shifts are analytically evaluated as ζ_{n2} $(j = \frac{5}{2})$ and $\frac{3}{2}\zeta_{n2}$ $(j = \frac{3}{2})$, *i.e.*, $\Delta\epsilon_{nd_{\frac{5}{2}}-nd} : \Delta\epsilon_{nd_{\frac{3}{2}}-nd} = 2 : 3$. We can confirm that these analytical relationships are satisfied in all Figs. 3.1 (a)-(e). This clearly indicates the validity of the present method.

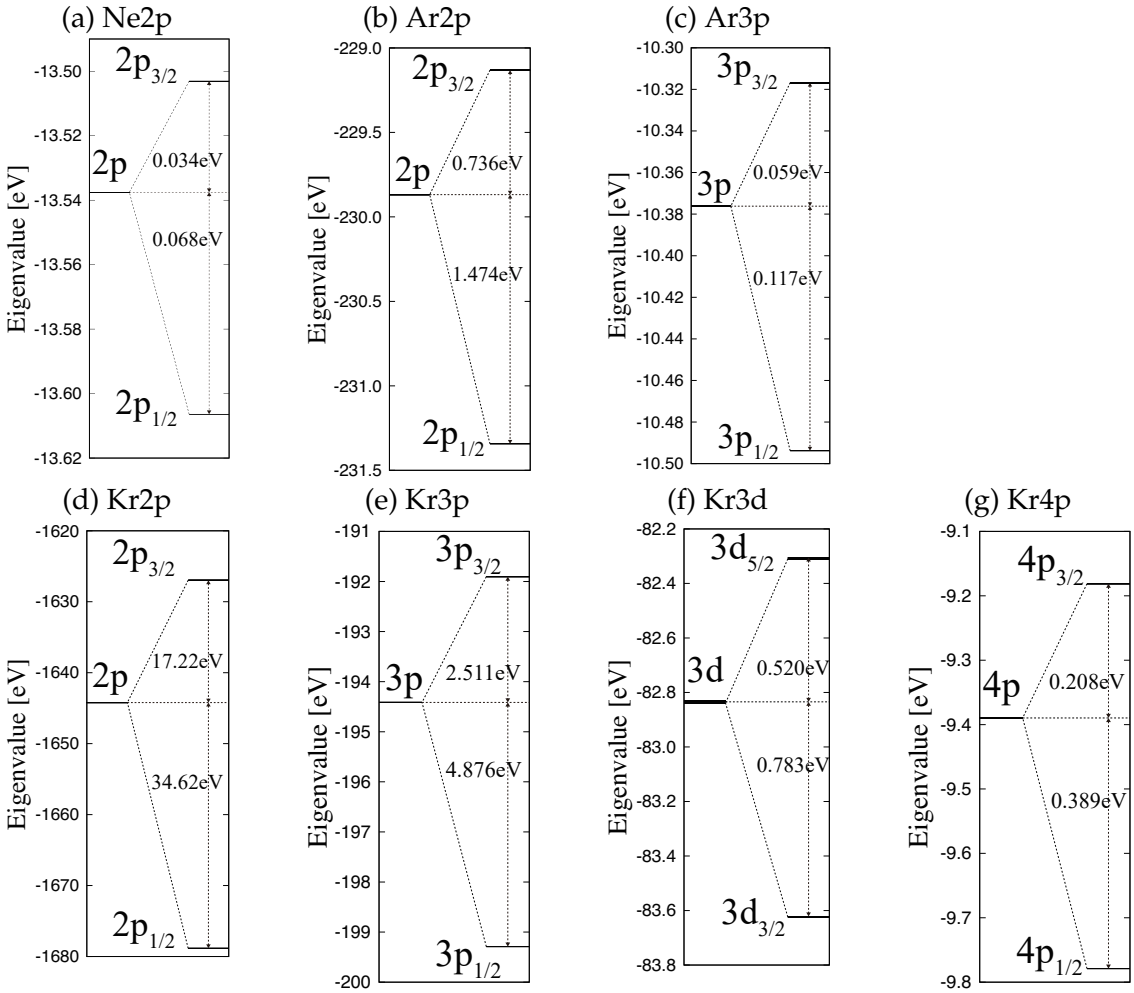

FIGURE 3.1: Energy diagram of rare gas atoms: (a) Ne (2p), (b) Ar (2p), (c) Ar (3p), (d) Kr (2p), (e) Kr (3d), (f) Kr (2p), and (g) Kr (4p) (Figures from the publication[1])

In Table 3.2, I show the calculated SOS of several open shell atoms Na, Mg, Al, Si, P, S, and Cl, which have nonzero spin magnetic moment. The error bars are the width of the slightly split levels due to the spin polarization of these systems. I also list experimental data [80–87] for comparison. The results are fairly good for all atoms, indicating again the validity of the present method.

TABLE 3.2: SOS of the open shell atoms in units of eV. Experimental values are listed for comparison. (Table from the publication[1])

Atom		Level	$\Delta E^{\text{calc}}_{\text{SOC}}$	Experiment
^{11}Na	$^2S_{\frac{1}{2}}$	$2p$	$0.182_{\pm 0.040}$	0.14[f]
^{12}Mg	$^1S_0$	$2p$	0.286	0.28[g]
^{13}Al	$^2P_{\frac{1}{2}}$	$2p$	$0.441_{\pm 0.05}$	$0.415^{\text{h}}_{\pm 0.015}$
^{14}Si	$^3P_0$	$2p$	$0.660_{\pm 0.154}$	$0.615^{\text{i}}_{\pm 0.015}$
^{15}P	$^4S_{\frac{3}{2}}$	$2p$	$0.941_{\pm 0.279}$	0.87[j]
^{16}S	$^3P_0$	$2p$	$1.274_{\pm 0.274}$	1.13[k]
^{17}Cl	$^2P_{\frac{3}{2}}$	$2p$	$1.68_{\pm 0.16}$	1.6[k]

[f] Ref.[80]
[g] Ref.[81]
[h] Ref.[82, 83]
[i] Ref.[84, 85]
[j] Ref.[86]
[k] Ref.[87]

TABLE 3.3: SOS in units of eV calculated for several molecules using full eigenvalue problem of $H + H_{\text{SOC}}$ without and with the scalar relativistic correction. For comparison, experimental data are listed together. (Table from the publication[1])

Molecule		MO	$\Delta E^{\text{calc}}_{\text{SOC}}$	$\Delta E^{\text{calc}}_{\text{SOC}}(+\text{SR})$	Experiment
HBr	$^1\Sigma$	π	0.290	0.282	0.33[l]
BrCN	$^1\Sigma$	2π	0.169	0.168	0.18[l]
		1π	0.061	0.081	(0.09)[l]
HCl	$^1\Sigma$	π	0.083	0.083	0.08[l]
HI	$^1\Sigma$	π	0.558	0.523	0.67[l]
I_2	$^1\Sigma_g$	π_g	0.603	0.563	0.63[m]
		π_u	0.592	0.547	0.79[m]
		$4d$	$1.942_{\pm 0.651}$	$1.875_{\pm 0.696}$	1.76[n]

[l] Ref.[88].
[m] Ref.[89].
[n] Ref.[90].

Next, I calculated the SOS for several molecules, HBr, BrCN, HCl, HI, and I_2. For the bond length, I used the following values: H-Br=1.414 Å, Br-C=1.159 Å, C-N=1.159 Å, H-Cl=1.274 Å, H-I=1.609 Å, and I-I=2.666 Å[91]. Table 3.3 shows the results of the SOS calculated for these molecules together with the previous experiments [88, 90]. From this table, $\Delta E^{\mathrm{calc}}_{\mathrm{SOC}}(+\mathrm{SR})$ calculated by the full $H + H_{\mathrm{SOC}}$ diagonalization with the scalar relativistic correction shows good agreement with the experimental values. Figures 3.2 (a)-(e) show the energy diagram for each molecular orbital. From these figures, we can identify how the molecular orbital levels split. In the case of molecules, the split is not simply 1:2 or 2:3 as in the rare gas atoms. This is of course because the complicated nature of the molecular orbitals.

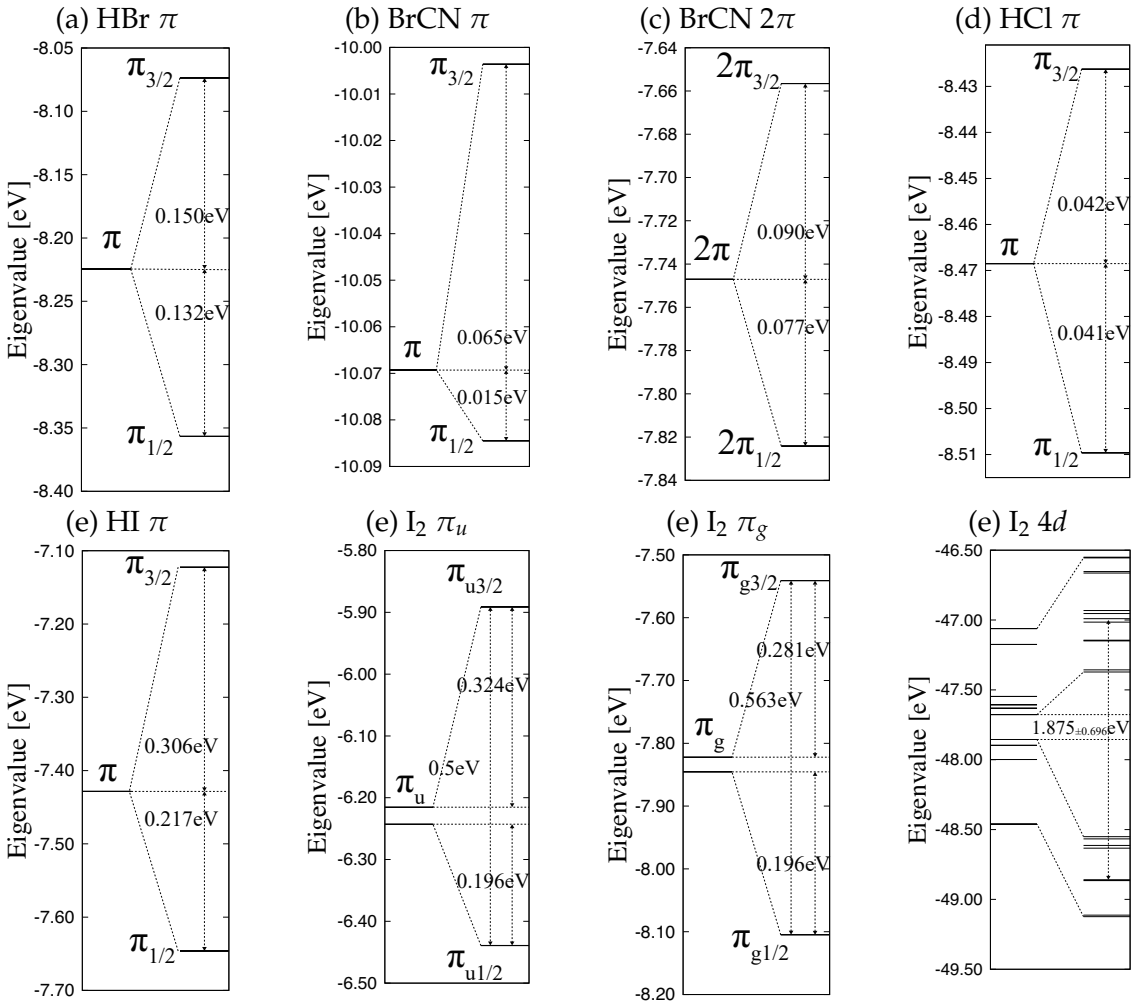

FIGURE 3.2: Energy diagram of some molecules: (a) HBr (π), (b) BrCN (2π), (c) BrCN (π), (d) HCI (π), (e) HI (π), (f) I_2 (π_g), (g) I_2 (π_u), and (h) I_2 ($4d$) (Figures from the publication[1])

In order to see how much PWs contribute to the SOS, I estimated the SOS with and without PWs in the calculation. As shown in Table 3.4, the AOs only results slightly overestimate the results using both AOs and PWs. The PW contribution is about 0.1-0.4%. Thus we can conclude that PW-PW and PW-AO parts can be safely neglected thus saving the effort for computation of large blocks of the H_{SOC} matrix. In this case, the calculation using only the AO-AO block becomes similar to the atomic mean-field integral (AMFI) approximation by Hess et al.[92]

TABLE 3.4: PW contribution to the SOS in units of eV. (Table from the publication[1])

Molecule		MO	AOs only	AOs and PWs
HBr	$^1\Sigma$	π	0.2833	0.2828
BrCN	$^1\Sigma$	2π	0.1679	0.1676
		1π	0.0812	0.0809
HCl	$^1\Sigma$	π	0.0834	0.0832
HI	$^1\Sigma$	π	0.5240	0.5237
I_2	$^1\Sigma_g$	π_g	0.565	0.563
		π_u	0.548	0.547
		$4d$	1.876	1.875

Finally, I calculated Si2p core level of silicon crystal at the Γ point. I used a simple cubic unit cell including 64 Si atoms. The calculated SOS $\Delta E_{\rm SOC}^{\rm calc} = 0.62 \pm 0.1$ eV, and the shifts from the original KS eigenvalue without SOC are $\Delta\epsilon_{2p_{\frac{3}{2}}-2p} = 0.205 \pm 0.05$ eV and $\Delta\epsilon_{2p_{\frac{1}{2}}-2p} = -0.415 \pm 0.05$ eV. Experimentally we know that the splitting value is 0.615 ± 0.15 eV[84, 85]. This result shows excellent agreement with the experimental value.

Table 3.5 lists the size of the assumed cubic unit cell, the PW cut-off energy, and the number of basis functions, and the number of KS levels used for the SOS calculation. It should be emphasized that the PW cut-off energy is relatively small (typically $\sim 50 - 170$ eV) compared to the usual PW expansion method accompanied with pseudopotential or APW method (typically $\sim 300 - 500$ eV). As demonstrated above, this is a distinct merit of using the all-electron mixed basis (AEMB) approach. The number of KS levels used in the diagonalization of $H + H_{\rm SOC}$ is typically 100-300 except for silicon crystal. I confirmed the result does not change even if I increase these numbers.

For the calculations of molecules, non-overlapping atomic spheres are selected so that they do not overlap each other and the total energy becomes smaller with a sufficient cutoff energy for PWs (given in Table 3.5). In each atomic sphere, the effective potential in the KS equation is assumed spherically symmetric. So, using large atomic spheres probability gives an error. Concrete values for the radius of the atomic sphere used in this study are listed in Table 3.6.

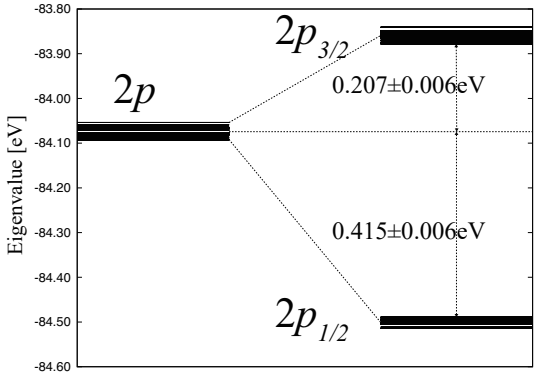

FIGURE 3.3: Energy diagram of the core 2p level of silicon crystal. (Figure from the publication[1])

3.3 Conclusion

I have implemented the spin-orbit coupling (SOC) in the all-electron mixed basis code, TOMBO. For this purpose, I have presented the explicit matrix form of the SOC Hamiltonian using the cubic harmonics, which is useful in any kind of first-principles calculations. There is a distinct merit of using the all-electron mixed basis approach in the evaluation of the SOC, because AOs are well confined in the non-overlapping atomic sphere, where the potential is spherically symmetric and the standard $\boldsymbol{S} \cdot \boldsymbol{L}$ form can be used (see Fig. 2.3). The AO-AO matrices were explicitly derived for p, d, and f orbitals in the cubic harmonics representation. The PW-AO matrices can be calculated in a similar way when PWs are expanded in spherical waves. On the other hand, the PW-PW matrices can be accurately treated in Fourier space without using the $\boldsymbol{S} \cdot \boldsymbol{L}$ form. I showed several results for the spin-orbit splitting (SOS) of atoms and molecules as well as silicon crystal. All the results are in good agreement with available experimental data, suggesting the validity of the present method. The present method is applicable to transition elements and rare earth elements also and even solid compounds as well. Such calculations will be planned as a future study.

Here, I discussed the SOS, *i.e.*, the relative energies, only, but it is also very important to determine the absolute energy values in XPS. For such a purpose, we have to go beyond density functional theory and adopt GW approximation [40]. Moreover, although the present method allows us to calculate the SOC interaction between core electrons and valence electrons, we have not focused the SOS of the conduction levels at all. In order to see how the present method works on the conduction levels, further investigations are necessary. All these studies are left for the future subjects.

TABLE 3.5: Cell size and cut-off energy for each systems. (Table from the publication[1])

System	Unit cell [Å]	$E_{\text{cut-off}}$ (PWs) [eV]	basis (AOs + PWs)	levels used for SOS
Ne	12.0	104.4	4174 (5+4169)	108
Ar	14.0	129.6	9180 (9+9171)	116
Kr	14.0	76.7	4187 (18+4169)	134
Xe	18.0	46.4	4196 (27+4169)	152
HBr	14.0	172.6	14166 (19+14147)	234
BrCN	14.0	129.7	9196 (25+9171)	246
HCl	14.0	76.7	4179 (10+4169)	216
HI	12.0	176.5	9199 (28+9171)	252
I_2	18.0	150.4	24459 (54+24405)	304
Si_{64} (crystal)	10.86	81.6	2429 (320+2109)	914
Na	18	46.4	4175 (6+4169)	114
Mg	16	58.7	4169 (6+4175)	110
Al	16	58.7	4178 (9+4169)	116
Si	16	58.7	4178 (9+4169)	118
P	16	71.0	5584 (9+5575)	122
S	16	84.6	7162 (9+7153)	120
Cl	18	46.4	7162 (9+7153)	120

TABLE 3.6: Radius of non-overlapping atomic sphere. (Table from the publication[1])

Molecule	Atom	Radius of Atomic Sphere [Å]
HBr	H	0.260
	Br	1.139
BrCN	Br	1.000
	C	0.780
	N	0.318
HCl	H	0.200
	Cl	0.999
H	H	0.369
	I	0.900
I_2	I	0.800

Chapter 4

Normalization of the QPWFs with the Ward identity

The first-principles calculation treats a lot of physical properties. Especially, Kohn-Sham (KS) density functional theory (DFT) is one of the powerful methods to be applied for various fields with low computational cost because the one-particle effective Schrödinger equation, which is called the KS equation, plays the key role and shows the great performance[3, 4, 25]. However, KS DFT is invalid to the cases if we need to calculate excitation properties, *i.e.*, precise band structures or phenomena related to such as spectroscopic transitions obtained from optical experiments. In order to perform the calculation of those properties including excitations precisely, it is important to take into account the self-energy correction in quasiparticle (QP) theory[18–20, 28]. As intuition, the self-energy correction is a kind of the effect affected by surrounding electrons (see Fig. 1.2). However, in the QP calculation, it is very cumbersome to solve Hedin's original 5 coupled equations, simultaneously[6, 7, 54]. It is also difficult to obtain the practical form of the self-energy (which is a key factor in QP theory) by taking sum of the infinite number of terms in many-body perturbation theory (MBPT) (see section 2.4).

Hedin(1965) proposed to take the screened Coulomb interaction W [52] and the one-particle Green's function G as the main factors in his theory[6, 54]. The Hedin's theory gave the intuition of the screening and the GW approximation, which shows great performance (see subsection 2.4.3)[6, 7, 14, 18, 29, 54, 58]. In Hedin's calculation, the treatment of the screened Coulomb interaction corresponds to the random phase approximation (RPA) in another aspect[64, 65], and it is well known that the method is great and appropriate for the metallic system. Therefore, the GW calculation has become the main method for various excitation calculations including semiconductors or correlated systems.

As computers have been advanced, self-consistent GW calculations have also been performed[57, 58, 93]. There are, however, still some problems in self-consistent GW calculation, *i.e.*, the wider band gap and reduced plasmon satellite which worsen the agreement with experiments, compared with one-iteration GW calculations (sometimes called one-shot GW calculation or denoted by G_0W_0 symbolically). It is noteworthy that the self-consistent GW increases the QP life-time, which corresponds to modifying the QP peak narrower. In order to improve these errors, it is considered that the vertex function correction beyond the GW approximation is needed [58].

Additionally, there is another main problem in self-consistent GW calculations, which I tried to solve through the present study[2]. Self-consistent GW calculations lead to the contradiction that the number of QPs are finite although the number of QPs are infinite theoretically. This problem implies that the number of electron in the system is not conserved. The nonconservation is derived from the fact that the norm of quasiparticle wave functions (QPWF) is less than one; $\langle \phi_\lambda \,|\, \phi_\lambda \rangle \leq 1$. For

the sake of the conservation of the number of electrons in the system, generalized self-consistent calculations have to be done with the renormalization of QPWFs.

The relation between the renormalization of QPWFs and the vertex correction is implied in some previous papers[58, 94, 95]. In order to improve the nonconservation of electron number, the QPWFs have to be renormalized but the justification for the renormalization procedure has not been discussed thoroughly. The present study discusses the cancellation between the renormalization of QPWFs and the vertex correction, and try to explain the validity of the renormalization of QPWFs in terms of the Ward identity[2]. (It is well known that the gauge invariance, specifically the generalized Ward-Takahashi identity, leads to the electron number conservation law, *i.e.*, continuity equation of the electron density and current density[7, 67, 68].) In addition, I gives the extended KS equation based on Baym-Kadanoff's conservation law, given the validity of the renormalization of QPWFs. The studies about the validity of the normalization for QPWFs and the extended KS equation based on Baym-Kadanoff's conservation law are reported in the following paper; Takeru Nakashima, Hannes Raebiger, and Kaoru Ohno. "Normalization of exact quasiparticle wave functions in the Green's function method guaranteed by the Ward identity". *Physical Review B*, 104 20: L201116 (2021).[2]. The present study gives the one solution for the uncertain connection between KS theory and QP theory, that is, the hermitized QP equation with normalized QPWFs is interpreted as extended KS equation.

4.1 The problem of the electron density

The electron density is defined by

$$\rho(\boldsymbol{r}) = \langle \Psi_0^N \mid \psi^\dagger(\boldsymbol{r})\psi(\boldsymbol{r}) \mid \Psi_0^N \rangle, \tag{4.1}$$

which is also expressed with an infinite number of occ quasiparticle wave functions (QPWFs) (see chapter 2.4.5),

$$\rho(\boldsymbol{r}) = \sum_{\mu \in \mathrm{occ}} |\phi_\mu(\boldsymbol{r})|^2, \tag{4.2}$$

which makes rigorous analysis very difficult in quasiparticle (QP) theory. On the other hand, including Kohn-Sham (KS) theory, the electron density is expressed by a finite number of KS wave functions

$$\rho(\boldsymbol{r}) = \sum_{i=1}^{N} |\phi_i(\boldsymbol{r})|^2. \tag{4.3}$$

The actual GW calculation gives the finite number of quasiparticle wave functions (QPWFs), which is inconsistent with the theoretical equation (4.2). This leads to the contradiction that the electron number is not conserved, *i.e.*, $\int d\boldsymbol{r}\rho(\boldsymbol{r}) \leq N$, in N electron system because the norm of the QPWF is less than one $\langle \phi_\mu \mid \phi_\mu \rangle \leq 1$.

The number of the electron density is related to the Green's function as

$$\rho(\boldsymbol{r}) = +i \int \frac{d\omega}{2\pi} G(\boldsymbol{r}, \boldsymbol{r}|\omega) e^{+i\omega 0^+}, \tag{4.4}$$

which means that in the case the electron density is composed of the finite number of the QPWFs, the Green's function is expressed with the finite number of the QPWFs too. Therefore, in order to normalize the QPWFs for the electron number conservation law, we have to discuss justification of the normalization procedure of QPWFs.

4.2 QP equation and the Ward identity

In subsection 2.4.1, the basic knowledge about the one-particle Green's function and the Dyson equation is explained. In this chapter, I explain the relation between the quasiparticle wave functions (QPWFs) and the vertex correction with the Ward identity. In recent studies, self-consistent Hedin's calculations are done with the Kohn-Sham (KS) orbitals and eigenvalues as initial information, and where the Green's function composed of the normalized QPWFs with no justification. The present discussion gives the validity to renormalize the QPWFs in Hedin's calculations.

4.2.1 QP equation under Baym-Kadanoff's conservation law

The one-particle Green's function for zero temperature is defined by the ground state Ψ_0^N for many-particle hamiltonian, and electron creation and annihilation Heisenberg operators, and Wick's time ordered operator $T[\cdots]$ as

$$G_s(1,2) = -i\langle\, \Psi_0^N \,|\, T[\psi_s(1)\psi_s^\dagger(1)] \,|\, \Psi_0^N \,\rangle, \tag{4.5}$$

where suffixes s denote the spin state and we suppose that the spin states is good quantum number. (Please notice that spin is not good quantum number in the case as a hamiltonian includes the spin-orbit coupling (SOC).) In the following, we omit the spin suffixes for simplicity. Green's function is also represented by

$$G(1,2) = -i\sum_{\mu\in\mathrm{occ}} \phi_\mu(1)\phi_\mu^*(2)\Theta(t_1-t_2) + i\sum_{\nu\in\mathrm{emp}} \phi_\nu(1)\phi_\nu^*(2)\Theta(t_2-t_1), \tag{4.6}$$

where QPWFs $\phi_\lambda(1)$ are defined by

$$\phi_\lambda(1) = \phi_\lambda(\boldsymbol{r}_i)e^{-i\varepsilon_\lambda t_i}, \tag{4.7}$$

where $\phi_\lambda(\boldsymbol{r}_i)$ is the space component of the QPWFs

$$\phi_\mu(\boldsymbol{r}_i) = \langle\, \Psi_\mu^{N-1} \,|\, \psi_s(\boldsymbol{r}_i) \,|\, \Psi_0^N \,\rangle \;;\; \mu \in \mathrm{occ}, \tag{4.8a}$$

$$\phi_\nu(\boldsymbol{r}_i) = \langle\, \Psi_0^N \,|\, \psi_s(\boldsymbol{r}_i) \,|\, \Psi_\nu^{N+1} \,\rangle \;;\; \nu \in \mathrm{emp}, \tag{4.8b}$$

and ε_λ are quasiparticle (QP) energies, which are interpreted as excitation energies, *i.e.*, $\varepsilon_\mu = E_0^N - E_\mu^{N-1}$ and $\varepsilon_\mu = E_\nu^{N+1} - E_0^N$. These QP energies's information is obtained from the photoelectron experiments, *i.e.*, photoemission, inverse photoemission, photoabsorption, and so on. Taking the time Fourier transformation of Eq. (4.6) gives

$$G(\boldsymbol{r}_1,\boldsymbol{r}_2|\omega) = \sum_{\mu\in\mathrm{occ}} \frac{\phi_\mu(\boldsymbol{r}_1)\phi_\mu^*(\boldsymbol{r}_2)}{\omega-\varepsilon_\mu-i0^+} + \sum_{\nu\in\mathrm{emp}} \frac{\phi_\nu(\boldsymbol{r}_1)\phi_\nu^*(\boldsymbol{r}_2)}{\omega-\varepsilon_\nu+i0^+}. \tag{4.9a}$$

For simplicity, the abstract form corresponding to Eq. (4.9a) is introduced as

$$G(\omega) = \sum_{\mu\in\mathrm{occ}} \frac{|\,\phi_\mu\,\rangle\langle\,\phi_\mu\,|}{\omega-\varepsilon_\mu-i0^+} + \sum_{\nu\in\mathrm{emp}} \frac{|\,\phi_\nu\,\rangle\langle\,\phi_\nu\,|}{\omega-\varepsilon_\nu+i0^+}, \tag{4.9b}$$

where $G(\boldsymbol{r}_1,\boldsymbol{r}_2|\omega) = \langle\, \boldsymbol{r}_1 \,|\, G(\omega) \,|\, \boldsymbol{r}_2 \,\rangle$ and $\phi_\lambda(\boldsymbol{r}) = \langle\, \boldsymbol{r} \,|\, \phi_\lambda \,\rangle$[71].

One-particle Green's function $G(\omega)$ follows the Dyson equation

$$(\omega - h - \Sigma(\omega))\, G(\omega) = 0, \tag{4.10a}$$

and also under Baym–Kadanoff's conservation law[67, 68]; the one-particle Green's function follows also left hand equation

$$G(\omega)\left(\omega - h - \Sigma(\omega)\right) = 0, \tag{4.10b}$$

where one-body term and the self-energy are written in similar operator forms; h and $\Sigma(\omega)$ which are defined by $\langle\, r \,|\, h \,|\, r' \,\rangle = h(r)\delta(r - r')$ and $\langle\, r \,|\, \Sigma(\omega) \,|\, r' \,\rangle = \Sigma(r, r'|\omega)$. This comes from the Dyson equation in two equivalent forms $G(\omega) = G^0(\omega) + G^0(\omega)\Sigma(\omega)G(\omega) = G^0(\omega) + G(\omega)\Sigma(\omega)G^0(\omega)$, which correspond to $\Sigma = \bar{\Sigma}$ in Eq. (6.6) of Ref. [7]. From Eqs. (4.10) and (4.9b) and the Cauchy's residue integral around each QP energy, we obtain the following Dyson equations for QPWFs

$$\left(\varepsilon_\lambda - h_s - \Sigma(\varepsilon_\lambda)\right) \,|\, \phi_\lambda \,\rangle = 0, \tag{4.11a}$$

$$\langle\, \phi_\lambda \,|\, \left(\varepsilon_\lambda - h_s - \Sigma(\varepsilon_\lambda)\right) = 0. \tag{4.11b}$$

These are also called the QP equations for left- and rigth-eigenvalue equation. Please note that the self-energy is energy dependent, which makes the solutions of this equation not orthogonal to each other and have the norm between 0 and 1 [71, 96, 97]. The Hermitian conjugate of Eq. (4.11b) is

$$\left[\, \varepsilon_\lambda^* - h - \Sigma^\dagger(\varepsilon_\lambda) \,\right] \,|\, \phi_\lambda \,\rangle = 0. \tag{4.12}$$

Eqs. (4.11) and (4.12) lead the following hermitian equation

$$\mathrm{Re}(\varepsilon_\lambda) \,|\, \phi_\lambda \,\rangle = \left[h_s + \frac{1}{2}\left(\Sigma(\varepsilon_\lambda) + \Sigma^\dagger(\varepsilon_\lambda)\right)\right] \,|\, \phi_\lambda \,\rangle. \tag{4.13a}$$

That is, we can hermitize the self-energy just like the effective potential in density functional theory (DFT) when we solve the QP eigenvalue problem, although the QP energies are complex numbers. This equation gives validity of the the general treatment to make the self-energy Hermitian. This treatment is somewhat similar to the V^{xc} choice in Kotani's quasiparticle self-consistent GW method[98]. It is seen that

$$\{G^{-1}(\varepsilon_\lambda)G^{-1\dagger}(\varepsilon_\lambda) - G^{-1\dagger}(\varepsilon_\lambda)G^{-1}(\varepsilon_\lambda)\} \,|\, \phi_\lambda \,\rangle = 0,$$

and it should be understood that, inside $\Sigma^\dagger(\varepsilon_\lambda)$ and $G^{-1\dagger}(\varepsilon_\lambda)$, ε_λ is replaced by ε_λ^*. Also, Eqs. (4.11) and (4.12) give the following equation, the imaginary part of the QP energies is obtained by

$$\frac{1}{2i}\left\{\Sigma(\varepsilon_\lambda) - \Sigma^\dagger(\varepsilon_\lambda)\right\} \,|\, \phi_\lambda \,\rangle = \mathrm{Im}\left[\varepsilon_\lambda\right] \,|\, \phi_\lambda \,\rangle. \tag{4.13b}$$

From the imaginary value of the QP energy derived from Eq. (4.13b), we can estimate the QP life-times. The interesting point is that Eqs. (4.13a) and (4.13b) have the simultaneous eigenstates.

Now, I would like to briefly comment on some simple approximations apart from the main story of the present theory. Under the assumption of translational symmetry, the Fourier transforms in space for Eq. (4.13) give

$$[h(\boldsymbol{k}) + \mathrm{Re}\Sigma(\boldsymbol{k}|\varepsilon_\lambda)] \langle \boldsymbol{k} \,|\, \phi_\lambda \rangle = \mathrm{Re}\,[\varepsilon_\lambda] \langle \boldsymbol{k} \,|\, \phi_\lambda \rangle, \tag{4.14a}$$

$$\mathrm{Im}\Sigma(\boldsymbol{k}|\varepsilon_\lambda) \langle \boldsymbol{k} \,|\, \phi_\lambda \rangle = \mathrm{Im}\,[\varepsilon_\lambda] \langle \boldsymbol{k} \,|\, \phi_\lambda \rangle, \tag{4.14b}$$

where

$$\langle \boldsymbol{k} \,|\, \phi_\lambda \rangle = \int d\boldsymbol{r} \langle \boldsymbol{r} \,|\, \phi_\lambda \rangle e^{-i\boldsymbol{r}\cdot\boldsymbol{k}}.$$

Note that in k-space, the operators can be treated as the scalar functions, and the convolution product gets the simple product, which leads tos

$$\mathrm{Re}\,[\varepsilon_\lambda] = h(k) + \mathrm{Re}\Sigma(k|\varepsilon_\lambda), \tag{4.15a}$$

$$\mathrm{Im}\,[\varepsilon_\lambda] = \mathrm{Im}\Sigma(k|\varepsilon_\lambda). \tag{4.15b}$$

These results are consistent with the relationship assumed in the conventional electron gas model calculations[50], that is, the imaginary part of the self-energy gives the life-time of the QP states. Moreover, this equation gives the validity of taking only the real part of the self-energy neglecting the imaginary part in actual calculations for the QP energy peaks position. Generally, the self-energy is treated as the function of the real part of the QP energy $\mathrm{Re}[\varepsilon_\lambda]$ neglecting the imaginary part of the QP energy $\mathrm{Im}[\varepsilon_\lambda]$ as[57]

$$\Sigma(\varepsilon_\lambda) \simeq \Sigma(\mathrm{Re}[\varepsilon_\lambda]). \tag{4.16}$$

In this case, the real part of the QP energy is calculated by only Eq. (4.13a) self-consistently, and we can neglect Eq. (4.13b) and the imaginary effect of the QP energy.

$$\left[h + \frac{1}{2}\left\{\Sigma(\mathrm{Re}[\varepsilon_\lambda]) + \Sigma^\dagger(\mathrm{Re}[\varepsilon_\lambda])\right\}\right] |\, \phi_\lambda \rangle = \mathrm{Re}\,[\varepsilon_\lambda] \;|\, \phi_\lambda \rangle. \tag{4.17}$$

After the self-consistent calculation get convergence, the life-time of the QP state is estimated by using Eq. (4.13b)[99].

Under Baym-Kadanoff conservation law, it is very interesting to get the QP energy (the real part) by solving such a Hermitized QP equation.

4.2.2 Normalization with the Ward identity

Firstly, I explain the norm of the QPWFs. It is well known that the norm of the QPWFs is less than one[71, 96, 97]. Combining Eqs. (4.9b) and (4.10a) shows

$$(\omega - h - \Sigma(\omega)) \sum_{\lambda} \frac{|\,\phi_\lambda\,\rangle\langle\,\phi_\lambda\,|}{\omega - \varepsilon_\lambda} = 1, \tag{4.18}$$

where $\delta(\boldsymbol{r}_1 - \boldsymbol{r}_2)h(\boldsymbol{r}_1) = \langle\,\boldsymbol{r}_1\,|\,h\,|\,\boldsymbol{r}_2\,\rangle$ and $\Sigma(\boldsymbol{r}_1, \boldsymbol{r}_2|\omega) = \langle\,\boldsymbol{r}_1\,|\,\Sigma(\omega)\,|\,\boldsymbol{r}_2\,\rangle$, and the infinitesimal number in denominator is omitted for simplicity

$$\left(\frac{\omega - h - \Sigma(\omega)}{\omega - \varepsilon_\alpha}\right) |\,\phi_\alpha\,\rangle\langle\,\phi_\alpha\,|\,\phi_\alpha\,\rangle + \sum_{\lambda\neq\alpha}\left(\frac{\omega - h - \Sigma(\omega)}{\omega - \varepsilon_\lambda}\right) |\,\phi_\lambda\,\rangle\langle\,\phi_\lambda\,|\,\phi_\alpha\,\rangle = |\,\phi_\alpha\,\rangle. \tag{4.19}$$

In the limit $(\omega \to \varepsilon_\alpha)$, therefore, the above equation becomes

$$\left(1 - \left.\frac{\partial\Sigma(\omega)}{\partial\omega}\right|_{\omega=\varepsilon_\alpha}\right) |\,\phi_\alpha\,\rangle = \frac{1}{\langle\,\phi_\alpha\,|\,\phi_\alpha\,\rangle}\left(1 - \sum_{\lambda\neq\alpha}\left(\frac{\varepsilon_\alpha - h - \Sigma(\omega)}{\varepsilon_\alpha - \varepsilon_\lambda}\right) |\,\phi_\lambda\,\rangle\langle\,\phi_\lambda\,|\right) |\,\phi_\alpha\,\rangle. \tag{4.20a}$$

Also, in similar way, combining Eqs. (4.9b) and (4.10b) shows

$$\langle\,\phi_\alpha\,|\left(1 - \left.\frac{\partial\Sigma(\omega)}{\partial\omega}\right|_{\omega=\varepsilon_\alpha}\right) = \frac{1}{\langle\,\phi_\alpha\,|\,\phi_\alpha\,\rangle}\langle\,\phi_\alpha\,|\left(1 - \sum_{\lambda\neq\alpha} |\,\phi_\lambda\,\rangle\langle\,\phi_\lambda\,|\left(\frac{\varepsilon_\alpha - h - \Sigma(\omega)}{\varepsilon_\alpha - \varepsilon_\lambda}\right)\right). \tag{4.20b}$$

The second term in the second factor on the right-hand side of Eqs. (4.20) become 0 after sandwiching by ϕ_α, and finally we can obtain the following equation

$$\langle\,\phi_\alpha\,|\left(1 - \left.\frac{\partial\Sigma(\omega)}{\partial\omega}\right|_{\omega=\varepsilon_\alpha}\right) |\,\phi_\alpha\,\rangle = 1, \tag{4.21}$$

due to left- and right-eigenvalue equation, Eqs. (4.11). This means that $1 - \partial_\omega\Sigma(\varepsilon_\lambda)$ plays a role of the normalization factor for the QP state ϕ_λ. This factor is identified with the vertex correction by the Ward identity $\widetilde{\Gamma}_{q=0}$ in the limit $q = (\boldsymbol{q}, \eta) \to 0$, *i.e.*, the situation is that the momentum-energy transfer in terms of the Coulomb interaction is 0.

Gauge invariance leads to various conservations[68]. As one of them, the Ward identity is the very famous conservation equation in quantum electrodynamics as following form[7, 22–24]

$$i(t_1 - t_2)\Sigma(1,2) = \delta(1,2) - \int d3\,\widetilde{\Gamma}(1,2;3), \tag{4.22a}$$

and taking the time Fourier transformation gives that

$$\frac{\partial\Sigma(\boldsymbol{r}_1, \boldsymbol{r}_2|\omega)}{\partial\omega} = \delta(\boldsymbol{r}_1 - \boldsymbol{r}_2) - \int d\boldsymbol{r}_3\,\widetilde{\Gamma}(\boldsymbol{r}_1, \boldsymbol{r}_2; \boldsymbol{r}_3|\omega, \omega), \tag{4.22b}$$

where the Fourier transformation for $\widetilde{\Gamma}$ is defined by

$$\widetilde{\Gamma}(\boldsymbol{r}_1, \boldsymbol{r}_2; \boldsymbol{r}_3|t_1 - t_3, t_2 - t_3) = \int \frac{d\omega d\eta}{(2\pi)^2} e^{-i(\omega+\eta)(t_1-t_3)} e^{+i\omega(t_2-t_3)} \widetilde{\Gamma}(\boldsymbol{r}_1, \boldsymbol{r}_2; \boldsymbol{r}_3|\omega + \eta, \omega). \tag{4.23}$$

Therefore, Eq. (4.22b) shows that

$$\widetilde{\Gamma}(\boldsymbol{r}_1, \boldsymbol{r}_2; \boldsymbol{q} = 0|\omega, \omega) = \delta(\boldsymbol{r}_1 - \boldsymbol{r}_2) - \frac{\partial \Sigma(\boldsymbol{r}_1, \boldsymbol{r}_2|\omega)}{\partial \omega}, \tag{4.24a}$$

where $\widetilde{\Gamma}(\boldsymbol{r}_1, \boldsymbol{r}_2; \boldsymbol{q} = 0|\omega, \omega) = \int \boldsymbol{r}_3 \widetilde{\Gamma}(\boldsymbol{r}_1, \boldsymbol{r}_2; \boldsymbol{r}_3|\omega, \omega)$, which corresponds to the limit that the momentum and the energy transfer via Coulomb interaction is 0, that is, $q = (\boldsymbol{q}, \eta) \to 0$. The above equation is represented as functions of position coordinates $\boldsymbol{r}$. For convenience, abstract form of Eq. (4.24a) is designated as

$$\widetilde{\Gamma}_{q=0}(\omega) = 1 - \frac{\partial \Sigma(\omega)}{\partial \omega}, \tag{4.24b}$$

where $\langle\, \boldsymbol{r}_1 \,|\, \widetilde{\Gamma}_{q=0}(\omega) \,|\, \boldsymbol{r}_2 \,\rangle = \widetilde{\Gamma}(\boldsymbol{r}_1, \boldsymbol{r}_2; k = 0|\omega, \omega)$. Finally, Eqs. (4.21) and (4.24) show

$$\int d\boldsymbol{r}_1 d\boldsymbol{r}_2 \phi^*_\alpha(\boldsymbol{r}_1) \widetilde{\Gamma}(\boldsymbol{r}_1, \boldsymbol{r}_2; \boldsymbol{q} = 0|\varepsilon_\alpha, \varepsilon_\alpha) \phi_\alpha(\boldsymbol{r}_2) = 1, \tag{4.25a}$$

$$\langle\, \phi_\alpha \,|\, \widetilde{\Gamma}_{q=0}(\varepsilon_\alpha) \,|\, \phi_\alpha \,\rangle = 1, \tag{4.25b}$$

which implies that the vertex function $\widetilde{\Gamma}_{q=0}$ plays a role of the normalization factor for the QPWFs. The vertex function, which connects the dynamical interaction to a pair of Green's functions, has an effect to make the system gauge invariant by the Ward–Takahashi identity, and guarantees the local charge conservation by the continuity equation [7, 100]. However, in the limit that the momentum and energy transfer; $q = (\boldsymbol{q}, \eta) \to 0$, no multiple excitation is possible by taking into account the multiple excitations not related to the main QP state. Specifically, when there is no momentum-energy transfer via the Coulomb interaction, those multiple excitations are not important for the main QP calculation (the details are explained in later and see Figs. 4.1 and 4.2). Therefore, the vertex function in this limit counts the $(N \pm 1)$-electron states $|\, \Psi^{N\pm1}_\lambda \,\rangle$ with purely one electron or hole only, and has an effect to normalize the corresponding QPWFs to unity, ignoring all the other QPWFs involving multiple excitations. This is the physical meaning of Eq. (4.25).

Additionally as coffee break, in the expectation value, the following equation is apparently true

$$\langle \phi_\alpha \mid \Big(\mid \phi_\alpha \rangle\langle \phi_\alpha \mid \widetilde{\Gamma}_{q=0}(\varepsilon_\alpha) \Big) \mid \phi_\alpha \rangle = \langle \phi_\alpha \mid \phi_\alpha \rangle. \tag{4.26}$$

From this equation, the inverse of the vertex correction $\widetilde{\Gamma}^{-1}_{q=0}$ is approximated as

$$\widetilde{\Gamma}^{-1}_{q=0}(\varepsilon_\lambda) \simeq \mid \phi_\lambda \rangle\langle \phi_\lambda \mid . \tag{4.27}$$

When this approximation is applied to Eq. (4.9b), the one-particle Green's function is approximated as

$$G(\omega) \simeq \sum_\lambda \frac{\widetilde{\Gamma}^{-1}_{q=0}(\varepsilon_\lambda)}{\omega - \varepsilon_\lambda}. \tag{4.28}$$

But, notice that this is just approximation under Eq. (4.27) and this gives the intuition of the validity of the Hedin's GW approximation because the GW approximation treating the KS results as initial values yields the one-particle Green's function composed of the normalized QPWFs only, which means the one-particle Green's function is represented by

$$G_0(\omega) = \sum_\lambda \frac{1}{\omega - \varepsilon_\lambda}.$$

Specifically, mass term is calculated by $\int G_0(\omega)W(\omega+\eta)d\eta$ and this implies that the vertex $\widetilde{\Gamma}^{-1}$ in Eq. (4.28) and vertex $\widetilde{\Gamma}$ in the original mass form are canceled each other (where the poles of QP energies from the normalized one-particle Green's function are considered only). The similar discussion for the homogeneous space is attached in the appendix B.

From Eqs. (4.25) and (4.28), when we focus on the expectation value, the 2-points vertex correction plays a central role of the normalization factor for the QPWFs. Now, only for the purpose of the normalization of QPWFs, the present study introduces a renormalization function, which satisfies

$$\sum_s \int \phi^*_\lambda(\boldsymbol{r}_1, s)\, \Gamma^{\mathrm{ren}}_{q=0\,s}(\boldsymbol{r}_1, \boldsymbol{r}_2; \varepsilon_\lambda)\phi_\lambda(\boldsymbol{r}_2, s) d\boldsymbol{r}_1 d\boldsymbol{r}_2 = 1,$$

as

$$\begin{aligned} \Gamma^{\mathrm{ren}}_{q=0\,s}(\boldsymbol{r}_1, \boldsymbol{r}_2; \omega) &= \langle\, \boldsymbol{r}_1, s \mid \Gamma^{\mathrm{ren}}_{q=0}(\omega) \mid \boldsymbol{r}_2, s \,\rangle = \delta(\boldsymbol{r}_1 - \boldsymbol{r}_2) f(\omega), \\ f(\omega) &= \sum_{\lambda \in \text{all}} \frac{1}{\langle \phi_\lambda \mid \phi_\lambda \rangle} \frac{\prod_{\alpha\neq\lambda}(\omega - \varepsilon_\alpha)}{\prod_{\beta\neq\lambda}(\varepsilon_\lambda - \varepsilon_\beta)}. \end{aligned} \tag{4.29}$$

This is spin-coordinate independent, and $f(\omega)$ satisfies

$$f(\varepsilon_\lambda) = \frac{1}{\langle \phi_\lambda \mid \phi_\lambda \rangle} = \frac{\langle \phi_\lambda \mid \widetilde{\Gamma}_{q=0}(\varepsilon_\lambda) \mid \phi_\lambda \rangle}{\langle \phi_\lambda \mid \phi_\lambda \rangle}. \tag{4.30}$$

Then, the normalized QP states $\mid \bar{\phi}_\lambda; \varepsilon_\lambda \rangle = \mid \bar{\phi}_\lambda \rangle$, which satisfy $\langle \bar{\phi}_\lambda; \varepsilon_\lambda \mid \bar{\phi}_\lambda; \varepsilon_\lambda \rangle = 1$

but generally obey $\langle\, \bar{\phi}_\lambda; \varepsilon_\lambda \,|\, \bar{\phi}_\zeta; \varepsilon_\zeta \,\rangle \neq 0$ for $\lambda \neq \zeta$, can be constructed from the ω-dependent states

$$|\, \bar{\phi}_\lambda; \omega \,\rangle = \Gamma^{\mathrm{ren}\,1/2}_{q=0}(\omega)\; |\, \phi_\lambda \,\rangle = \sqrt{f(\omega)}\; |\, \phi_\lambda \,\rangle. \tag{4.31}$$

As well, the normalized Green's function is defined by

$$\bar{G}(\omega) = \Gamma^{\mathrm{ren}\,1/2}_{q=0}(\omega)\, G(\omega)\, \Gamma^{\mathrm{ren}\,1/2}_{q=0}(\omega) = G(\omega) f(\omega), \tag{4.32}$$

which satisfies $\bar{G}_s(1,2) = i\rho_s(1,2)$ for $t_1 < t_2$. That is, $f(\omega)$ becomes $f(\varepsilon_\lambda)$ by taking the pole of the Green's function. It is clear that the normalized QP states satisfy the QP equation

$$\varepsilon_\lambda \,|\, \bar{\phi}_\lambda; \varepsilon_\lambda \,\rangle = [\, h + \Sigma(\varepsilon_\lambda) \,]\; |\, \bar{\phi}_\lambda; \varepsilon_\lambda \,\rangle, \tag{4.33}$$

which corresponds to taking the pole of Eq. (4.32) with Eq. (4.9b) in the Dyson equation. The renormalization function $\Gamma^{\mathrm{ren}}_{q=0\,s}(1,2)$ connects the original and renormalized vertex functions as

$$\widetilde{\Gamma}_s(1,2;3) = \int d1'\, \Gamma^{\mathrm{ren}}_{q=0\,s}(1,1')\bar{\Gamma}_s(1',2;3). \tag{4.34}$$

There are two possibilities of choosing $i = 1$ or 2 of $\widetilde{\Gamma}_s(1,2;3)$ to connect $\widetilde{\Gamma}^{\mathrm{ren}}_{q=0\,s}(1,1')$ or $\Gamma^{\mathrm{ren}}_{q=0\,s}(2',2)$. This has to be selected to make the resulting form with G replaced by $\bar{G}$ symmetric. The renormalized vertex function $\bar{\Gamma}$ is the vertex function with factoring out a renormalization function $\Gamma^{\mathrm{ren}}_{q=0}(i,i')$, $\Gamma^{\mathrm{ren}}_{q=0}(i',i)$.

The separation of the renormalization function $\Gamma^{\mathrm{ren}}_{q=0}$ corresponds to removing the spontaneous multiple excitations, not related to the relevant pure QP states (see Fig. 4.1). The limit of the vertex function $\Gamma^{\mathrm{ren}}_{q=0}$ has no momentum-energy transfer in terms of the Coulomb interaction; $\boldsymbol{q} = (q, \omega) \to 0$. The point is that the spontaneous multiple excitations are not related to the main QP calculation intrinsically. The important multiple excitations, such as the bubbles of electron-hole pairs, have contributions to QP in terms of Coulomb interaction through momentum-energy transfer $q = (\boldsymbol{q}, \omega) \neq 0$. In many-body perturbation theory (MBPT), the bubbles of electron-hole pairs is the electron density polarization in the material, which screens Coulomb interaction (see Fig. 4.1 (a)). However, the limit of the vertex function $\Gamma_{q=0}$ does not give the momentum-energy transfer in terms of the Coulomb interaction (see Fig. 4.1 (b)). Therefore, in the case that there is no momentum-energy transfer, those spontaneous multiple excitations can be factored out in using the renormalized factor $\Gamma^{\mathrm{ren}}_{q=0}$ (see Fig. 4.1 (c)).

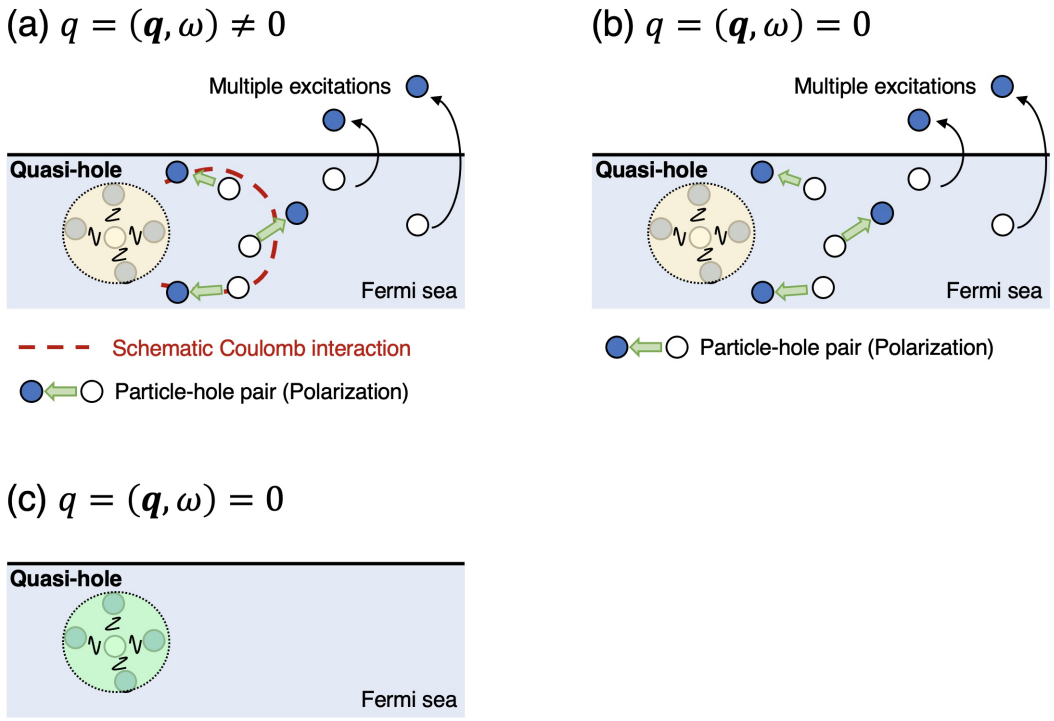

FIGURE 4.1: (a) In the case that there is the momentum-energy transfer $q = (\boldsymbol{q}, \omega) \neq 0$ in terms of the Coulomb interaction, the Coulomb interaction is screened by the multiple excitations such as bubbles of electron-hole pairs. Therefore, their multiple excitations are important. (b) In the case that there is no momentum-energy transfer $q = (\boldsymbol{q}, \omega) = 0$ in terms of the Coulomb interaction, there are spontaneous multiple excitations not related to main QP state. These multiple excitations are not important for each QP calculation. (c) The unimportant spontaneous multiple excitations can be renormalized to the renormalized factor, as the Ward identity $\Gamma^{\text{ren}}_{q=0}$. This situation allows us to treat the normalized pure QP states, which leads to the normalized one-particle Green's function.

4.3 The time-dependent QP equation

Here, the present study proposes to solve the norm problem of the quasiparticle wave functions (QPWFs) as follows. (This problem is explained in section 4.1.) Multiplying both sides of Eq. (2.78a) by $e^{-i\varepsilon_\lambda t_1}$ and using the original Fourier transformation definition $\Sigma_s(r_1, r_2|\varepsilon_\lambda) = \int d(t_1 - t_2)\Sigma_s(1,2)e^{i\varepsilon_\lambda(t_1-t_2)}$, we obtain the time-dependent quasiparticle (QP) equation [54, 63]

$$i\partial_{t_1}\phi_\lambda(1,s) = h_s(\boldsymbol{r}_1)\phi_\lambda(1,s) + \int d2\,\Sigma_s(1,2)\phi_\lambda(2,s). \tag{4.35}$$

Now, we can define the two-time spin density matrix $D_s^{(-)}(1,2)$ and its complementary function $D_s^{(+)}(1,2)$ as

$$D_s^{(-)}(1,2) \equiv \langle\, \Psi_0^N \mid \psi_s^\dagger(2)\psi_s(1) \mid \Psi_0^N \,\rangle = \sum_{\mu\,\in\,\mathrm{occ}} \phi_\mu(1,s)\phi_\mu^*(2,s), \tag{4.36a}$$

$$D_s^{(+)}(1,2) \equiv \langle\, \Psi_0^N \mid \psi_s(1)\psi_s^\dagger(2) \mid \Psi_0^N \,\rangle = \sum_{\nu\,\in\,\mathrm{emp}} \phi_\nu(1,s)\phi_\nu^*(2,s), \tag{4.36b}$$

which are equal to $\mp iG_s(1,2)$ for $t_1 \lessgtr t_2$ and satisfy an equation that is similar to Eq. (2.49) and readily derived from Eq. (4.35),

$$i\partial_{t_1} D_s^{(\pm)}(1,2) = h_s(\boldsymbol{r}_1)D_s^{(\pm)}(1,2) + \int d3\,\Sigma_s(1,3)D_s^{(\pm)}(3,2). \tag{4.37}$$

Next, we can assume that these functions are expressed by normalized QPWFs $\bar{\phi}_i(1,s)$ ($i = 1,2,...,N,N+1,N+2,...$) as

$$D_s^{(-)}(1,2) = \sum_{i=1}^{N} \bar{\phi}_i(1,s)\bar{\phi}_i^*(2,s), \tag{4.38a}$$

$$D_s^{(+)}(1,2) = \sum_{i=N+1}^{\infty} \bar{\phi}_i(1,s)\bar{\phi}_i^*(2,s). \tag{4.38b}$$

Then, the necessary condition for the electron spin density

$$\sum_s \int d\boldsymbol{r}_1 \rho_s(\boldsymbol{r}_1) = \sum_s \int d\boldsymbol{r}_1 D_s^{(-)}(1,1) = N,$$

and the completeness condition Eq. (2.74) is automatically satisfied. At each time t_1, we can introduce the dual orbitals $\widetilde{\phi}_j(1,s)$ ($j = 1,2,...,N,N+1,N+2,...$), which satisfy the biorthogonality condition; such a dual basis can be constructed from Gram–Schmidt orthogonalization method

$$\int \bar{\phi}_i^*(1,s)\widetilde{\phi}_j(1,s)d\boldsymbol{r}_1 = \delta_{ij} \quad (i,j \leq N \text{ or } i,j > N), \tag{4.39}$$

and derive $\int D_s^{(\mp)}(1,2)\widetilde{\phi}_i(2,s)d\boldsymbol{r}_2 = \bar{\phi}_i(1,s)$ ($\mp$ for $i \lessgtr N$). Using this, I readily find that Eq. (4.37) yields the equation

$$i\partial_{t_1}\bar{\phi}_i(1,s) = h_s(\boldsymbol{r}_1)\bar{\phi}_i(1,s) + \int d2\,\Sigma_s(1,2)\bar{\phi}_i(2,s). \tag{4.40}$$

Eqs. (4.35) and (4.40) have exactly the same form, and thus we can conclude that $\bar{\phi}_i(1,s)$ is equivalent to the QPWF $\phi_\mu(1,s)$ except for a normalization factor under the condition the electron spin density is constructed by the finite number of the normalized QPWFs. Therefore, the electron spin density $\rho_s(\boldsymbol{r}_1) = D_s^{(-)}(1,1)$ is expressed by N normalized QPWFs except for normalization. Those functions are not necessarily mutually orthogonal. Here is a hint to solve the problem. There are a lot of independent excitations that are not directly associated with the PE and IPE processes in the $(N \pm 1)$-electron states $\mid \Psi_\lambda^{N\pm1} \,\rangle$ (see Fig. 4.2 (a)). However, they can be eliminated in the summation over all occupied and empty states in Eqs. (2.78a), (4.2), (4.6), (4.9) and (4.36b), and instead we accept that the QP energies have an imaginary part, which represents the peak width and the inverse of the QP life-time; see Fig. 4.2 (b). Then, each hole (electron) QP state associated with one final PE $\mid \Psi_\mu^{N-1} \,\rangle$

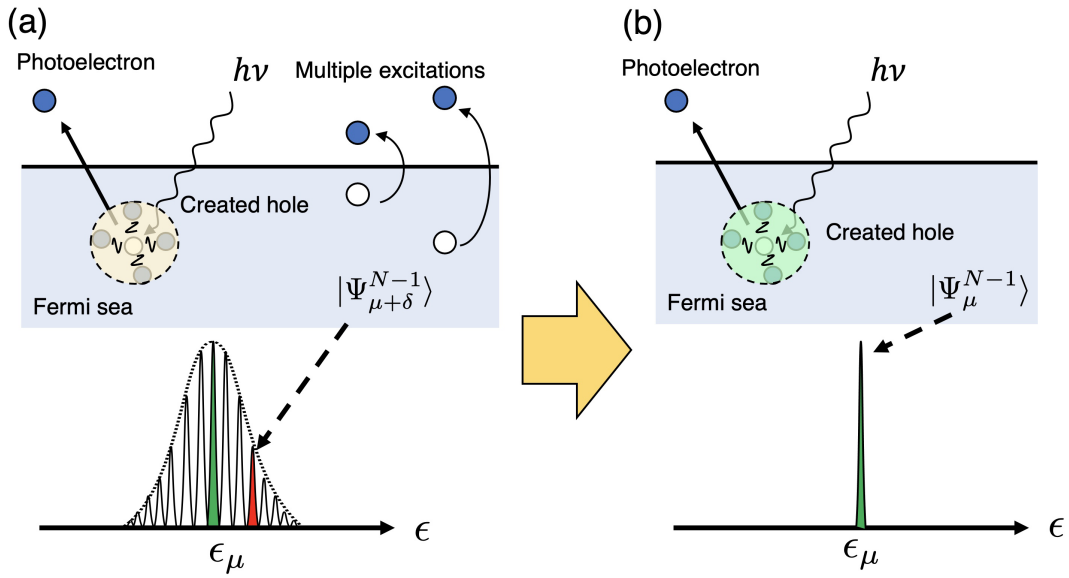

FIGURE 4.2: Illustration of (a) infinite number of $(N-1)$-electron eigenstates $|\,\Psi^{N-1}_{\mu+\delta}\,\rangle$ with multiple excitations around the created hole and (b) the relevant $(N-1)$-electron state $|\,\Psi^{N-1}_{\mu}\,\rangle$ with the created hole.

(IPE $|\,\Psi^{N+1}_{\nu}\,\rangle$) state, which does not include any multiple excitations or Auger-like process involving the recombination and the second excitations, etc., may have a norm equal to the amount of one electron exactly (see Fig. 4.1 (a)-(c)). Normalizing the QPWFs corresponds to ignoring the multiple excitations not related to the main QP states, which appears in the case there are no momentum-energy transfer via the Coulomb interaction. That case is represented by the limited vertex function mathematically.

4.4 Vertex Correction

The present study shows that changing the Green's function from G to $\bar{G}$ is equivalent to replacing the vertex function Γ with $\bar{\Gamma}$ in the exact manner. Firstly, following Baym and Kadanoff [67] and Strinati [7], the two-particle Green's function is separated as $K_{ss';ss'}(1,2;1',2') = G_s(1,1')G_{s'}(2,2') - L_{ss';ss'}(1,2;1',2')$. Then, the first GG term can be included in the one-body term as the Hartree potential $v^{\rm H}(\boldsymbol{r}_1)$ in Eq. (2.46). This corresponds to separating the self-energy into two terms, $\Sigma_s(1,2) = \Sigma^{\rm H}(1,2) + M_s(1,2)$; the first and second terms represent, respectively, the Hartree term $v^{\rm H}(\boldsymbol{r}_1)\delta(1,2)$ and the exchange-correlation (xc) term [7]. The density-density correlation function χ is related to L as [7]

$$\chi(1,2) = \int d3\, \widetilde{\chi}(1,3)\varepsilon^{-1}(3,2) = -i\sum_{ss'} L_{ss';ss'}(1,2;1^+,2^+),$$

where $\widetilde{\chi}$ and ε^{-1} denote, respectively, the polarization function (which is also called irreducible polarizability, Eq. (2.57)) and the inverse of the dielectric function. The polarization function $\widetilde{\chi}(1,3) = -i\sum_s R_s(1,3,1^+,3^+)$ can be calculated from

$$R_s(1,3;2,3^+) = \int d(44')G_s(1,4)G_s(4',2)\widetilde{\Gamma}_s(4,4';3), \tag{4.41}$$

where the scalar vertex function satisfies the Bethe–Salpeter equation (BSE) [6, 7, 50, 54] (see also Fig. 4.3)

$$\begin{aligned}\widetilde{\Gamma}_s(1,2;3) &= \delta(1,3)\delta(2,3) + \sum_{s''}\int d(44'55') \\ &\times \frac{\delta M_s(1,2)}{\delta G_{s''}(4',4)} G_{s''}(4',5)G_{s''}(5',4)\widetilde{\Gamma}_{s''}(5,5';3).\end{aligned} \tag{4.42}$$

Then, the dielectric function is given by

$$\varepsilon(1,2) = \delta(1,2) - \int d(33')\, \frac{\delta\, v^{\rm H}(\boldsymbol{r}_1)}{\delta G_{s''}(3',3)} R_{s'}(3',2;3,2^+), \tag{4.43}$$

and

$$\begin{aligned}\sum_{s'} L_{ss';ss'}(1,3;2,3^+) &= \int d4\, R_s(1,4;2,4^+)\varepsilon^{-1}(4,3) \\ &= \int d(455')G_s(1,5)G_s(5',2)\widetilde{\Gamma}_s(5,5';4)\varepsilon^{-1}(4,3).\end{aligned}$$

Inserting this expression into Eq. (2.46) and rewriting Eq. (2.49) as

$$i\partial_{t_1}G_s(1,2) - [\,h_s(\boldsymbol{r}_1) + v^{\rm H}(\boldsymbol{r}_1)\,]G_s(1,2) - \int d3\, M_s(1,3)G_s(3,2) = \delta(1,2), \tag{4.44}$$

We find Hedin's GWΓ expression [6, 54] for $M_s(1,3)$

$$M_s(1,2) = i\int d(34)G_s(1,3)W(1^+,4)\widetilde{\Gamma}_s(3,2;4), \tag{4.45}$$

where W denotes the dynamically screened Coulomb interaction defined by $W(1,2) = \int d3\, \varepsilon^{-1}(1,3)V(3,2)$.

All the above is the exact formulation satisfying the conservation laws [7, 67].

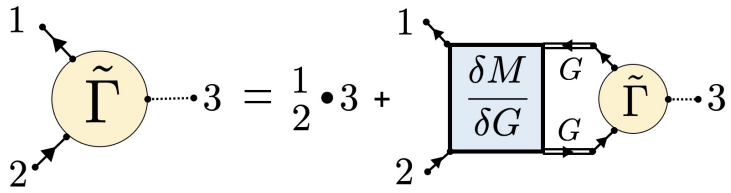

FIGURE 4.3: Diagrammatic representation of the BSE for the vertex function $\widetilde{\Gamma}_s(1,2;3)$.

Now please notice that, although $\widetilde{\Gamma}_{q=0}(1,2)$ does not have the third argument "3", it satisfies the BSE

$$\widetilde{\Gamma}_{q=0\,s}(1,2) = \delta(1,2) + \sum_{s''}\int d(44'55') \times \frac{\delta M_s(1,2)}{\delta G_{s''}(4',4)} G_{s''}(4',5) G_{s''}(5',4) \widetilde{\Gamma}_{q=0\,s''}(5,5'), \tag{4.46}$$

which has exactly the same form as the BSE for $\widetilde{\Gamma}_s(1,2;3)$ Eq. (4.42) (see Fig. 4.3). Equation (4.46) can be obtained by integrating Eq. (4.42) with respect to "3" because $\int d3\,\widetilde{\Gamma}_s(1,2;3) = \widetilde{\Gamma}_{q=0\,s}(1,2)$; see, for example, Eq. (7.22) of Ref. [7]. Since the $q \to 0$ limit corresponds to ignoring all multiple excitations produced by energy-momentum transfer in terms of Coulomb interaction, the replacement of $\Gamma_s(1,2;3)$ with $\Gamma_{q=0\,s}(1,2)$ corresponds to treating everything as if there is only one electron or hole in the $(N \pm 1)$-electron states $|\,\Psi_\lambda^{N\pm1}\,\rangle$ (see Fig. 4.1). Therefore, the function associated with it's expectation value $\Gamma^{\rm ren}_{q=0\,s}(1,2)$ has a meaning of the renormalization factor of such a purely one-electron or one-hole quasiparticle (QP) state. The procedure to factor out $\Gamma^{\rm ren}_{q=0\,s}(1,1')$ or $\Gamma^{\rm ren}_{q=0\,s}(2',2)$ symmetrically from $\Gamma_s(1,2;3)$ as Eq. (4.34) is now possible by construction. Then, the BSE for the vertex function (see Eq. (4.42) and Fig. 4.3) becomes that for the renormalized one with $\Gamma^{\rm ren}_{q=0\,s}$ factored out:

$$\bar{\Gamma}_s(1,2;3) = \Gamma^{{\rm ren}\,-1}_{q=0\,s}(1,3)\delta(2,3) + \sum_{s''}\int d(1'44'55') \times \Gamma^{{\rm ren}\,-1}_{q=0\,s}(1,1')\frac{\delta M_s(1',2)}{\delta \bar{G}_{s''}(4',4)} \bar{G}_{s''}(4',5)\bar{G}_{s''}(5',4)\bar{\Gamma}_{s''}(5,5';3). \tag{4.47}$$

Next, we can find that the exchange-correlation part of the self-energy Eq. (4.45) becomes

$$M_s(1,2) = i\int d(34)\bar{G}_s(1,3)W(1^+,4)\bar{\Gamma}_s(3,2;4), \tag{4.48}$$

and the dielectric function Eq. (4.43) with $R_{s'}(3',2;3,2^+)$ becomes

$$\varepsilon(1,2) = \delta(1,2) - \int d(33'44')\,\frac{\delta\, v^{\rm H}(\boldsymbol{r}_1)}{\delta \bar{G}_{s''}(3',3)}\bar{G}_s(3',4)\bar{G}_s(4',3)\bar{\Gamma}_s(4,4';2). \tag{4.49}$$

Although the calculation of the Hartree potential $v^{\rm H}(\boldsymbol{r}_1)$ by the original QP wave functions, *i.e.*, the original G, was difficult, it is now easy by using the renormalized

$\bar{G}$ as

$$v^{\mathrm{H}}(\boldsymbol{r}_1) = -i\sum_s \int d2\, v(1,2)\bar{G}_s(2,2^+). \tag{4.50}$$

Then, Eq. (4.49) becomes $\varepsilon(1,2) = \delta(1,2) - \int d3\, v(1,3)\widetilde{\chi}(3,2)$ with the polarization function,

$$\widetilde{\chi}(3,2) = -i\sum_s \int d(44')\bar{G}_s(3,4)\bar{G}_s(4',3^+)\bar{\Gamma}_s(4,4';2). \tag{4.51}$$

Finally, the dynamically screened Coulomb interaction W and the exchange-correlation part of the self-energy as well as the Hartree potential are completely expressed only by $\bar{G}$ and $\bar{\Gamma}$. This form is no other than the full $GW\Gamma$ formula but with G and Γ replaced by $\bar{G}$ and $\bar{\Gamma}$. Thus the present study succeeded in including the renormalization function Eq. (4.29) in the formulation, and established the exact self-consistent $GW\Gamma$ form with the normalized QPWFs.

4.5 Conclusion

In summary, what we have to do is to simply normalize all the quasiparticle wave functions (QPWFs) to unity, although the quasiparticle (QP) energies are complex. The point is that the two-time spin density matrix Eq. (4.36b) is expressed by N normalized wave functions $\bar{\phi}_i(1)$. Then, the present theory proved that these functions exactly satisfy the same equation as the time-dependent QP equation (4.35). Thus, the exact equivalence between the normalized wave functions $\bar{\phi}_i(1)$ and the QPWFs $\phi_\mu(1)$ (except for the normalization factor) was established for the time-dependent case. This is a very reasonable conclusion because each hole (electron) QP state associated with one final photoemission (PE) $|\,\Psi_\mu^{N-1}\,\rangle$ (inverse photoemission (IPE) $|\,\Psi_\nu^{N+1}\,\rangle$) state should have a norm equal to the amount of one electron exactly. It is clear that the same statement holds for the time-independent case also. If the spin density matrix defined by $\rho_s(\boldsymbol{r}_1,\boldsymbol{r}_2) = \langle\,\Psi_0^N\,|\,\psi_s^\dagger(\boldsymbol{r}_2)\psi_s(\boldsymbol{r}_1)\,|\,\Psi_0^N\,\rangle$ is expressed by N normalized wave functions $\bar{\phi}_i(\boldsymbol{r})$ as $\rho_s(\boldsymbol{r}_1,\boldsymbol{r}_2) = \sum_i^N \bar{\phi}_i(\boldsymbol{r}_1,s)\bar{\phi}_i^*(\boldsymbol{r}_2,s)$, these functions satisfy exactly the same equation as the time-independent QP equation (2.78a). All these facts imply that one can normalize the QPWFs, although they are not necessarily mutually orthogonal. Here, Baym-Kadanoff's conservation law [7, 67] guarantees that we can solve the QP equation with the hermitized self-energy Eq. (4.13a).

I emphasize that to normalize the QPWFs is equivalent to taking into account the Ward identity. The vertex function in the limit $q \to 0$ counts the $(N \pm 1)$-electron states $|\,\Psi_\lambda^{N\pm1}\,\rangle$ with purely one electron or hole only, and has an effect to normalize the corresponding QPWFs as Eq. (4.25), ignoring all spontaneous multiple excitations not related to the momentum-energy transfer in terms of Coulomb interaction (see Fig. 4.1). Therefore, to normalize the QPWFs is equivalent to replace G and Γ, respectively, with $\bar{G}$ normalized by $\Gamma^{\rm ren}_{q=0}$ and $\bar{\Gamma}$ factored out by $\Gamma^{\rm ren}_{q=0}$ everywhere. If we assume $\bar{\Gamma}_s(1,2;3) = \delta(1,3)\delta(2,3)$, we obtain the renormalized self-consistent GW approximation, in which G is replaced everywhere by $\bar{G}$. This is not equivalent to the original self-consistent GW approximation because $\widetilde{\Gamma}_s(1,2;3) = \Gamma^{\rm ren}_{q=0\,s}(1,3)\delta(2,3)$ is not equal to $\delta(1,3)\delta(2,3)$. The procedure is similar to that proposed by Holm and von Barth [57, 93] but the QP energies should be treated as complex numbers. Although the present theory was explained for the ground state as the initial state, it is applicable to the excited states also by using the approach given by Ohno *et al.* [44, 45].

Finally, let me make a comment on Kohn-Sham's formulation of density functional theory (DFT). In their original paper[4], they never wrote that the Kohn-Sham (KS) orbitals are mutually orthogonal, although they assumed their normalization. If we accept this interpretation for KS theory (see Eqs. 4.13), the present formulation of the self-consistent $GW\Gamma$ (or self-consistent GW) approach using the normalized QPWFs can be regarded as an extension of KS theory. Although an indirect relationship between the KS potential and the self-energy has been achieved by Sham and Schlüter [20, 27], what the present study achieved is their direct equivalence in a hermitized form Eq. (4.13a), which is exact. The only difference from the traditional DFT is that the QPWFs are not necessarily orthogonal to each other, because the self-energy is energy dependent. This consideration implicitly shows the justification of the non-local effective potential and of their energy dependent (which is equal to orbital dependent, such as Hubbard $+U$ scheme) in the KS framework, which gives the favor to the generalized KS framework also[37]. A non-orthogonality actually implies that the QPWFs are interacting, or correlated, in contrast to the fictitious non-interacting KS orbitals.

Chapter 5

Summary

This doctoral thesis consists of an overview of two papers; (i) Takeru Nakashima and Kaoru Ohno. "Spin-Orbit Coupling in All-electron Mixed Basis Approach". *Annalen der Physik*, 531 9: 1900060 (2019)[1] and (ii) Takeru Nakashima, Hannes Raebiger, and Kaoru Ohno. "Normalization of exact quasiparticle wave functions in the Green's function method guaranteed by the Ward identity". *Physical Review B* 104 20: L2011116 (2021)[2].

As the first study, I developed the method to calculate the spin-orbit coupling (SOC) in all-electron mixed basis approach, and which takes into account the SOC contributed from the valence electrons and the core electrons efficiently. The calculation results show the good agreement with the experimental results, which suggests the present method.

As the second study, I gave the justification to normalize the quasiparticle wave functions in quasiparticle (QP) theory and introduced the extended Kohn-Sham (KS) equation (see Eqs. 4.13). In the case of the limit of the vertex function $q \to 0$, I introduce the interpretation that there are spontaneous multiple excitations not related to momentum-energy transfer in terms of the Coulomb interaction (see Figs. 4.1 and 4.2). Therefore, the factoring out the limit of the vertex function $\Gamma^{\mathrm{ren}}_{q=0}$ corresponds to the elimination of spontaneous multiple excitations (see Fig. 4.1). Additionally, I showed that under the Baym-Kadanoff's conservation law, the one-particle Green's function satisfies the left- and right-eigenvalue equation, which gives the two type equations having the real part of the QP energy and the imaginary part of the QP energy as eigenvalues, respectively (see Eqs. 4.13). This equation is obtained from hermitizing the self-energy of the original QP equation and which is interpreted as extended KS equation.

Appendix A

Green's function and quasiparticle

Mathematically, the Green's function method is the very famous technique which solve integral problems and which has been widely applied in many-body problems[48]. This appendix is devoted to the explanation for the mathematical Green's function and the quasiparticle wave functions (QPWFs) derived from the bilinear diagonal expansion.

A.1 What is Green's function mathematically?

The Green's function is the useful technique combining the differential and integral equations. Firstly, suppose the differential equation

$$\hat{F}(x)h(x) = g(x), \tag{A.1}$$

where $\hat{F}(x)$ is the differential operator in the function space. For simplicity, introducing the abstract form $\langle x \,|\, h \rangle = h(x)$, $\langle x \,|\, g \rangle = g(x)$, and $\delta(x - x')\hat{F}(x) = \langle x \,|\, F \,|\, x' \rangle$, Eq. (A.1) becomes

$$F \,|\, h \rangle = |\, g \rangle, \tag{A.2}$$

where F is assumed as hermitian linear operator. Also, we can introduce a linear operator G and a linear transformation as

$$|\, h \rangle = G \,|\, g \rangle, \tag{A.3}$$

Substituting Eq. (A.3) into Eq. (A.2) shows that

$$FG = 1. \tag{A.4}$$

In the function space, G in Eq. (A.3) corresponds to the integral kernel

$$h(x) = \int dx' G(x, x') g(x'),$$

where $G(x, x') = \langle x \,|\, G \,|\, x' \rangle$ and Eq. (A.4) is equal to $\hat{F}(x)G(x, x') = \delta(x - x')$. Generally, this integral kernel or linear operator G is called Green's function. This kernel G can convert the original complex Eq. (A.2) to simple Eq. (A.4).

Consider the Hermitian eigenvalue problems

$$F \,|\, f_i \rangle = a_i \,|\, f_i \rangle, \ \langle f_i \,|\, f_j \rangle = \delta_{i,j} \tag{A.5}$$

where f_i and a_i are eigenstates and eigenvalues, respectively. Using these eigenstates, any state $|\, \phi \rangle$ is expanded as $|\, \phi \rangle = \sum_i |\, f_i \rangle \langle f_i \,|\, \phi \rangle$. Combining Eqs. (A.2)

and (A.5) gives

$$a_i \langle f_i \,|\, h \rangle = \langle f_i \,|\, g \rangle. \tag{A.6}$$

If $a_i \neq 0$, $|\, h \rangle$ can be expanded as

$$|\, h \rangle = \sum_i \frac{1}{a_i} |\, f_i \rangle \langle f_i \,|\, g \rangle, \tag{A.7}$$

and both Eqs. (A.3) and (A.7) show that the Green's function G is

$$G = \sum_i \frac{|\, f_i \rangle \langle f_i \,|}{a_i} \; ; \; a_i \neq 0. \tag{A.8}$$

Here, the point is that the Green's function is expanded by the orthogonal normalized basis. This bilinear diagonal expansion is used for the first QPWFs derivation (see appendix A.2) There is difference between the QPWFs appearing in the first derivation[71] and the QPWFs appearing in the main part of this doctoral thesis. The QPWFs appearing in the main part of this doctoral thesis are not orthogonal mutually because those QPWFs are the eigenstates for the Dyson equation. Therefore, we can not treat QPWFs in similar way shown here. This difference is important.

A.2 Quasiparticle approximation

The concept of the quasiparticle (QP) is treated as approximation and called QP approximation[26, 50, 71]. It is true that the original concept of QPs, introduced by Landau, is approximation. However, the QPs appearing in the main part of this doctoral thesis is not approximation In this appendix, I explain the derivation of the QP concept by approximation method using left- and right-eigenvalue problems.

In the Klein and Prange's paper (1968)[63], the QP equation is introduced firstly, and in few years later the derivation for the QP equation is given using the left- and right-eigenvalue problems. The derivation using the left- and right-eigenvalue problem is basic method. In this method, the one-particle Green's function is assumed to be spectral form, that is, the one-particle Green's function is expanded by the diagonal bilinear expansion in the sets of eigenfunctions for left- and right-eigenvalue problems[26, 71, 101]. Specifically, the one-particle Green's function is assumed to be expanded as follows

$$G(\omega) = \sum_{\lambda} \frac{|\,\phi_\lambda(\omega)\,\rangle\langle\,\psi_\lambda(\omega)\,|}{\omega - E_\lambda(\omega)}, \tag{A.9}$$

where $\langle\,\psi_\lambda(\omega)\,|$ and $|\,\phi_\lambda(\omega)\,\rangle$ are eigenstates for the left-eigenvalue equations and the right-eigenvalue equations, respectively,

$$\langle\,\psi_\lambda(\omega)\,|\;(h+\Sigma(\omega)) = \langle\,\psi_\lambda(\omega)\,|\,E_\lambda(\omega), \tag{A.10a}$$
$$(h+\Sigma(\omega))\;|\,\phi_\lambda(\omega)\,\rangle = E_\lambda(\omega)\,|\,\phi_\lambda(\omega)\,\rangle. \tag{A.10b}$$

In the following discussion, the representation $L(\omega) = h + \Sigma(\omega)$ is used for simplicity. Eqs. (A.10) show that the eigenstates orthogonality; $\langle\,\psi_\lambda(\omega)\,|\,\phi_{\lambda'}(\omega)\,\rangle = \delta_{\lambda,\lambda'}$

$$\{\langle\,\psi_\lambda(\omega)\,|\,L(\omega)\}\;\;|\,\phi_{\lambda'}(\omega)\,\rangle = E_\lambda(\omega)\langle\,\psi_\lambda(\omega)\,|\,\phi_{\lambda'}(\omega)\,\rangle, \tag{A.11a}$$
$$\langle\,\psi_\lambda(\omega)\,|\;\;\{L(\omega)\,|\,\phi_{\lambda'}(\omega)\,\rangle\} = E_{\lambda'}(\omega)\langle\,\psi_\lambda(\omega)\,|\,\phi_{\lambda'}(\omega)\,\rangle. \tag{A.11b}$$

Eqs. (A.11) lead the orthogonality for the left- and right- eigenstates

$$\langle\,\psi_\lambda(\omega)\,|\,\phi_{\lambda'}(\omega)\,\rangle = \delta_{\lambda,\lambda'}. \tag{A.12}$$

From this orthogonality, the representation for the one-particle Green's function Eq. (A.9) is valid, which is easily verified through the discussion in appendix A.1. (This frame work using the spectral form Eq. (A.9) is also called h approximation[71])

In the QP approximation, the one-particle Green's function has simple poles, *i.e.* $\epsilon_\lambda = E_\lambda(\epsilon_\lambda)$. Taking into account the norm of the QPs, the one-particle Green's function is represented by

$$G(\omega) \simeq \sum_{\lambda} g_\lambda \frac{|\,\phi_\lambda\,\rangle\langle\,\psi_\lambda\,|}{\omega - \varepsilon_\lambda}, \tag{A.13}$$

where $\phi_\lambda = \phi_\lambda(\varepsilon_\lambda)$, $\psi_\lambda = \psi_\lambda(\varepsilon_\lambda)$, and $g_\lambda^{-1} = 1 - (\partial/\partial\omega)\,E_\lambda|_{\omega=\varepsilon_\lambda}$. The first derivation for the QP equation is done in the Layzer ' s paper[71]. In this Layzer's derivation, the QPWFs are defined through the left- and right-eigenvalue equations. This Green's function spectra form is the QP approximation, which takes into account the norm of the QP states unlike the h approximation. However, please notice that in this

doctoral paper, the QPWFs are defined by Eqs. (2.70) using the electron field Heisenberg operator and the many-body eigenstates Ψ_0^N, $\Psi_\lambda^{N\pm1}$, and through the discussion in subsection 2.4.5, there are no approximation in the introduction of quasiparticle wave functions representing the one-particle Green's function. Therefore, the quasiparticle wave functions appearing in our discussion are not approximation.

Appendix B

Homogeneous system

The fundamental theories on the Green's function and the quasiparticle wave functions (QPWFs) have been established for a homogeneous system, *i.e.*, translational symmetry in space, in condensed matter physics. In this doctoral thesis, the Green's function is not restricted to a homogeneous system, but it is very helpful to know the knowledge of the Green's function in the homogeneous system. Therefore, I put the brief explanation of the theories for the homogeneous system.

B.1 The coherent and incoherent part of the Green's function

In the case where the system has the translational symmetry, the Green's function has the following form

$$G(\boldsymbol{r}_1 - \boldsymbol{r}_2|\omega) = G(\boldsymbol{r}_1, \boldsymbol{r}_2|\omega), \tag{B.1}$$

and the Fourier transformation is

$$G(\boldsymbol{k}|\omega) = \int d\boldsymbol{r}\, G(\boldsymbol{r}|\omega) e^{-i\boldsymbol{k}\cdot\boldsymbol{r}}. \tag{B.2}$$

Using the above Fourier transformation, the Dyson equation becomes

$$\left(\omega - h(\boldsymbol{k}|\omega) - \Sigma(\boldsymbol{k})\right) G(\boldsymbol{k}|\omega) = 1, \tag{B.3}$$

where convolution product becomes the direct product through the Fourier transformation and $\omega - h(\boldsymbol{k}) - \Sigma(\boldsymbol{k}|\omega)$ is a scalar function. Therefore, in the system the translational symmetry is satisfied, the Green's function is represented by

$$G(\boldsymbol{k}|\omega) = \frac{1}{\omega - h(\boldsymbol{k}) - \Sigma(\boldsymbol{k}|\omega)}. \tag{B.4}$$

The pole of the Green's is obtained from the solution for $\omega - h(\boldsymbol{k}) - \Sigma(\boldsymbol{k}|\omega) = 0$. Here, the self-energy is supposed as smooth function and the root is $\varepsilon_{\boldsymbol{k}}$. From this consideration, the Green's function is considered as following form

$$G(\boldsymbol{k}|\omega) = \frac{f_{\boldsymbol{k}}(\omega)}{\omega - \varepsilon_{\boldsymbol{k}}}, \tag{B.5}$$

where $\varepsilon_{\boldsymbol{k}} = h(\boldsymbol{k}) + \Sigma(\boldsymbol{k}|\varepsilon_{\boldsymbol{k}})$ (which is the pole of $G(\boldsymbol{k}|\omega)$) and $f_{\boldsymbol{k}}(\omega)$ is defined by

$$f_{\boldsymbol{k}}(\omega) = \left(1 - \frac{\Sigma(\boldsymbol{k}|\omega) - \Sigma(\boldsymbol{k}|\varepsilon_{\boldsymbol{k}})}{\omega - \varepsilon_{\boldsymbol{k}}}\right)^{-1}. \tag{B.6}$$

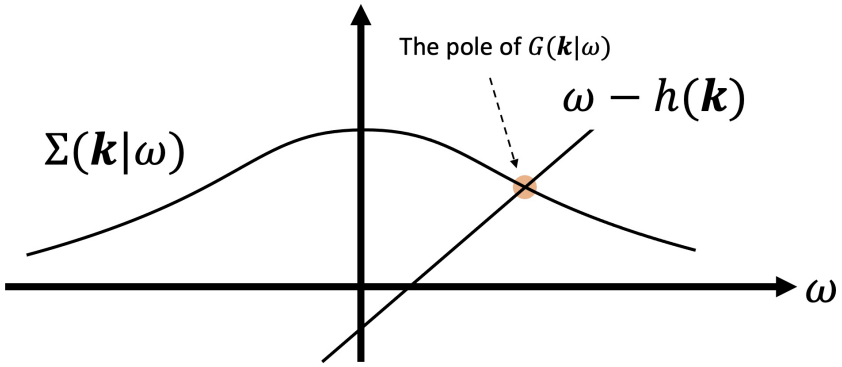

FIGURE B.1: The pole of the Green's function in the homogeneous system

Please notice that $f_{\boldsymbol{k}}(\omega)$ is considered smooth function. Considering the Taylor expansion of $f_{\boldsymbol{k}}(\omega)$ around the pole $\varepsilon_{\boldsymbol{k}}$, the Green's function is divide to two part, *i.e.*, coherent part, which is the first term in Eq. (B.7), and incoherent part,

$$G(\boldsymbol{k}|\omega) = \frac{Z_{\boldsymbol{k}}}{\omega - \varepsilon_{\boldsymbol{k}}} + (\text{incoherent part}), \tag{B.7}$$

where $Z_{\boldsymbol{k}} = f_{\boldsymbol{k}}(\varepsilon_{\boldsymbol{k}})$ and the incoherent part is the sum of a remaining terms except 0-th Taylor expansion term of $f_{\boldsymbol{k}}(\omega)$, which are regular at the pole; $\omega = \varepsilon_{\boldsymbol{k}}$, specifically,

$$Z_{\boldsymbol{k}} = \left(1 - \frac{\partial \Sigma(\boldsymbol{k}|\omega)}{\partial \omega}\bigg|_{\omega=\epsilon_{\boldsymbol{k}}}\right)^{-1}. \tag{B.8}$$

The Ward identity for the homogeneous space is

$$\Gamma(\boldsymbol{k}; \boldsymbol{q} = 0|\omega, \omega) = 1 - \frac{\partial \Sigma(\boldsymbol{k}|\omega)}{\partial \omega}, \tag{B.9}$$

which shows that

$$Z_{\boldsymbol{k}} \times \Gamma(\boldsymbol{k}; \boldsymbol{q} = 0|\epsilon_{\boldsymbol{k}}, \epsilon_{\boldsymbol{k}}) = 1. \tag{B.10}$$

Equation (B.10) shows that the one-particle Green's function is represented by

$$G(\boldsymbol{k}|\omega) = \frac{\Gamma^{-1}(\boldsymbol{k}; \boldsymbol{q} = 0|\epsilon_{\boldsymbol{k}}, \epsilon_{\boldsymbol{k}})}{\omega - \varepsilon_{\boldsymbol{k}}} + (\text{incoherent part}). \tag{B.11}$$

Using abbreviation, $\Gamma_{q=0}(\boldsymbol{k}|\omega)$ and $W_q = W(\boldsymbol{q}, \eta)$, the above equation yields

$$G(\boldsymbol{k}|\omega)W_{q=0}\Gamma_{q=0}(\boldsymbol{k}|\epsilon_{\boldsymbol{k}}) = \bar{G}(\boldsymbol{k}|\omega)W_{q=0} + W_{q=0}\Gamma_{q=0}(\boldsymbol{k}|\epsilon_{\boldsymbol{k}}) \times (\text{incoherent part}), \tag{B.12}$$

where $\bar{G}(\boldsymbol{k}|\omega) = 1/(\omega - \epsilon_{\boldsymbol{k}})$ denotes the renormalized Green's function composed of the normalized QPWFs. Please notice that the coherent part and the incoherent part are defined in the wave vector space and Eq. (B.7) is definition, which means that the incoherent part is not defined in real position vector space, generally.

Bibliography

[1] Takeru Nakashima and Kaoru Ohno. "Spin-Orbit Coupling in All-Electron Mixed Basis Approach". In: *Annalen der Physik* 531.9 (2019), p. 1900060.

[2] Takeru Nakashima, Hannes Raebiger, and Kaoru Ohno. "Normalization of exact quasiparticle wave functions in the Green's function method guaranteed by the Ward identity". In: *Physical Review B* 104.20 (2021), p. L201116.

[3] Pierre Hohenberg and Walter Kohn. "Inhomogeneous electron gas". In: *Physical review* 136.3B (1964), B864.

[4] Walter Kohn and Lu Jeu Sham. "Self-consistent equations including exchange and correlation effects". In: *Physical review* 140.4A (1965), A1133.

[5] Ulf Von Barth and Lars Hedin. "A local exchange-correlation potential for the spin polarized case. i". In: *Journal of Physics C: Solid State Physics* 5.13 (1972), p. 1629.

[6] Lars Hedin. "New method for calculating the one-particle Green's function with application to the electron-gas problem". In: *Physical Review* 139.3A (1965), A796.

[7] Giancarlo Strinati. "Application of the Green's functions method to the study of the optical properties of semiconductors". In: *La Rivista del Nuovo Cimento (1978-1999)* 11.12 (1988), pp. 1–86.

[8] Gy Csanak, HS Taylor, and Robert Yaris. "Green's function technique in atomic and molecular physics". In: *Advances in atomic and molecular physics*. Vol. 7. Elsevier, 1971, pp. 287–361.

[9] Giovanni Onida, Lucia Reining, and Angel Rubio. "Electronic excitations: density-functional versus many-body Green's-function approaches". In: *Reviews of modern physics* 74.2 (2002), p. 601.

[10] Lev Davidovich Landau. "The theory of a Fermi liquid". In: *Soviet Physics Jetp-Ussr* 3.6 (1957), pp. 920–925.

[11] LD Landau. "SOV PHYS JETP". In: *Sov. Phys. JETP* 5 (1957), p. 101.

[12] Lev Davidovich Landau and Evgenii Mikhailovich Lifshitz. *Course of theoretical physics*. Elsevier, 2013.

[13] Leslie L Foldy and Siegfried A Wouthuysen. "On the Dirac theory of spin 1/2 particles and its non-relativistic limit". In: *Physical Review* 78.1 (1950), p. 29.

[14] Mark S Hybertsen and Steven G Louie. "Electron correlation and the band gap in ionic crystals". In: *Physical Review B* 32.10 (1985), p. 7005.

[15] Mark S Hybertsen and Steven G Louie. "Spin-orbit splitting in semiconductors and insulators from the ab initio pseudopotential". In: *Physical Review B* 34.4 (1986), p. 2920.

[16] Giovanni B Bachelet and M Schlüter. "Relativistic norm-conserving pseudopotentials". In: *Physical Review B* 25.4 (1982), p. 2103.

[17] Shota Ono et al. "TOMBO: All-electron mixed-basis approach to condensed matter physics". In: *Computer physics communications* 189 (2015), pp. 20–30.

[18] Mark S Hybertsen and Steven G Louie. "First-principles theory of quasiparticles: calculation of band gaps in semiconductors and insulators". In: *Physical review letters* 55.13 (1985), p. 1418.

[19] RW Godby, M Schlüter, and LJ Sham. "Accurate exchange-correlation potential for silicon and its discontinuity on addition of an electron". In: *Physical review letters* 56.22 (1986), p. 2415.

[20] Rex W Godby, Michael Schlüter, and LJ Sham. "Self-energy operators and exchange-correlation potentials in semiconductors". In: *Physical Review B* 37.17 (1988), p. 10159.

[21] Patrick Rinke et al. "Combining GW calculations with exact-exchange density-functional theory: an analysis of valence-band photoemission for compound semiconductors". In: *New Journal of Physics* 7.1 (2005), p. 126.

[22] John Clive Ward. "An identity in quantum electrodynamics". In: *Physical Review* 78.2 (1950), p. 182.

[23] Yasushi Takahashi. "On the generalized Ward identity". In: *Il Nuovo Cimento (1955-1965)* 6.2 (1957), pp. 371–375.

[24] G Strinati, HJ Mattausch, and W Hanke. "Dynamical aspects of correlation corrections in a covalent crystal". In: *Physical Review B* 25.4 (1982), p. 2867.

[25] Robert O Jones and Olle Gunnarsson. "The density functional formalism, its applications and prospects". In: *Reviews of Modern Physics* 61.3 (1989), p. 689.

[26] L. J. Sham and W. Kohn. "One-particle properties of an inhomogeneous interacting electron gas". In: *Physical Review* 145.2 (1966), pp. 561–567. ISSN: 0031899X. DOI: 10.1103/PhysRev.145.561.

[27] Lu J Sham and Michael Schlüter. "Density-functional theory of the energy gap". In: *Physical Review Letters* 51.20 (1983), p. 1888.

[28] RW Godby, M Schlüter, and LJ Sham. "Trends in self-energy operators and their corresponding exchange-correlation potentials". In: *Physical Review B* 36.12 (1987), p. 6497.

[29] Mark S Hybertsen and Steven G Louie. "Electron correlation in semiconductors and insulators: Band gaps and quasiparticle energies". In: *Physical Review B* 34.8 (1986), p. 5390.

[30] CS Wang and WE Pickett. "Density-functional theory of excitation spectra of semiconductors: application to Si". In: *Physical review letters* 51.7 (1983), p. 597.

[31] WE Pickett and CS Wang. "Local-density approximation for dynamical correlation corrections to single-particle excitations in insulators". In: *Physical Review B* 30.8 (1984), p. 4719.

[32] Klaus Capelle and Vivaldo L Campo Jr. "Density functionals and model Hamiltonians: Pillars of many-particle physics". In: *Physics Reports* 528.3 (2013), pp. 91–159.

[33] Victor L Moruzzi, James F Janak, and Arthur R Williams. *Calculated electronic properties of metals*. Elsevier, 2013.

[34] Leonard Kleinman. "Exchange density-functional gradient expansion". In: *Physical Review B* 30.4 (1984), p. 2223.

[35] Axel D Becke. "Density-functional exchange-energy approximation with correct asymptotic behavior". In: *Physical review A* 38.6 (1988), p. 3098.

[36] DM Bylander, Leonard Kleinman, and Seongbok Lee. "Self-consistent calculations of the energy bands and bonding properties of B 12 C 3". In: *Physical Review B* 42.2 (1990), p. 1394.

[37] A Seidl et al. "Generalized Kohn-Sham schemes and the band-gap problem". In: *Physical Review B* 53.7 (1996), p. 3764.

[38] Paul Adrien Maurice Dirac. "The quantum theory of the electron". In: *Proceedings of the Royal Society of London. Series A, Containing Papers of a Mathematical and Physical Character* 117.778 (1928), pp. 610–624.

[39] Steven G Louie, Kai-Ming Ho, and Marvin L Cohen. "Self-consistent mixed-basis approach to the electronic structure of solids". In: *Physical Review B* 19.4 (1979), p. 1774.

[40] Tsubasa Aoki and Kaoru Ohno. "Accurate quasiparticle calculation of x-ray photoelectron spectra of solids". In: *Journal of Physics: Condensed Matter* 30.21 (2018), 21LT01.

[41] Riichi Kuwahara and Kaoru Ohno. "Linearized self-consistent GW approach satisfying the Ward identity". In: *Physical Review A* 90.3 (2014), p. 032506.

[42] Riichi Kuwahara, Yoshifumi Noguchi, and Kaoru Ohno. "GW Γ+ Bethe-Salpeter equation approach for photoabsorption spectra: Importance of self-consistent GW Γ calculations in small atomic systems". In: *Physical Review B* 94.12 (2016), p. 121116.

[43] Kaoru Ohno, Francesco Mauri, and Steven G Louie. "Magnetic susceptibility of semiconductors by an all-electron first-principles approach". In: *Physical Review B* 56.3 (1997), p. 1009.

[44] Kaoru Ohno, Shota Ono, and Tomoharu Isobe. "A simple derivation of the exact quasiparticle theory and its extension to arbitrary initial excited eigenstates". In: *The Journal of chemical physics* 146.8 (2017), p. 084108.

[45] Kaoru Ohno, Keivan Esfarjani, and Yoshiyuki Kawazoe. *Computational materials science: from ab initio to Monte Carlo methods*. Springer, 2018.

[46] Richard Phillips Feynman. "Space-time approach to non-relativistic quantum mechanics". In: *Feynman's Thesis—A New Approach To Quantum Theory* (2005), pp. 71–109.

[47] Julian Schwinger. "On the Green's functions of quantized fields. I". In: *Proceedings of the National Academy of Sciences* 37.7 (1951), pp. 452–455.

[48] Viktor Mikhailovich Galitskii and Arkadii Beinusovich Migdal. "Application of quantum field theory methods to the many body problem". In: *Sov. Phys. JETP* 7.96 (1958), p. 18.

[49] Joaquin Mazdak Luttinger and John Clive Ward. "Ground-state energy of a many-fermion system. II". In: *Physical Review* 118.5 (1960), p. 1417.

[50] Philippe Nozieres. *Theory of interacting Fermi systems*. CRC Press, 2018.

[51] Jeffrey Goldstone. "Derivation of the Brueckner many-body theory". In: *Proceedings of the Royal Society of London. Series A. Mathematical and Physical Sciences* 239.1217 (1957), pp. 267–279.

[52] John Hubbard. "The description of collective motions in terms of many-body perturbation theory". In: *Proceedings of the Royal Society of London. Series A. Mathematical and Physical Sciences* 240.1223 (1957), pp. 539–560.

[53] David Pines. *The many-body problem: a lecture note and reprint volume*. WA Benjamin, 1962.

[54] Lars Hedin and Stig Lundqvist. "Effects of electron-electron and electron-phonon interactions on the one-electron states of solids". In: *Solid state physics*. Vol. 23. Elsevier, 1970, pp. 1–181.

[55] DNA Zubarev. "Double-time Green functions in statistical physics". In: *Soviet Physics Uspekhi* 3.3 (1960), p. 320.

[56] Gian-Carlo Wick. "The evaluation of the collision matrix". In: *Physical review* 80.2 (1950), p. 268.

[57] Bengt Holm and Ulf von Barth. "Fully self-consistent GW self-energy of the electron gas". In: *Physical Review B* 57.4 (1998), p. 2108.

[58] Ferdi Aryasetiawan and Olle Gunnarsson. "The GW method". In: *Reports on Progress in Physics* 61.3 (1998), p. 237.

[59] Murray Gell-Mann and Francis Low. "Bound states in quantum field theory". In: *Physical Review* 84.2 (1951), p. 350.

[60] C Bloch and C De Dominicis. "A DEVELOPMENT OF THE GIBBS POTENTIAL OF A QUANTIC SYSTEM COMPOSED OF A LARGE NUMBER OF PARTICLES". In: *Nuclear Phys.* 7 (1958).

[61] M Gaudin. "A SIMPLIFIED DEMONSTRATION OF WICK'S THEOREM IN STATISTICAL MECHANICS". In: *Nuclear Phys.* 15 (1960).

[62] Alexander L Fetter and John Dirk Walecka. *Quantum theory of many-particle systems*. Courier Corporation, 2012.

[63] Abraham Klein and Richard Prange. "Perturbation Theory for an Infinite Medium of Fermions". In: *Physical Review* 112.3 (1958), p. 994.

[64] Stephen L Adler. "Quantum theory of the dielectric constant in real solids". In: *Physical Review* 126.2 (1962), p. 413.

[65] Nathan Wiser. "Dielectric constant with local field effects included". In: *Physical Review* 129.1 (1963), p. 62.

[66] Xia Leng et al. "GW method and Bethe–Salpeter equation for calculating electronic excitations". In: *Wiley Interdisciplinary Reviews: Computational Molecular Science* 6.5 (2016), pp. 532–550.

[67] Gordon Baym and Leo P Kadanoff. "Conservation laws and correlation functions". In: *Physical Review* 124.2 (1961), p. 287.

[68] Gordon Baym. "Self-consistent approximations in many-body systems". In: *Physical review* 127.4 (1962), p. 1391.

[69] JM Luttinger. "Fermi surface and some simple equilibrium properties of a system of interacting fermions". In: *Physical Review* 119.4 (1960), p. 1153.

[70] Abraham Klein. "Perturbation theory for an infinite medium of fermions. II". In: *Physical Review* 121.4 (1961), p. 950.

[71] AJ Layzer. "Properties of the One-Particle Green's Function for Nonuniform Many-Fermion Systems". In: *Physical Review* 129.2 (1963), p. 897.

[72] David Awschalom and Nitin Samarth. "Spintronics without magnetism". In: *Physics* 2 (2009), p. 50.

[73] B Merabet et al. "Spin-orbit coupling effect on the electronic structure of Sr2FeHfO6 alloy for spintronics application". In: *Journal of Magnetism and Magnetic Materials* 518 (2021), p. 167374.

[74] Charlotte Emma Moore. *Atomic energy levels as derived from the analyses of optical spectra*. Vol. 1. US Department of Commerce, National Bureau of Standards, 1949.

[75] B Vincent Crist. "Argon implanted into graphite, by XPS". In: *Surface Science Spectra* 1.4 (1992), pp. 376–380.

[76] PH Citrin and DR Hamann. "Measurement and calculation of polarization and potential-energy effects on core-electron binding energies in solids: X-ray photoemission of rare gases implanted in noble metals". In: *Physical Review B* 10.12 (1974), p. 4948.

[77] Edward B Saloman. "Energy levels and observed spectral lines of ionized argon, Ar II through Ar XVIII". In: *Journal of Physical and Chemical Reference Data* 39.3 (2010), p. 033101.

[78] Edward B Saloman. "Energy levels and observed spectral lines of krypton, Kr I through Kr XXXVI". In: *Journal of physical and chemical reference data* 36.1 (2007), pp. 215–386.

[79] CD Wagner et al. "Handbook of X-ray photoelectron spectroscopy, Perkin-Elmer Corp". In: *Eden Prairie, MN* 38 (1979).

[80] E Lundgren et al. "Layer dependent core level binding energy shifts: Na, K, Rb and Cs on Al (111)". In: *Surface science* 281.1-2 (1993), pp. 83–90.

[81] PM Th M Van Attekum and JM Trooster. "The resolution obtainable in x-ray photoelectron spectroscopy with unmonochromatized Mg Kα radiation". In: *Journal of Electron Spectroscopy and Related Phenomena* 18.1 (1980), pp. 135–143.

[82] W Theis and K Horn. "Temperature-dependent line broadening in core-level photoemission spectra from aluminum". In: *Physical Review B* 47.23 (1993), p. 16060.

[83] SBM Hagström et al. "Oxidation of aluminum surfaces studied by synchrotron radiation photoelectron spectroscopy". In: *Physica Scripta* 16.5-6 (1977), p. 414.

[84] L Ley et al. "Initial stages in the formation of PtSi on Si (111) as followed by photoemission and spectroscopic ellipsometry". In: *Thin Solid Films* 270.1-2 (1995), pp. 561–566.

[85] GM Ingo et al. "X-ray photoelectron spectroscopy investigation on the chemical structure of amorphous silicon nitride (a-SiN x)". In: *Journal of Vacuum Science & Technology A: Vacuum, Surfaces, and Films* 7.5 (1989), pp. 3048–3055.

[86] M Taniguchi et al. "Valence band and core-level photoemission spectra of black phosphorus single crystals". In: *Solid State Communications* 45.2 (1983), pp. 59–61.

[87] A Barrie, IW Drummond, and QC Herd. "Correlation of calculated and measured 2p spin-orbit splitting by electron spectroscopy using monochromatic x-radiation". In: *Journal of Electron Spectroscopy and Related Phenomena* 5.1 (1974), pp. 217–225.

[88] RF Lake and Harold Warris Thompson. "The photoelectron spectra of some molecules containing the C≡ N group". In: *Proceedings of the Royal Society of London. A. Mathematical and Physical Sciences* 317.1529 (1970), pp. 187–198.

[89] AB Cornford et al. "Photoelectron spectra of the halogens". In: *The Journal of Chemical Physics* 54.6 (1971), pp. 2651–2657.

[90] RA Pollak et al. "Evolution of Core States from Energy Bands in the 4 d 5 s 5 p Region from Pd to Xe". In: *Physical Review Letters* 29.5 (1972), p. 274.

[91] Russell D Johnson III et al. "NIST Computational Chemistry Comparison and Benchmark Database, NIST Standard Reference Database Number 101, Release 19, April 2018". In: *URL http://cccbdb. nist. gov/. Accessed March 05th* (2019).

[92] Bernd A Heß et al. "A mean-field spin-orbit method applicable to correlated wavefunctions". In: *Chemical Physics Letters* 251.5-6 (1996), pp. 365–371.

[93] Ulf von Barth and Bengt Holm. "Self-consistent GW 0 results for the electron gas: Fixed screened potential W 0 within the random-phase approximation". In: *Physical Review B* 54.12 (1996), p. 8411.

[94] F Bechstedt et al. "Compensation of dynamical quasiparticle and vertex corrections in optical spectra". In: *Physical review letters* 78.8 (1997), p. 1528.

[95] R Del Sole and Raffaello Girlanda. "Optical properties of solids within the independent-quasiparticle approximation: Dynamical effects". In: *Physical Review B* 54.20 (1996), p. 14376.

[96] AB Migdal. "The momentum distribution of interacting Fermi particles". In: *Soviet Phys. JETP* 5 (1957).

[97] Falco Hüser, Thomas Olsen, and Kristian S Thygesen. "Quasiparticle GW calculations for solids, molecules, and two-dimensional materials". In: *Physical Review B* 87.23 (2013), p. 235132.

[98] Takao Kotani, Mark Van Schilfgaarde, and Sergey V Faleev. "Quasiparticle self-consistent G W method: A basis for the independent-particle approximation". In: *Physical Review B* 76.16 (2007), p. 165106.

[99] Fabio Caruso et al. "Self-consistent G W: All-electron implementation with localized basis functions". In: *Physical Review B* 88.7 (2013), p. 075105.

[100] John Robert Schrieffer. *Theory of superconductivity*. CRC press, 2018.

[101] Philip M Morse and Herman Feshbach. "Methods of theoretical physics". In: *American Journal of Physics* 22.6 (1954), pp. 410–413.